Department of Biology
University of Fribourg (Switzerland)

UNI FR
UNIVERSITÉ DE FRIBOURG
UNIVERSITÄT FREIBURG

Regulation of the Rag GTPase Gtr2 in TORC1 signaling

THESIS

Presented to the Faculty of Sciences of the University of Fribourg (Switzerland) in consideration for the award of the academic grade *Doctor rerum naturalium*

by

Alessandro Sardu

from

Olbia, Italy

2016

"Studia, ca ua' dì tindi asa accattai."
Erminio Sardu

List of abbreviations:

ADP: Adenosine diphosphate
AMP: Adenosine monophosphate
ATP: Adenosine triphosphate
ATPase: Adenosine triphosphatase
CORVET: Class C core vacuole/endosome tethering
EGOC: Exit from rapamycin-induced GrOwth arrest Complex
EGO-TC: Ego ternary complex
FBP: F-Box Protein
FKBP12: FK506 Binding Protein 12
GAD: G protein activated by nucleotide-dependent dimerization
GAP: GTPase activating protein
GATOR: GAP activity toward Rags
GDI: Guanine dissociation inhibitors
GDP: Guanosine diphosphate
GEF: Guanine nucleotide exchange factors
GGTase II: Geranylgeranyl Transferase II
GPCR: G Protein Coupled Receptor
GTP: Guanosine triphosphate
GTPase: Guanosine triphosphatase
HOPS: HOmotypic fusion and vacuole Protein Sorting
LeuRS: Leucyl t-RNA synthetase
mRNA: Messenger RNA
mTORC1: Mammalian TORC1
NLS: Nuclear Localization Signal
ORF: Open Reading Frame
P_i: Inorganic Phosphate
PI3K: Phosphatidyl Inositol 3' Kinase
PKA: Protein Kinase A
Rag: Ras-related GTP binding protein
REP: Rab escort protein
RGS: Regulators of G protein signaling
RNA: RiboNucleic Acid
SEAC: Seh1-associated complex
SEACAT: SEAC subcomplex activating TORC1 signaling
SEACIT: SEAC subcomplex inhibiting TORC1 signaling
TOR: Target Of Rapamycin
TORC1: Target Of Rapamycin Complex I
v-ATPase: Vacuolar ATPase

Summary

Growth, proliferation, differentiation and survival of all living organisms highly depend on their capacity to sense and adapt to environmental changes, such as fluctuations in nutrients availability. Thus, living organisms have evolved several mechanisms to sense and respond to availability or changes in environmental nutrient levels. The target of rapamycin complex 1 (TORC1) defines one of the central nutrient sensing networks, which has emerged in the eukaryotic kingdom during evolution. Among all the nutrients, amino acids are the best-known TORC1 nutritional input, and their presence is communicated to TORC1 via the highly conserved family of Rag GTPases. Gtr1 and Gtr2 define the Rag family GTPases in *S. cerevisiae* and together they form a heterodimer. RagA, RagB, RagC and RagD represent the Rag family GTPases in higher eukaryotes and, similarly to Gtr1/Gtr2, RagA/B and RagC/D heterodimerize. The Rag GTPase heterodimer activates TORC1 when Gtr1 or RagA/B is GTP-loaded and Gtr2 or RagC/D is GDP-loaded, a state promoted by amino acid availability. Vice versa, when Gtr1 or RagA/B is GDP-loaded and Gtr2 or RagC/D is GTP-loaded, the dimer inhibits TORC1. Although several regulators of Gtr1 have been identified, regulators of Gtr2 have remained instead elusive.

The work presented in this thesis is focused on the identification of novel regulators of Gtr2. In the first chapter of this thesis, we present the Lst4-Lst7 heterodimeric complex as a positive regulator for Gtr2. The Lst4-Lst7 complex acts as a GAP and thus stimulates GTP hydrolysis activity of Gtr2, favoring its GDP-loaded form. Interestingly, the Lst4-Lst7 complex is recruited to and released from the vacuolar membrane following amino acid deprivation and refeeding, respectively. In parallel, this complex interacts well, but transiently, with Gtr2 only when cells are re-fed with amino acids. We conclude that the Lst4-Lst7 complex is a GAP for Gtr2 and mediates the presence of amino acids to activate TORC1 downstream of Gtr2.

In the second chapter, we present a proof of concept for a genetic screen that was aimed to identify novel regulators of Gtr1/Gtr2 and/or TORC1. The over-production of a nucleotide-free form of Gtr1 ($Gtr1^{S20L}$) causes downregulation of TORC1 and impairs growth in budding yeast. The screening protocol described in this chapter aimed to identify suppressor mutations that could alleviate the growth inhibitory phenotype

caused by Gtr1^{S20L} over-expression. Most of the isolated mutations were located in genes whose products were previously known to be involved in the TORC1 signaling network. We also present in this chapter an initial analysis of the respective mutants (including the assessment of their TORC1-related phenotypes) and discuss the data in the context of the current literature.

In the third chapter, we describe of attempt to investigate the role of the Mrs6 protein as a regulator for Gtr2. Mrs6 has a positive effect on TORC1 activity by an unknown mechanism. Our data indicate a functional link between Mrs6 and Rag GTPases that remain to be studied in more detail in the future.

In the final chapter, we provide some concluding remarks regarding unsolved questions and experiments that may follow up on the discoveries presented in Chapters I, II and III.

Résumé

La croissance, la prolifération, la différenciation ainsi que la survie des cellules au sein d'organismes uni ou pluricellulaires dépendent de leur capacité à sentir et à répondre rapidement au moindre changement susceptible de survenir dans leur environnement. Pour percevoir et adapter au mieux leur réponse, les cellules font appel à des voies moléculaires de signalisation, conservées au cours de l'évolution. Au cœur de l'une d'elles, le complexe protéine kinase TORC1 joue un rôle central en permettant, entre autres, de moduler le niveau de croissance cellulaire en fonction de la disponibilité en acides aminés. La présence d'acides aminés est communiquée à TORC1 par les Rag GTPases, qui appartiennent à une famille conservée de GTPases. Chez la levure *S. cerevisiae*, les deux représentants de cette famille, Gtr1 et Gtr2, s'associent pour former un hétérodimère. Celui-ci se concentre à la surface de la vacuole. RagA, RagB, RagC et RagD représentent la famille des Rag GTPases dans les eucaryotes supérieurs et, tout comme Gtr1/Gtr2, RagA/B et RagC/D s'assemblent en hétérodimères. Lorsque Gtr1 ou RagA/B est lié au GTP et Gtr2 ou RagC/D est lié au GDP, condition favorisée par la disponibilité en acides aminés, le complexe est actif et contribue à l'activation de TORC1. Au contraire, quand Gtr1 ou RagA/B est chargé avec du GDP et Gtr2 ou RagC/D est chargé avec du GTP, le dimère inhibe TORC1. Bien que plusieurs régulateurs de Gtr1 aient été identifiés, les régulateurs de Gtr2 sont, jusqu'à présent, restés plutôt insaisissables.

Dans cette thèse, nous présentons notre travail, réalisé dans le but d'identifier de possibles régulateurs de Gtr2. Dans le premier chapitre, nous présentons le complexe hétérodimérique Lst4-Lst7 comme régulateur positif pour Gtr2. En effet, ce complexe agit comme une GAP, stimulant l'activité d'hydrolytique de Gtr2, favorisant donc sa conversion de la forme Gtr2-GTP vers celle Gtr2-GDP. De plus, le complexe Lst4-Lst7 est recruté puis relâché de la membrane vacuolaire en conditions de privation et de réapprovisionnement en acides aminés, respectivement. Seulement lorsque les niveaux d'acides aminés sont satisfaisants, Lst4-Lst7 interagit avec Gtr2, l'active et informe ainsi TORC1 des conditions favorables de croissance.

Dans le deuxième chapitre, nous présentons un criblage génétique à petite échelle entrepris dans le but d'identifier de nouveaux régulateurs de Gtr1/Gtr2 et/ou TORC1.

Cette approche génétique est basée sur l'observation que la surproduction de la forme Gtr1 libre de nucléotides (Gtr1S20L) a un effet négatif sur TORC1 et, de ce fait, empêche la formation de colonies. Des mutations spontanées capables de supprimer l'inhibition de croissance découlant de la surexpression de Gtr1S20L ont donc été recherchées, identifiées et leur caractérisation entamée. La plupart des mutations isolées ont été localisées dans des gènes dont les produits étaient précédemment connus pour être impliqués dans le réseau de signalisation TORC1. Nous présentons également dans ce chapitre une analyse initiale de ces mutants (notamment l'évaluation de leurs phénotypes liés à TORC1) et discutons les données dans le contexte de la littérature actuelle.

Dans le troisième chapitre, nous rapportons notre tentative d'étudier le rôle de la protéine Mrs6 comme régulateur de Gtr2. Mrs6 a un effet positif sur l'activité TORC1 mais son mécanisme d'action est inconnu. Nos données indiquent un lien fonctionnel entre Mrs6 et les Rag GTPases qui reste à étudier plus en détail.

Dans le dernier chapitre, nous formulons quelques remarques sur des questions demeurées ouvertes et proposons des expériences qui pourraient donner suite aux découvertes présentées dans les chapitres précédents.

Introduction

1 Signaling in living organisms

Interaction with the environment is a critical aspect for growth, proliferation, differentiation and survival of all living organisms. Indeed, many biological processes are tightly regulated by environmental changes which, when sensed, generate appropriate biochemical responses in cells. For example, cells could exhaust a particular resource from their environment and have to utilize others in order to survive. This choice would require internal changes depending on which nutrient can be metabolized by the cells and what the environment is actually "offering". Adaptation to a new condition can happen in many different forms, like synthesis of new enzymes, modification of the activities of pre-existing ones, and alteration of membrane-transport processes. A typical signaling response starts with the perception of an environmental signal by receptors. This may happen via different mechanisms such as recognition of a chemical that can directly diffuse through the cell membrane or can be transported by a protein, or changes in the cell membrane tension (Kozlov and Chernomordik, 2015; Zaman et al., 2008). Following detection, many players orchestrate the signaling transduction up to the final effectors often requiring crosstalk and coordination between the components of distinct molecular pathways. Among all the mechanisms used by living organisms to react to any change in their environment, protein phosphorylation, dephosphorylation and ubiquitination are historically the most studied. However, a wide set of dedicated proteins called GTP-binding proteins or GTPases has as well a key role in signaling control and propagation. The next paragraphs will give a general outlook on this family of proteins and their regulators.

1.1 GTPases

GTP-binding proteins, or GTPases, represent a large family of proteins of key importance in the regulation of diverse processes such as protein biosynthesis, differentiation, signal transduction and transport of vesicles (Bourne et al., 1990; Gilman, 1987; Pfeffer, 2012; Trahey and McCormick, 1987). The family is characterized by its ability to bind and hydrolyze GTP through a so-called G domain yielding GDP and inorganic phosphate P_i. GTPases are often described as "molecular switches", being active and signaling competent in their GTP-bound form and inactive when GDP-bound. Indeed, the nucleotide loading status of the GTPase typically induces conformational changes that allow or deny binding to its target effectors (Fig.1) (Bourne et al., 1990).

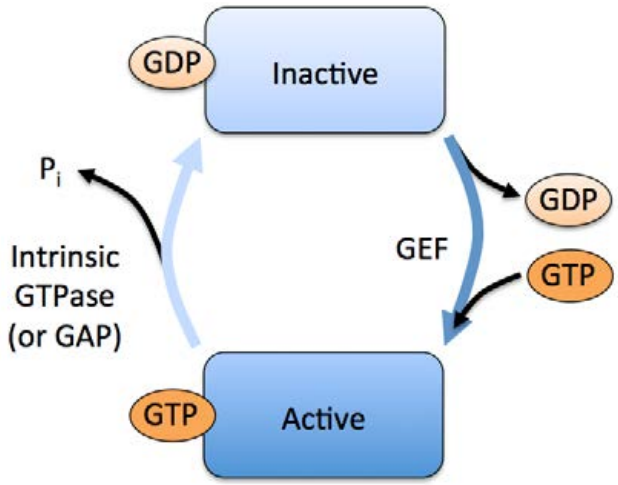

Figure 1 The "molecular switch" concept. GTPases are active in their GTP-bound form and inactive when GDP-bound. Additional regulators such as GEFs and GAPs may be needed to progress through the GTP/GDP cycle (see 1.3.1, 1.3.2 and 1.3.3).

Historically, GTPases have been classified in two groups: the "heterotrimeric G-proteins" and the "small GTPases" (Scheffzek and Ahmadian, 2005). More recently, an additional group has been proposed: the G proteins activated by nucleotide-dependent dimerization (GADs) (Gasper et al., 2009).

1.1.1 Heterotrimeric G proteins

Heterotrimeric G proteins are best known for their role in signal transduction activated by extracellular signals such as hormones and neurotransmitters (Siderovski and Willard, 2005). This group can be divided into four main families of G proteins: G_i/G_o,

G_q, G_s, and G_{12}. As suggested by their name, they are composed of three different subunits: Gα, Gβ and Gγ (Wittinghofer and Vetter, 2011). Gα is often myristoylated and/or palmitoylated, while Gγ is prenylated. These lipid modifications are necessary to tether the G proteins to membranes (Wedegaertner et al., 1995). Among the three subunits, Gα is the only catalytic subunit as it bears a G domain and the GTPase activity (Gilman, 1987). When Gα is GDP-loaded, it associates with Gβ and Gγ to form a heterotrimer. This complex binds a seven transmembrane domain receptor named G Protein Coupled Receptor (GPCR) (Cabrera-Vera et al., 2003; Siderovski and Willard, 2005). The ligand-activated GPCR favors the release of GDP and the binding of GTP to Gα. GTP-bound Gα exhibits weak affinity for both GPCR and the dimer Gβγ, hence dissociates from both of them. Gα and Gβγ can now freely associate with their target effectors. The GTP-GDP cycle is restored upon GTP hydrolysis of Gα which, when GDP-loaded, reassembles with Gβγ and reassociates with the GPCR, thereby stopping signal propagation (Fig.2A). Regulators of G protein signaling (or RGS) decreases the lifespan of GTP-bound Gα by favoring the GTP hydrolysis (Siderovski and Willard, 2005).

1.1.2 Small GTPases

The small GTPases group is composed of small globular proteins of approximately 25-30 kDa. The archetypes are the Ras GTPases. Since the other members have been discovered based on their similarity to this subfamily, the small GTPases group is also called Ras GTPase superfamily (Wennerberg et al., 2005). Small GTPases can be divided into six family groups: (1) the Ras family which is important for cell proliferation, (2) the Rho family that regulates cytoskeletal dynamics and morphology, (3) the Rab and (4) Arf family that control membrane trafficking and vesicle transport, (5) the Ran family which is involved in nuclear transport, and (6) the Rag family (together with Rheb from the Ras family) that regulate cell growth. The major Ras family can be further divided into six subfamilies called Ras, Ral, Rit, Rap, Rheb, and Rad (Reiner and Lundquist, 2016; Wennerberg et al., 2005). A typical feature of the Ras superfamily proteins is their post-translational modification by lipids, necessary for their membrane anchorage (Mishra and Lambright, 2016; Wennerberg et al., 2005). Rho and Ras GTPases often possess a CAAX motif (C= Cysteine, A= aliphatic, X= any amino acid) at their C-terminus in which the cysteine thiol group can be modified to form a stable

thioether linkage to one polar farnesyl or geranylgeranyl isoprenoid (Cox and Der, 2002; Mishra and Lambright, 2016). Rab GTPases have different C-terminal motifs (CC, CXC, CCX, CCXX, or CCXXX) that are similarly modified by the addition of geranylgeranyl groups while Arf GTPases are instead myristoylated at their N-terminus (Wennerberg et al., 2005). Ran and Rag GTPases do not have any clear motif for lipid modification (Reiner and Lundquist, 2016; Rush et al., 1996). Rab, Arf and Ran GTPase activities differ depending on their nucleotide-bound form, therefore they need to cycle between the GTP and GDP-bound states for proper functioning. Since in most cases small GTPases have low intrinsic GTPase activity and low GDP to GTP exchange rate, regulators acting *in trans* such as GEFs and GAPs are necessary to control the GDP/GTP cycling (Fig. 2B) (see 1.3.1, 1.3.2 and 1.3.3) (Wennerberg et al., 2005).

1.1.3 G proteins activated by nucleotide-dependent dimerization

G proteins activated by nucleotide-dependent dimerization (GADs) are a relatively new group of GTPases. Several studies demonstrated their involvement in processes such as protein targeting across signal recognition, cytokinesis, secretion, membrane remodeling, and protein transport via the chloroplast membrane in plants (Barral and Kinoshita, 2008; Connolly and Gilmore, 1989; Gasper et al., 2009; Schleiff et al., 2003). GADs have low affinity for nucleotides and high intrinsic nucleotide-exchange rates (Gasper et al., 2009; Moser et al., 1997). When GTP-bound, the γ phosphate is believed to induce a conformational change into the G domain allowing GAD proteins to dimerize across their nucleotide-binding sites. The GTP-loaded dimer can interact with its effectors and is considered as the active form of the GTPase. GADs do not have enzymatic activity when monomeric because of an incomplete catalytic domain, but dimerization activates their GTP hydrolysis function (Gasper et al., 2009). The GTP hydrolysis determines the end of the interactions with effectors or co-regulators and the disassembly of the dimer (Fig. 2C) (Gasper et al., 2009).

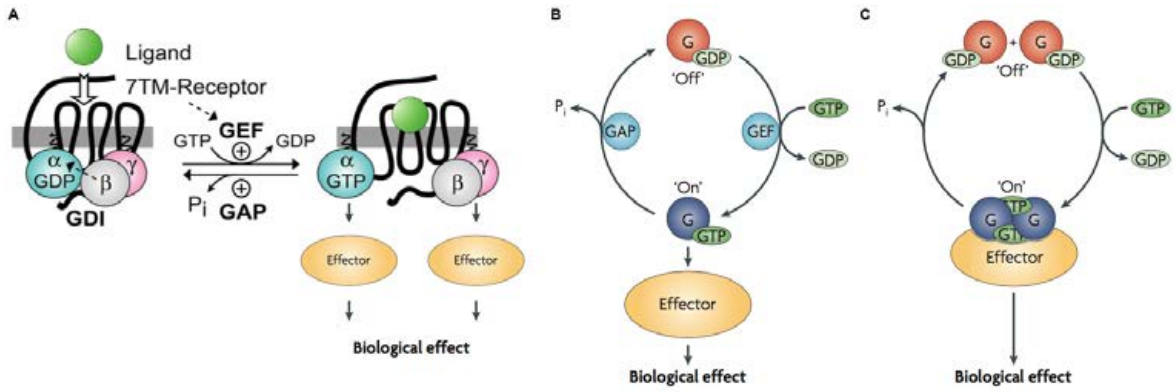

Figure 2 GTP/GDP cycle of the three main GTPase families. Standard models of the GTP/GDP cycle for Heterotrimeric G proteins coupled to transmembrane receptors (A), Small GTPases (B), and GADs (C). GTPases alternate between GTP and GDP thanks to GAP and GEF proteins. The former class promotes the GTP hydrolysis while the latter the exchange of GDP for GTP. Figure 2A has been adapted from (Siderovski and Willard, 2005), while figures 2B and 2C from (Gasper et al., 2009).

1.2 Structure and functioning of G proteins

In all G proteins, GTP binding and hydrolysis are achieved via a nucleotide-binding domain also called the "G domain" (Syrovatkina et al., 2016). This domain is composed of a six-stranded mixed β-sheet and five α-helices on both sides. G domains are usually defined by the presence of specific conserved sequence motifs called G for "G binding" (Fig.3) (Wittinghofer and Vetter, 2011). An alternative nomenclature instead divides them into PM for "Phosphate and Metal binding" and G' motifs (here I will use the apostrophe to differentiate between the two nomenclatures) for "Guanine specificity" (Valencia et al., 1991).

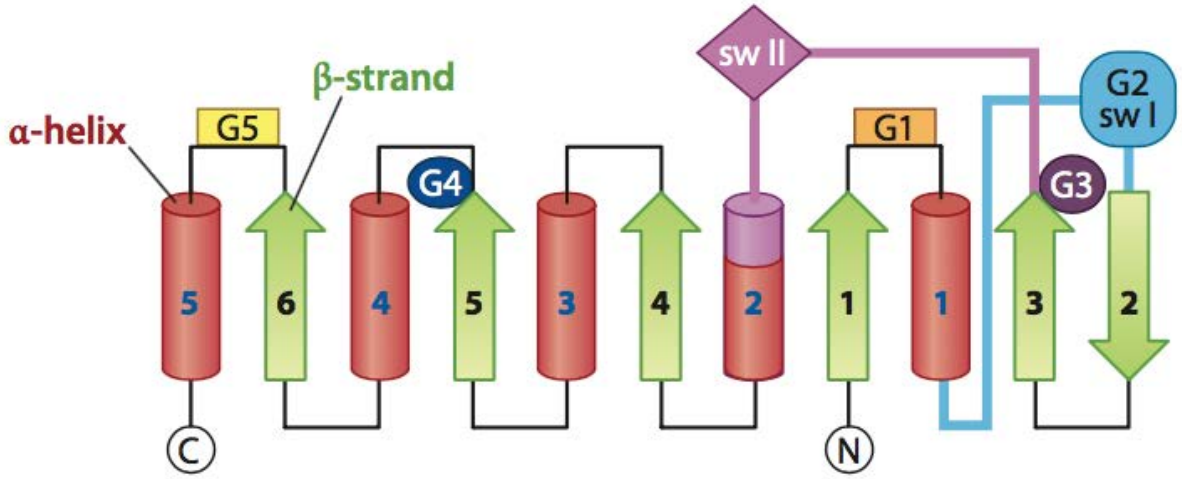

Figure 3 Topology of the G domain. β-strands and α-helices are colored in green and red, respectively. Conserved motifs, N and C termini are indicated. Figure taken from (Wittinghofer and Vetter, 2011).

G1/PM1 is the motif GxxxxGKS/T, also called P-loop for "phosphate binding", and it is common to both GTP- and ATP- binding proteins (Saraste et al., 1990). Its main function is the binding of the nucleotide β phosphate (Rensland et al., 1995). The G2/PM2 motif is one highly conserved threonine (T) in the switch I region that directly binds the GTP γ phosphate and an Mg^{2+} ion, which is a cofactor (Wittinghofer and Pai, 1991; Wittinghofer and Vetter, 2011). The sequence DxxG defines the G3/PM3 motif, and its aspartate (D) indirectly coordinates the Mg^{2+} ion, which is necessary for GTP hydrolysis and nucleotide binding in many GTPases via interaction with the non-bridging oxygen of GTP. It can be found close or within the switch II region. G4/G2', with the N/TKxD sequence motif, and G5/G3' consisting of one conserved alanine (A) critically determine the specificity for guanine base binding and contribute, together with the G1/P-loop, to the tight nucleotide binding (Wittinghofer and Vetter, 2011). In a GTP-loaded G protein, the threonine (T) in Switch I and the glycine (G) in Switch II regions make each one a hydrogen bond with the GTP γ phosphate, defining an overall conformation for the GTPase that can interact with its effectors (Wittinghofer and Vetter, 2011). Following GTP hydrolysis, the Switch I and II regions, connected to the γ phosphate, undergo a conformational change, rendering the GTPase inactive (Scheffzek and Ahmadian, 2005). The hydrolysis reaction consists of a nucleophilic attack by a "catalytic" water molecule on the GTP γ phosphate that results in the cleavage of the phospho-monoester bond and the production of GDP and inorganic phosphate (P_i) (Carvalho et al., 2015).

1.3 Regulators of GTPases

Most GTPases slowly hydrolyze GTP and slowly exchange GDP to GTP (Bourne et al., 1990; Feuerstein et al., 1987; John et al., 1993). The conversion between the two nucleotide-loading states has a timescale slower than that of relevant biological processes (Mishra and Lambright, 2016). Therefore, to accelerate the switch between their active/inactive states, two types of proteins are fundamental: Guanine nucleotide Exchange Factors (GEFs) and GTPase-Activating Proteins (GAPs). GEFs accelerate the GDP/GTP exchange while GAPs stimulate the intrinsic GTP hydrolytic activity of the GTPase (Scheffzek and Ahmadian, 2005).

1.3.1 Guanine nucleotide exchange factors (GEFs)

Most of the GTPases have high affinity for guanine nucleotides and, consequently, slowly dissociate from both GTP and GDP. GADs are an exception because of their low affinity for nucleotides and high intrinsic nucleotide-exchange rate and therefore the they do not seem to require any GEF (Gasper et al., 2009; Moser et al., 1997). Without external help, the GTP hydrolysis would lead to an inactive GTPase that would then require one or more hours to exchange the loaded GDP for GTP. GEFs accelerate this exchange by catalyzing the dissociation of the loaded nucleotide from the G protein. Different domains and specificity toward their target/s characterize many known GEFs. The mode of interaction with the target GTPase changes among GEFs but, when bound, they operate using similar principles. (Bos et al., 2007). GEFs typically regulate heterotrimeric G proteins and small GTPases. The GDP/GTP exchange of the Gα subunit is favored by the ligand-activated GPCR which functions as a GEF (Siderovski and Willard, 2005).

GEFs have low affinity for the so-called "ternary complex" composed of the GTPase, the GDP and the GEF and high affinity for the nucleotide free GTPase. Briefly, the GEF binds to the G protein and induces conformational changes into the P-loop and the switch regions, such that the cofactor Mg^{2+} ion is displaced and the interaction surface in the phosphate-binding region is perturbed. Consequently, the GDP is released and the GEF-GTPase interaction is strengthened. Since the base-binding region of the GTPase remains unperturbed upon GEF binding, a new guanine nucleotide can bind to the GTPase. This new interaction eventually displaces the GEF (Bos et al., 2007). GTPases have comparable affinity for both GTP and GDP. However, GTP is favored over GDP after nucleotide release simply because GTP cellular concentration is 10 to 50 times higher than that of GDP (Bos et al., 2007; Trahey and McCormick, 1987). Destabilization of the Mg^{2+} ion is important to facilitate dissociation of the GDP molecule from the GTPase. Several GEFs provide a hydrophobic residue close to the Mg^{2+} binding site, which decreases its affinity for the GTPase, and therefore that of GDP. Some other GEFs induce conformational changes on the switch II region and consequently a conserved GTPase alanine re-orients its methyl group near the Mg^{2+}-binding site producing a hydrophobic repulsion (Cherfils and Zeghouf, 2013).

All GEFs interact extensively with the switch II of the GTPase. The large interacting surface is supposed to be important to prevent unfolding of the unstable nucleotide-free GTPase (Bos et al., 2007; Cherfils and Zeghouf, 2013).

GEFs are believed to interact specifically and induce dissociation of GDP and not GTP from the GTPase. A mechanism to discriminate between the two nucleotide-loading states would be necessary to avoid displacement of GTP from the GTPase. One example comes from the DOCK family of GEFs for Rho GTPases where a "nucleotide sensor" within the GEF was discovered. More precisely, DOCK9 GEF has an α-helix that senses the nucleotide loading status of the Cdc42 GTPase, a member of Rho GTPase family, through the Mg^{2+} ion in the nucleotide-binding pocket. When Cdc42 is GDP-loaded, the DOCK9 α-helix displaces the Mg^{2+} and induces GDP release. When Cdc42 is GTP-loaded, the Mg^{2+} ion is tightly bound to GTP, hence this stronger interaction displaces the α-helix "nucleotide sensor", inducing discharge of the GEF from the GTPase (Yang et al., 2009).

1.3.2 GTPase activating proteins (GAPs)

GTPases have low intrinsic GTPase activity and they require a GAP to achieve efficient GTP hydrolysis. GAPs are involved in proper orientation and polarization of the catalytic water molecule, and stabilization of the transition state. Once these conditions are fulfilled, the GTP hydrolysis can be more efficient by several orders of magnitude. (Bos et al., 2007). GAPs can differ among them depending on how they enhance the GTPase activity or they interact with the GTPase. The Gα subunits of heterotrimeric G proteins have already high intrinsic GTPase activity (Siderovski and Willard, 2005). It has been speculated that the higher GTPase activity in Gα is due to a catalytic arginine in the P-loop that is absent in most of the small GTPases (Bourne et al., 1991).However, a superfamily called RGS (“regulator of G-protein signaling”) proteins can bind Gα subunits via an “RGS-box” domain and substantially increase their intrinsic GTPase activity and attenuate the signal propagation (Siderovski and Willard, 2005). In small GTPases, Ras and RhoGAPs stabilize the glutamine 61 in the switch II region of the GTPase that coordinates the catalytic water molecule. These GAPs also provide *in trans* an arginine (called "arginine finger") that neutralizes the negative charge at the GTP γ-phosphate (Scheffzek and Ahmadian, 2005). The RabGAP provides an arginine finger

similarly to Ras and RhoGAPs. Additionally, it supplies a glutamine to stabilize the hydrolysis reaction by the Rab GTPases. The conserved glutamine in Rab switch II region is important only for binding of the RabGAP and it does not have catalytic functions (Pan et al., 2006). RapGAPs provide an asparagine (called the "asparagine thumb") with catalytic functions taking over the role of the glutamine in switch II (Daumke et al., 2004). Ran GTPases contain all the machinery for GTP hydrolysis. RanGAPs do not provide any catalytic residues to Ran GTPases but they are involved in stabilization of switch I and II regions (Cherfils and Zeghouf, 2013). Finally, GADs do not require GAPs because their dimerization activates their GTP hydrolysis function. It is speculated that the two subunits of the dimer complement each other by providing residues in the active site that stimulate the GTP hydrolysis, making the need of a GAP unnecessary. On the one hand those shared residues could directly take part into the catalysis process, on the other hand they could stabilize the flexible regions of the partner (Gasper et al., 2009).

1.3.3 Guanine nucleotide dissociation inhibitors (GDIs)

GDIs are a class of proteins that preferentially bind the GDP-bound GTPase and inhibit spontaneous exchange of GDP for GTP (Pfeffer et al., 1995). In the heterotrimeric G proteins the Gβγ heterodimer has the additional role of inhibitor of spontaneous GDP release from Gα, thereby functioning as GDI (Siderovski and Willard, 2005). Furthermore, a family of proteins containing a highly conserved 19-amino acid sequence called "GoLoco motif" act as a GDI for the Gα subunits of the adenylyl-cyclase-inhibitory subclass (Willard et al., 2004). Many GTPases of the Ras superfamily proteins have lipid modification at their N- or C-termini. Ras, Rho and Rab GTPases are prenylated at their C-terminus and this modification is necessary for membrane anchorage. As part of their regulation, they can be extracted from membranes and solubilized by GDIs (Pfeffer et al., 1995). The best-known GDIs are those for Rho and Rab proteins. These two GDI families do not share similar structure but both have two domains involved in the recognition of the GTPase core and the lipid modified C-terminus (Cherfils and Zeghouf, 2013). GDIs keep their target GTPase in the inactive state because they prevent GDP to GTP exchange and localization of the G protein at the membrane. The Rab escort protein (REP) is an exception to this rule. REP shares many

properties with GDIs but its function is to bind unprenylated GDP-bound Rabs and ensure their prenylation via recruitment of a prenyltransferase (Andres et al., 1993; Pfeffer et al., 1995).

2 Nutrient sensing

Nutrients like sugars, amino acids and lipids are organic compounds constituents of cellular biomass or are implicated in energy production processes. Since nutrients are essential for cell growth and proliferation, several mechanisms to sense and respond to availability or changes in environmental nutrient levels are required for life. Nutrient scarcity has been a strong selective force through evolution. Organisms characterized by efficient processes for nutrient sensing and assimilation, as well as adaptation to nutritional deficiencies, had an advantage in maximizing their survival rates. Unicellular organisms, such as the budding yeast *Saccharomyces cerevisiae*, have evolved signaling pathways to sense both intracellular and external nutrient levels. Multicellular eukaryotes like mammals also have intracellular and extracellular nutrient sensing mechanisms.

The target of rapamycin (TOR) pathway is one of the central nutrient sensing networks, which has emerged in the eukaryotic kingdom during evolution. Indeed, the essential functions regulated by the TOR pathway are conserved from yeast to human, emphasizing its general importance in living organisms (De Virgilio and Loewith, 2006; Efeyan et al., 2015). The following paragraphs will focus on key components that define and regulate the TOR pathway in the budding yeast *S. cerevisiae* and higher eukaryotes.

2.1 Target of Rapamycin (TOR) and TOR complexes

The target of rapamycin (TOR) proteins are highly conserved serine/threonine protein kinases, members of the phosphatidylinositol 3-kinase-related kinase protein family (Schmelzle and Hall, 2000). Their name derives from the effect of rapamycin treatment, a macrolide antibiotic with antifungal proprieties produced by the soil bacterium *Streptomyces hygroscopicus* (Sehgal et al., 1975; Vézina et al., 1975). Rapamycin binds to the yeast proline isomerase Fpr1 (ortholog of FKBP12 in human) creating a complex that targets and inhibits TOR kinases leading to cell cycle arrest (Heitman et al., 1991).

While higher eukaryotes have only one *TOR* gene (mTOR in mammals), *S. cerevisiae* has two *TOR* paralogs (named *TOR1* and *TOR2*) probably because of a whole genome duplication event concomitant to interspecies hybridization (Marcet-Houben and Gabaldón, 2015). Tor1 and Tor2 are ~70% identical and have semi-redundant functions. TOR proteins assemble into two structurally and functionally different complexes: TORC1 and TORC2 (Loewith et al., 2002). The two complexes are broadly conserved, and in mammals are called mTORC1 and mTORC2 (Hara et al., 2002; Jacinto et al., 2004; Kim et al., 2002; Sarbassov et al., 2004). In *S. cerevisiae*, deletion of *TOR2* results in cell cycle arrest and therefore in an unviable phenotype, while *TOR1* is not essential (De Virgilio and Loewith, 2006). TORC1 is a dimeric multiprotein complex composed of Tor1 and/or Tor2, Kog1, Lst8 and Tco89 (Loewith et al., 2002; Reinke et al., 2004). Mammalian TORC1 (mTORC1) also consists of a homodimer of mTOR, the Kog1 ortholog Raptor, mammalian Lst8 (mLst8) and two non-conserved subunits: PRAS40 and Deptor (Tab.1) (Peterson et al., 2009; Sancak et al., 2007; Wullschleger et al., 2006).

TORC1

S. cerevisiae	**Mammals**
Tor1 or Tor2	mTOR
Lst8	mLST8
Kog1	Raptor
Tco89	?
?	PRAS40
?	Deptor

TORC2

S. cerevisiae	**Mammals**
Tor2	mTOR
Lst8	mLST8
Avo1	mSin1
Avo2	?
Avo3	Rictor
Bit2, Bit61	Protor-1, -2
?	Deptor

Table 1 TORC1 and TORC2 components in *Saccharomyces cerevisiae* and their orthologs in mammals.

Tco89 seems to be exclusive to *S. cerevisiae* and no sequence homolog has been found in other species, not even in the fungal kingdom (Shertz et al., 2010). Although *TCO89* is not an essential gene, it is still required for proper TORC1 functioning (Binda et al., 2009). Interestingly, deletion of both *TOR1* and *TCO89* results in synthetic lethality that can be rescued by over-expression of Tor2 (Reinke et al., 2004).

TORC1 regulates cell growth in response to nutrient availability and cellular stresses by activating anabolic processes and inhibiting catabolic processes. Thus, events such as

protein synthesis or ribosome biogenesis are positively regulated while macroautophagy is inhibited (De Virgilio and Loewith, 2006). Additionally, mTORC1 is controlled by extracellular mitogens such as insulin (Sarbassov et al., 2005). In budding yeast, TORC1 localizes to the vacuole, a membrane-bound organelle with degradative and storage capabilities (Sturgill et al., 2008). In mammals, active mTORC1 localizes at lysosomal surface (Sancak et al., 2010). TORC2 is a dimer composed uniquely of Tor2, Avo1, Avo2, Avo3, Bit61 (or its paralog Bit2) and Lst8 (Loewith et al., 2002; Reinke et al., 2004; Wullschleger et al., 2006). Mammalian TORC2 (mTORC2) is an homodimer containing mTOR, the Avo1 and Avo3 orthologs mSin1 and Rictor, the Bit61/Bit2 ortholog Protor-1/Protor-2, mammalian LST8 and Deptor (Tab.1) (Gaubitz et al., 2016). TORC2 is involved in regulating membrane tension and homeostasis via processes such as actin cytoskeleton polarization during cell cycle progression, endocytosis, sphingolipid and ceramide biosynthesis (Cybulski and Hall, 2009; Eltschinger and Loewith, 2015). This thesis will not extensively describe TORC2 because our research is mainly focused on TORC1 and its regulation. However, recent reviews have extensively described TORC2, its organization and functions (Eltschinger and Loewith, 2015; Gaubitz et al., 2016).

Although many cellular processes are regulated in a TORC1 dependent manner, the number of well-characterized substrates directly phosphorylated by TORC1 is small. In *S. cerevisiae*, the known direct TORC1 substrates are the regulatory subunit of the "Atg1p signaling complex" Atg13, the PP2A phosphatase associated protein Tap42, the Ypk3 protein kinase, the Sfp1 transcription factor and the Sch9 protein kinase (Jiang and Broach, 1999; Kamada et al., 2010; Lempiäinen et al., 2009; Urban et al., 2007; Yerlikaya et al., 2016). Among these proteins, Sch9 is the best-characterized TORC1 target. TORC1 controls ribosome biogenesis and, in part, translation initiation via direct phosphorylation of the AGC kinase Sch9 at multiple C-terminal sites. Sch9 was initially considered the functional homolog of the mammalian S6 kinase (S6K) since they are both similarly regulated by TORC1 and they perform same functions (Urban et al., 2007). However, another group claimed the AGC kinase Ypk3 as S6K homolog (González et al., 2015). In support of this idea, Ypk3 is orthologous to Psk1, the *Schizosaccharomyces pombe* functional homolog of the S6K (Nakashima et al., 2012; Yerlikaya et al., 2016). Furthermore, Ypk3 has been shown to phosphorylate, in a TORC1 dependent manner, the conserved ribosomal protein S6 (Rps6), which is the

direct target of the S6K in mammals. (Yerlikaya et al., 2016). In conclusion, Ypk3 has been accepted as the homolog of the S6K.

Sch9 is phosphorylated in wild type cells growing in rich conditions. Conversely, deprivation of nutrients, or removal of positive regulator of the TORC1 pathway results in Sch9 dephosphorylation (Binda et al., 2009; Urban et al., 2007). Since the Sch9 phosphorylation state reflects the activation/inactivation state of TORC1, Sch9 is often used as readout for TORC1 activity.

3 Small GTPases involved in the TORC1 signaling cascade

In mammals, mTORC1 activity is tightly regulated by cooperation of two different types of small GTPases, Rags and Rheb. The following paragraphs will describe these two major players of the TORC1 signaling pathway.

3.1 Rheb

Rheb (Ras Homolog Enriched in Brain) is a ~21 kDa small GTPase member of the Ras family (Yamagata et al., 1994). When GTP-bound, it can directly bind and increase the kinase activity of mTORC1 (Saucedo et al., 2003). Rheb consists of 184 amino acids: the 169 N-terminal residues define the G domain and the remaining 15 C-terminal residues are part of a flexible structure ending with a CAAX motif necessary for Rheb farnesylation (Castro et al., 2003). Rheb is characterized by a very low intrinsic GTPase activity, hydrolyzing GTP at a rate of ~50 fold lower than that of wild type Ras (Im et al., 2002). Following GTP hydrolysis, Rheb undergoes conformational changes like many other small GTPases. Unlike other Ras family members however, during the GTP/GDP cycle profound rearrangements occur on switch I while the switch II region remains unperturbed (Fig.4) (Yu et al., 2005).

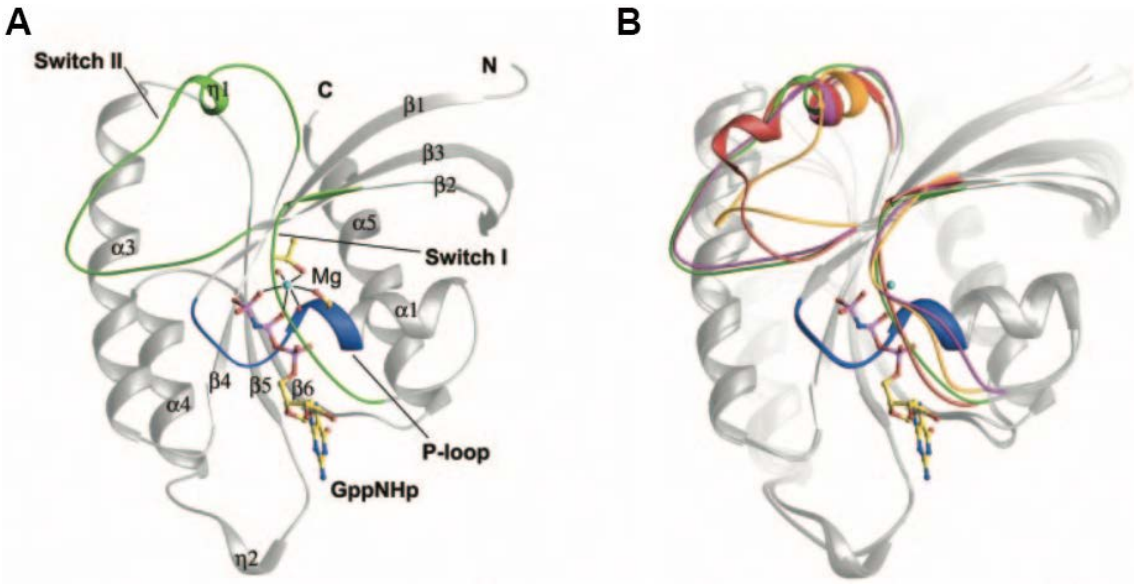

Figure 4 Conformational changes between GTP and GDP-loaded status of Rheb. A) Overall structure of the Rheb G module. P-loop, Switch I, and Switch II regions are indicated on the structure. Rheb is bound to the non-hydrolysable GTP analog GMPPNP (shown using a ball-and-stick representation). Magnesium atoms are represented as azure balls. B) Structure comparison between $Rheb^{GMPPNP}$ (green), $Rheb^{GDP}$ (magenta), Ras^{GTP} (red), Ras^{GDP} (gold). Figure taken from (Yu et al., 2005).

The switch II region of Rheb is rather unique, having a conformation different from the canonical long α-helix seen in Ras GTPases (Fig.4). The low intrinsic GTPase activity of Rheb can be explained by structural differences in the positioning of key residues. Glutamine 61 (Q61) in Ras switch II is directly implicated in GTP hydrolysis (Scheffzek et al., 1997). The corresponding glutamine in Rheb (Q64) is buried in a hydrophobic core and it interacts neither with the nucleotide nor with the catalytic site (Yu et al., 2005). Furthermore, tyrosine 35 (Y35) in Rheb shields the GTP γ-phosphate countering the contribution of the key catalytic residue aspartate 65 (D65) by restricting its access to the nucleotide-binding pocket. Y35 also restrains the position of the catalytic water molecule and decreases its polarization mediated by threonine 38 (T38), another Rheb catalytic residue (Mazhab-Jafari et al., 2012).

How Rheb cycles from GDP to GTP is not clear yet. The protein TCTP (Translationally Controlled Tumor Protein) has been proposed to function as a GEF for Rheb because it accelerates the release of GDP from human Rheb-GDP complexes. (Hsu et al., 2007). Nevertheless, two different reports questioned the role of TCTP as a GEF for Rheb (Rehmann et al., 2008; Wang et al., 2008). Rehmann et al. could not observe interaction between human Rheb and TCTP while *in vitro* they realized that the Rheb intrinsic

nucleotide exchange rate is already high. Wang et al. also concluded that hTCTP does not bind Rheb and has no impact on mTOR signaling. It could be that the Rheb intrinsic exchange rate is sufficiently high on its own and does not need a GEF. Alternatively, it is also possible that a clear GEF has not been discovered because there are multiple redundant GEFs for Rheb (Durán and Hall, 2012).

The TSC complex activates the low GTPase activity of Rheb thereby functioning as a GAP (Castro et al., 2003; Garami et al., 2003; Inoki et al., 2003a; Saucedo et al., 2003). This GAP consists of three proteins: TSC1 (or Hamartin), TSC2 (or Tuberine) and TBC1D7 (Nakashima et al., 2007). The C-terminal domain of TSC2 presents a GAP domain which is sufficient for the GAP activity toward Rheb (Scrima et al., 2008). TSC2 uses the asparagine-thumb mechanism for its GAP function by providing the asparagine 1643 (N1643) *in trans* to accelerate Rheb GTP hydrolysis by 50 fold. Arginine 15 (R15) in the P-loop and Q64 in Rheb coordinate TSC2 binding, but they are not involved in the hydrolysis reaction (Marshall et al., 2009). Regulation of Rheb involves mainly the TSC complex that senses many signals such as oxygen presence, growth factor availability, and cellular energy level. In presence of growth stimulating signals, the TSC complex is disrupted after Akt-dependent phosphorylation of TSC2 (Inoki et al., 2002; Manning et al., 2002). Mitogenic stimuli can start the Ras-Raf-MEK-Erk signaling cascade in which activated Erk1/2 directly phosphorylates TSC2 causing inactivation of the TSC complex (Ma et al., 2005). Conversely, AMPK activates the TSC complex via TSC2 phosphorylation during energy starvation conditions and consequent increase in the AMP levels (Inoki et al., 2003b). During amino acid starvation, the TSC complex is actively recruited at the lysosome via the Rag GTPases. Consequently, the active fraction of GTP-bound Rheb diminishes leading to inhibition of mTORC1 (Demetriades et al., 2014). The TSC complex localization is not only controlled by amino acids. Other stimuli, such as hyperosmotic stress, changes in pH, energetic stress and hypoxic stress, can result in TSC complex re-localization at the lysosomal surface (Demetriades et al., 2016). Rheb inactivation can also be obtained via direct phosphorylation by the p38β–PRAK signaling cascade during energy depletion (Zheng et al., 2011).

The microspherule protein 1 (MCRS1) is another essential link between Rheb and mTORC1 activation (Fawal et al., 2015). When GTP-loaded, Rheb binds the mTOR catalytic domain and activates mTORC1 (Sato et al., 2009). The interaction is stabilized by MCRS1 that binds both Rheb and mTOR functioning as a "molecular link" between

the two proteins. Furthermore, MCRS1 protects Rheb from the inhibitory effect of its GAP, the TSC complex. During amino acid starvation, MCRS1 dissociates from both mTOR1 and Rheb and departs from the lysosome leaving Rheb unprotected from the TSC complex GAP activity. These events result in a GTP to GDP switch of Rheb and therefore in delocalization of lysosomal Rheb (Fawal et al., 2015).

In *S. cerevisiae* a Rheb ortholog named Rhb1 is present. Rheb and Rhb1 have 26% sequence identity and 57% sequence similarity. Moreover, all the key features for nucleotide binding and Mg^{2+} coordination are conserved (Fig.5) (Urano et al., 2000).

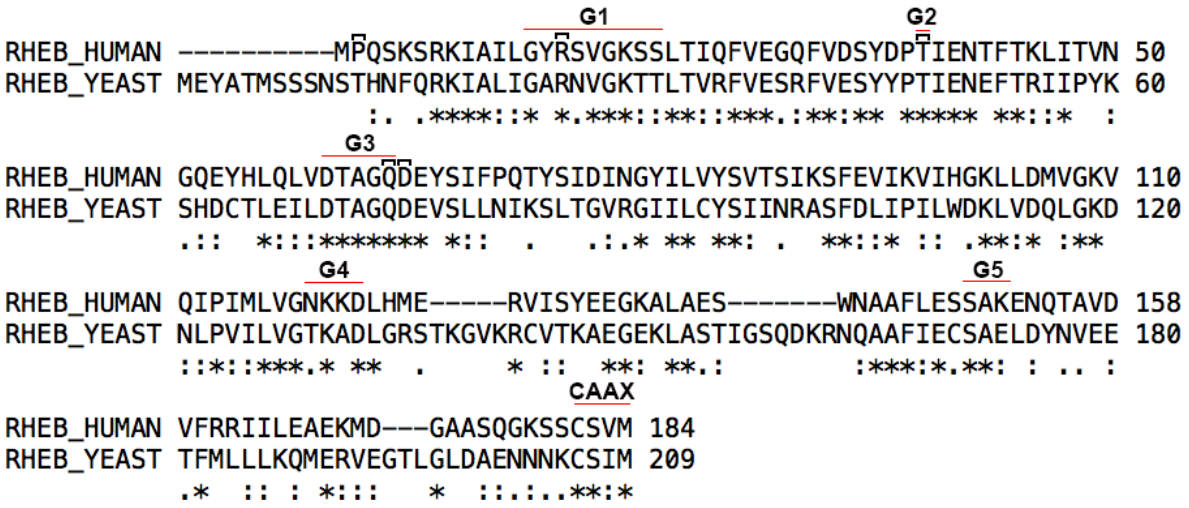

Figure 5 Sequence comparison of Rheb orthologs from human and budding yeast. Conserved G motifs and farnesylation site have been overlined and named. The asterisks, colons and dots indicate identical, strongly similar, and weakly similar residues, respectively. Black caps indicate important residues described in the text.

Currently, no evidences connecting Rhb1 to the TORC1 pathway has been found. Deletion of Rhb1 in budding yeast causes increased uptake of arginine and lysine. Accordingly, loss of Rhb1 provokes canavanine and thialysine sensitivity, which are toxic analogs of arginine and lysine. Mutation of arginine 25 (R25) in the G1 motif or removal of the CAAX motif decreases Rhb1 functionality (Urano et al., 2000). Intriguingly, the corresponding residue to R25 in human Rheb would be R15 in yeast, which is important for TSC2 binding. GFP-Rhb1 localizes to a distinct site close to the periphery of the cell, near to the plasma membrane (Chattopadhyay and Pearce, 2002). *S. cerevisiae* does not contain any obvious orthologs of TSC1, TSC2, or TBC1D7.

3.2 Rag family GTPases

The Ras-related GTP-binding protein (Rag) family of GTPases is of key importance to mediate the amino acid signaling to TORC1 (Binda et al., 2009; Kim et al., 2008; Sancak et al., 2008). Gtr1 and Gtr2 define the Rag family GTPases in *S. cerevisiae* and RagA, RagB, RagC and RagD in higher eukaryotes (Nakashima et al., 1999; Sekiguchi et al., 2001). RagA is homologous to RagB: they share 90% amino acid identity and differ by 7 conservative amino acid substitutions and 33 additional residues in the N terminus of RagB (Schürmann et al., 1995; Sekiguchi et al., 2001). Gtr1 is the yeast ortholog of RagA/B with 51.6% sequence identity to RagA (Schürmann et al., 1995). Similarly, RagC is homologous to RagD, sharing 81.1% amino acid identity, most of their variability lying in their N- and C-terminal regions. Gtr2 is the yeast ortholog of RagC/D with 46.1% sequence identity to RagC (Sekiguchi et al., 2001). Sequence similarity is predicted to be 75% between Gtr1 - RagA, and 76% between Gtr2 - RagC (Gong et al., 2011). Rag GTPases possess most of the sequence elements typically found in all GTPases (Fig.6). The G1/P-loop, G2 and G3 motifs involved in the phosphate/magnesium binding of Rag GTPases are well conserved with the Ras family (Schürmann et al., 1995; Sekiguchi et al., 2001). The guanine base-binding motifs (G4, and G5) differ instead from those found in all the other Ras homologs (Schürmann et al., 1995; Sekiguchi et al., 2014). Indeed, the G4 motif of Rag GTPases has an histidine (**H**KxD) instead of a conserved asparagine (**N**KxD) (Nakashima et al., 1999; Sekiguchi et al., 2001). Rag GTPases G5 motif has an isoleucine (I) instead of the common alanine (A) (Sekiguchi et al., 2014). The Rag GTPase family was initially defined because of these differences in the guanine base-binding motifs (Nakashima et al., 1999). Another peculiar characteristic of Rag GTPases is the C-terminal domain that is larger than those of other Ras family members (Fig.6) (Sekiguchi et al., 2001). Furthermore, they do not have a clear motif for lipid modifications and membrane anchorage (Bun-Ya et al., 1992). The C-terminal domain main function is involved in the assembly of Gtr1-Gtr2 in *S. cerevisiae* or RagA/B-RagC/D in higher eukaryotes (Gong et al., 2011; Sekiguchi et al., 2001). The Rag GTPase heterodimer is considered as an activator of TORC1 when Gtr1 or RagA/B is GTP-loaded and Gtr2 or RagC/D is GDP-loaded, a state promoted by amino acid availability. Vice versa, when Gtr1 or RagA/B is GDP-loaded and Gtr2 or RagC/D is

GTP-loaded, the dimer inhibits TORC1 (Binda et al., 2009; Demetriades et al., 2014; Gao and Kaiser, 2006; Kim et al., 2008; Kira et al., 2014; Sancak et al., 2008).

The concept of having different signaling functions when asymmetrically loaded is rather unique among GTPases that are normally active or inactive when GTP or GDP-loaded, respectively (Mishra and Lambright, 2016).

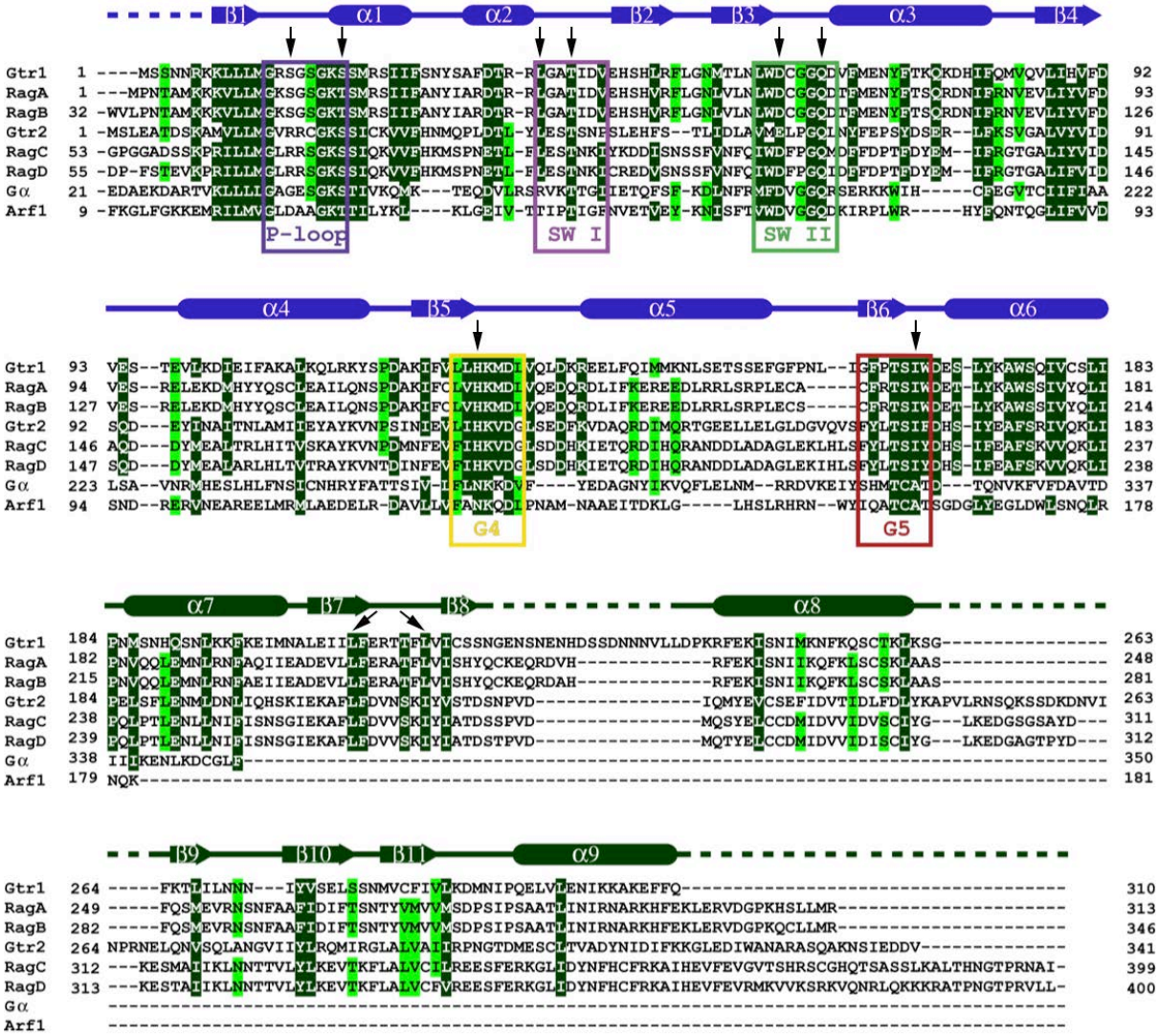

Figure 6 Rag GTPase family alignment. Amino acid sequence alignment of Rag GTPases together with Gα subunit and Arf1 GTPase. Highly conserved residues have been lightened in dark green. Sequence elements typical of GTPases have been enclosed by rectangles and their names have been noted. Secondary structures have been drawn above their corresponding residues and colored in blue or dark green to define the G domain and C terminal domain, respectively. Black arrows indicate important residues described in the text. Figure adapted from (Gong et al., 2011).

In higher eukaryotes, Rags localize at the lysosomal surface independently of amino acid availability, and consequently of their nucleotide loading status (Sancak et al., 2010). In the presence of amino acid stimuli, Rags are in their active conformation and they can recruit mTORC1 to the lysosome via direct binding with its subunit Raptor (Kim et al., 2008; Sancak et al., 2008; 2010). At the lysosomal surface, mTORC1 can interact with the small GTPase Rheb (Sancak et al., 2008). Following amino acid deprivation, RagA/B is switched to its GDP-bound form while RagC/D to its GTP-bound form. Therefore, their interaction with Raptor is weakened (Sancak et al., 2008). The RagA/B^{GDP}-RagC/D^{GTP} heterodimer recruits the TSC complex at the lysosomal membrane (Demetriades et al., 2014).

In budding yeast, Gtr1 and Gtr2 mainly localize at the vacuolar membrane, the yeast equivalent of the lysosome (Sturgill et al., 2008). Both Gtr1 and Gtr2 are essential to have proper activation of TORC1. Differently from higher eukaryotes, TORC1 does not move away from the vacuolar surface upon amino acid deprivation although TORC1 activity and its interaction with Gtr1-Gtr2 are still amino acid regulated (Binda et al., 2009).

3.2.1 Structure

Gtr1 and Gtr2 are part of a complex adopting a pseudo-twofold symmetry (Gong et al., 2011; Jeong et al., 2012). For each subunit two physical domains can be defined: the N-terminal GTPase domain (G domain), which is responsible for binding guanine nucleotides, and the C-terminal domain (CTD). The two GTPases dimerize through their CTDs while the G domains are not involved in the heterodimer formation (Fig.7) (Gong et al., 2011).

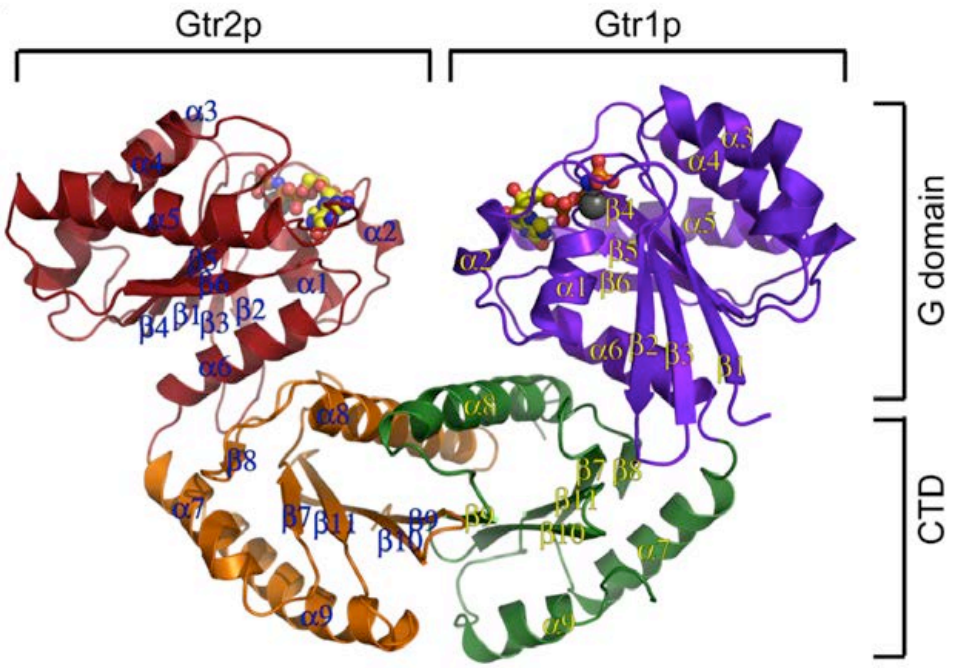

Figure 7 Structure of the Gtr1-Gtr2 heterodimer. Gtr1 and Gtr2 G domains are colored in blue and red, respectively, while CTDs are colored in green and orange, respectively. Gtr1 and Gtr2 are bound to the non-hydrolysable GTP analog GMPPNP (shown using a ball-and-stick representation). The name of each strand and helix has been written on top of the relative feature. Magnesium atoms are represented as black balls. Figure taken from (Gong et al., 2011).

As a result, the dimer interface is distant from the nucleotide-binding pocket defining a new architecture not yet found in any other GTPase structure. Indeed, reported structures for other GTPases that dimerize show a typical involvement of the G domain for the dimerization process (Chappie et al., 2010; Focia et al., 2004; Gao et al., 2010; Low et al., 2009). The CTDs are characterized by a central five-stranded anti-parallel β sheet with 2-1-4-5-3 topology surrounded by one long helix on the G domain side and two helices on the other side (Gong et al., 2011). The heterodimer formation is mediated by hydrogen bonds and hydrophobic interactions, mainly involving the Gtr2 α8 helix that interacts with α8 and four other β strands from Gtr1 (Fig.8). Impressively, the Gtr1 α8 helix is only involved in interactions with α8 helix and two other β strands from Gtr2 (Gong et al., 2011). Leucine 207 (L207) is a highly conserved amino acid across all Rag GTPases, which localizes in the β7 strand. This residue is extremely important for dimerization. Indeed, substitution of this residue in Gtr1 or Gtr2 with a proline is sufficient to abolish dimerization. Gtr1^{L207P} and Gtr2^{L207P} mutations also caused rapamycin and caffeine sensitivity showing how dimerization is necessary for

proper functioning of Gtr1 and Gtr2. The Gtr1-Gtr2 complex is also necessary for interaction with Ego1 and Ego3 (see paragraph 3.2.2.1) (Sekiguchi et al., 2014).

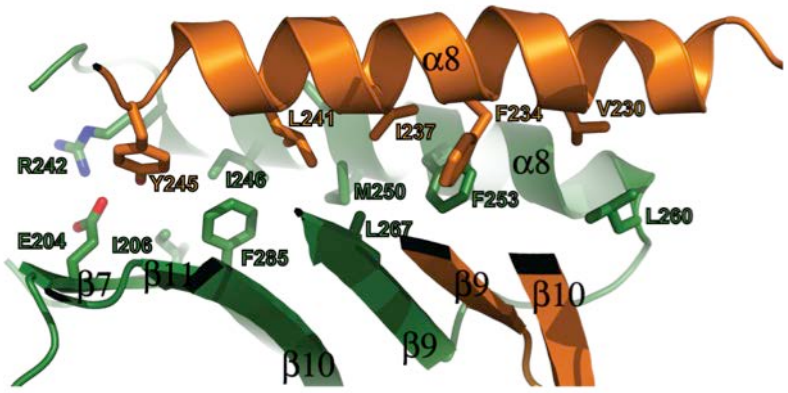

Figure 8 Residues involved in CTDs dimerization. Ribbon representation of Gtr1 and Gtr2 secondary structures, respectively colored in green and orange, involved into the dimer formation. Figure adapted from (Gong et al., 2011).

The CTDs of Gtr1 and Gtr2 are relatively stable and they do not change conformation after GTP hydrolysis of Gtr2. However, they contribute to the stabilization of the G domain after GTP hydrolysis. Indeed, in Gtr2, the Isoleucine 214 (I214) residue from the CTD is placed into a hydrophobic pocket created by the G domain α6 and α1 helices leading to an increase in the interdomain interaction of $Gtr2^{GDP}$ compared to $Gtr2^{GTP}$ (Jeong et al., 2012).

Unlike the CTDs of both proteins, which have really similar structure, the G domains show some structural and functional differences (Gong et al., 2011; Jeong et al., 2012). Similarly to other Ras-related GTPases, $Gtr1^{GTP}$ has a G domain composed of six β strands and six α helices, two switch regions that interact with the GTP γ phosphate via hydrogen bonds, and a Mg^{2+} ion in the nucleotide-binding site (Jeong et al., 2012).

Biochemical experiments have demonstrated that Gtr1 has extremely low intrinsic hydrolysis rate compared to other GTPases like G_{ial} or Ras (Sengottaiyan et al., 2012). Structural analysis can explain the reason of this low intrinsic GTPase activity. Gtr1, like members of the Arf GTPase family, is missing an important tyrosine (Y) in the switch I region that is instead conserved in Ras, Rho, and Ran GTPases (Jeong et al., 2012). It has been proposed that this tyrosine in Ras (Y32) has an important role via its hydroxyl group in stabilizing the transition state from GTP to GDP. The Ras^{Y32F} has a 2-fold decrease in GTP hydrolysis compared to the wild type (Buhrman et al., 2010). Leucine 38 (L38) in Gtr1 is the corresponding residue to Y32 in Ras, and it does not show

interaction with the GTP molecule (Fig.9) (Jeong et al., 2012). Gtr1 has a serine (S15) in the P-loop that can contact via hydrogen bond the GTP γ phosphate (Fig.9) while most of the Ras subfamily members have a glycine as a corresponding residue, which does not interact with the GTP (Jeong et al., 2012).

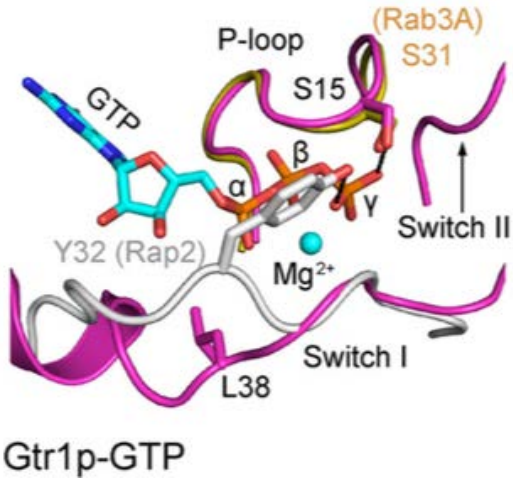

Figure 9 GTP-bound Gtr1 compared to Rap2 and Rab3A GTPases. Superimposed structures of $Gtr1^{GTP}$ (magenta), Rab3A (olive) and Rap2 (gray). Important regions of the three proteins are indicated. Residues implicated in the hydrogen bond formation (dashed lines) with the GTP γ phosphate are represented in sticks and labeled. Figure taken from (Jeong et al., 2012).

S15 is believed to cause a stereochemical constraint against GTP hydrolysis because mutation of the equivalent serine (S31) in Rab3A is sufficient to increase the GTPase activity (Brondyk et al., 1993). Mutation of the corresponding glycine residue to serine in Ras (G12S) weakens the GTPase activity and is oncogenic (Barbacid, 1987). Glutamine 65 (Q65) in the switch II region of Gtr1 has been proposed to be crucial for GTP hydrolysis on the basis of comparison with mutants of Ras subfamily (Nakashima et al., 1999). The corresponding residue in Ras is Q61 that is known to be oncogenic when mutated in any other amino acid residue (except Proline, Glutamate and Glycine) (Barbacid, 1987). Q61 in Ras has a direct catalytic role in correctly placing a water molecule and stabilizing together with Y32 the transition state of the GTP hydrolysis reaction (Buhrman et al., 2010). Mutation of Gtr1 Q65 in leucine is sufficient to hyper-activate TORC1 compared to a wild type Gtr1 (Binda et al., 2009). Furthermore, the $Gtr1^{Q65L}$ mutation protects TORC1 activity from over-production of the Iml1 GAP for Gtr1 (Panchaud et al., 2013). These data would support the hypothesis of a GTP-locked allele for $Gtr1^{Q65L}$ although there is not biochemical evidence confirming it.

Serine 20 (S20) in the P-loop of Gtr1 has been proposed to lock Gtr1 in its GDP-bound state when mutated in leucine based on comparison with the Ran^{T24N} mutant (Nakashima et al., 1999). Growth inhibition and decreased TORC1 activity have been observed during expression of $Gtr1^{S20L}$ (Binda et al., 2009). The serine / threonine residue following the lysine in the P-loop domain is usually highly conserved among all GTPases and is involved via its hydroxyl group in the coordination of the Mg^{2+} ion in any of the two nucleotide-bound states. The corresponding residue in Ras is S17 and when it is mutated in asparagine yields a dominant inhibitory protein resembling the inactive status of the protein (Farnsworth and Feig, 1991). However, it is not correct to define the mutation as "GDP-locked" allele because S17 seems to be critical for both GDP and GTP binding (John et al., 1993). Biochemical experiments have demonstrated that the absence of the Mg^{2+} ion leads to an increase of ~1000 fold in the GDP dissociation rate (Simon et al., 1996). Furthermore, the corresponding mutant $RagA^{T21N}$ shows weak nucleotide binding (Kim et al., 2008). It would be therefore more correct to define Ras^{S17N}, and by analogy $Gtr1^{S20L}$, as "nucleotide-free" mutants.

Gtr2 has been crystalized bound to GMPPNP or to GDP (Gong et al., 2011; Jeong et al., 2012). The P-loop of Gtr2 has an arginine in position 18 (R18) that is conserved with RagC/D but not with Gtr1 or RagA/B. The corresponding residue in Gtr1 would be S15, which is partially responsible for the low intrinsic GTPase activity. The $Gtr2^{GMPPNP}$ structure shows how R18 is close to the GMPPNP γ phosphate and likely involved in stabilizing its transition state (Jeong et al., 2012). A comparable feature can be found in the heterotrimeric GTPase subunit Gα where an arginine in the switch I region similarly stabilizes the transition state (Coleman et al., 1994). The difference in the P-loop between the inhibitory residue S15 of Gtr1 and the R18 of Gtr2 can explain why Gtr1 has almost not detectable GTPase activity while Gtr2 has basal GTPase activity (Jeong et al., 2012). Based on the overall similarity between Gtr2 and RagC/D, it is not surprising that the latter can hydrolyze ~40% of GTP to GDP within 4 hours (Sekiguchi et al., 2001). Glutamine 66 (Q66) and Serine 23 (S23) in Gtr2 are predicted to be important for GTPase activity and GTP binding, respectively. Based on comparison with Ras proteins, $Gtr2^{Q66L}$ and $Gtr2^{S23L}$ mutants were defined as GTP and GDP-locked form, respectively (Gao and Kaiser, 2006). $Gtr2^{Q66L}$ causes decreased TORC1 activity and a defect in recovery from rapamycin treatment (Binda et al., 2009). Sequence alignment of Rag GTPases shows how Gtr2 Q66 and Gtr1 Q65, described above, are both in the

switch II region and likely involved in a similar stabilizing function. Differently from $Gtr1^{Q65L}$, $Gtr2^{S23L}$ has normal TORC1 activity (Binda et al., 2009; Panchaud et al., 2013). $Gtr2^{S23L}$, similarly to the corresponding S20L mutant in Gtr1, would be supposed to be a "nucleotide free" form of the GTPase. Indeed, $Gtr2^{GDP}$ structure shows how S23 is one of the residues involved in interactions with GDP (Jeong et al., 2012). It could be speculated that a constitutive active Gtr1 has a more important role in TORC1 activation compared to a nucleotide free Gtr2. In cell cultures, GTP-locked RagA dominantly activates TORC1 independently from the nucleotide binding status of RagC/D (Kim et al., 2008).

The G domain structure of $Gtr2^{GDP}$ differs from the one of $Gtr1^{GTP}$ because it has five β strands and five α-helices instead of six, and lacks the Mg^{2+} ion in the nucleotide-binding site. However, this is the result of a large conformational transition due to the hydrolysis of GTP (Jeong et al., 2012). The structure of Gtr2 bound to GMPPNP shows indeed six β strands and six α-helices in the G domain, plus the Mg^{2+} ion in the nucleotide-binding pocket (Gong et al., 2011). The absence of the Mg^{2+} ion could explain the low binding affinity for GDP compared to GTP (Jeong et al., 2012). Since GTP loading is favored over GDP, it is possible that Gtr2 does not need a GEF protein to regulate the nucleotide exchange (Sekiguchi et al., 2001).

Most of the differences triggered by GTP to GDP conversion are related to the switch I and II, the βG2 and βG3 strands (Fig.10).

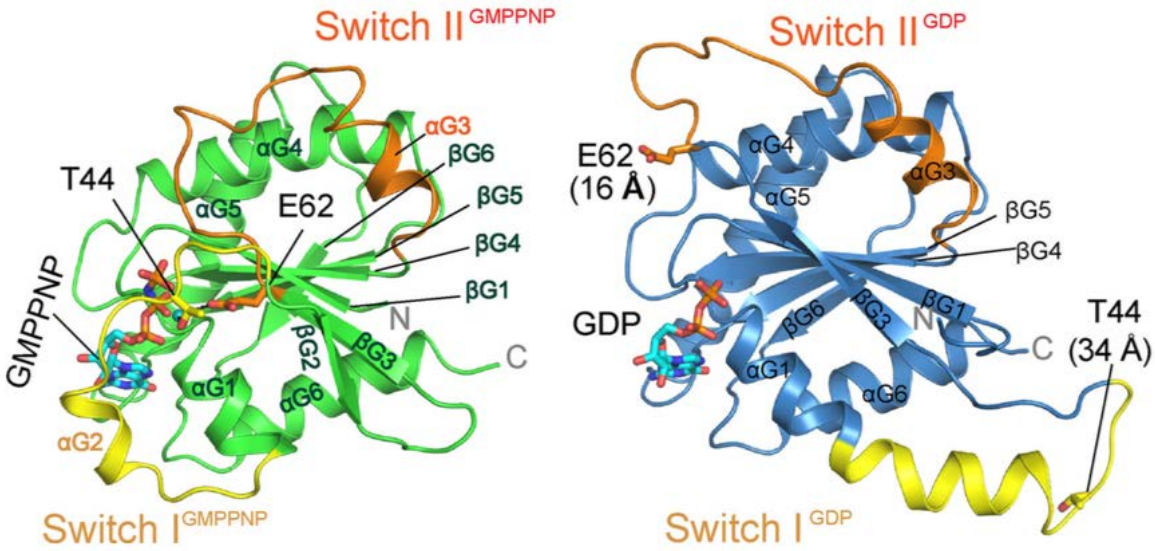

Figure 10 G domain comparison of $Gtr2^{GMPPNP}$ and $Gtr2^{GDP}$. Gtr2 is shown in complex with GMPPNP (left) and GDP (right). Residues coordinating the Mg^{2+} ion in $Gtr2^{GMPPNP}$ are defined, and the number in parentheses indicates the distance moved in the conformational transition. Figure taken from (Jeong et al., 2012).

Upon GTP hydrolysis, the switch I segment is converted in the C-terminal part of the helix αG1 while the βG2 strand leaves the central β-sheet and becomes a loop segment (Jeong et al., 2012). These events lead to the change in number for the β strands and α-helices. The switch I region relocates far from the bound GDP, and the threonine 44 (T44) residue, which was involved in coordination of the Mg^{2+} ion in $Gtr2^{GMPPNP}$, is now 34Å distant from its original position (Jeong et al., 2012). The switch II turns into a more flexible region, and the glutamate 62 (E62) side chain involved in coordination of the Mg^{2+} ion in $Gtr2^{GMPPNP}$ moves of about 16Å in $Gtr2^{GDP}$. The βG3 strand is now redefined and composed of different residues, but the chemical properties of its side chains remain unchanged. The interaction between βG3 and βG1 after GTP to GDP transition are still analogous (Jeong et al., 2012).

During GTP to GDP conversion, the Gtr2 G domain rotates of ~28° relative to its C domain and enters in contact with the Gtr1 G domain, which rotates of ~6° (Fig.11) (Jeong et al., 2012).

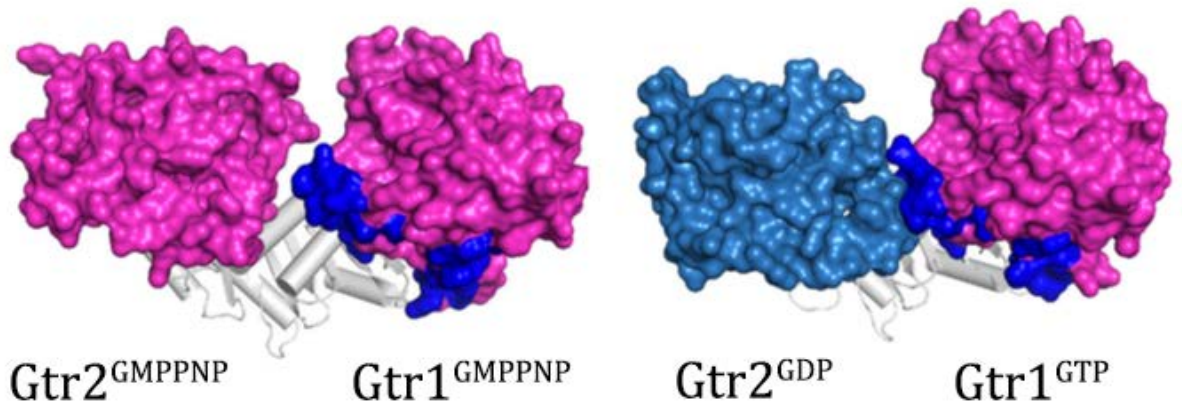

Figure 11 Conformational rotations after transition from $Gtr2^{GMPPNP}$ to $Gtr2^{GDP}$. C domains are colored in light gray and shown as drawings. G domains are refigured in space fill style, and colored in magenta if GTP-bound or in sky blue if GDP-bound. The dark blue area corresponds to the Raptor binding residues of RagA. A rotation of ~28° for Gtr2 and ~6° for Gtr1 can be noticed following transition from GTP to GDP for Gtr2. Figure adapted from (Jeong et al., 2012).

Based on the structural information known for Gtr1 and the high sequence similarity between Gtr1 and RagA, the regions important for interaction between RagA and the Kog1 ortholog Raptor have been mapped (Gong et al., 2011). The corresponding areas in Gtr1 are those close to $Gtr2^{GDP}$ that would form a continuous surface with it and likely involved in protein-protein interactions (Fig.11) (Jeong et al., 2012). In mammals, both RagB and RagC contribute to the binding of Raptor with the latter having a pivotal role

depending on its nucleotide binding status (Sancak et al., 2008; Tsun et al., 2013). In yeast, Gtr1 can interact with the TORC1 subunits Kog1 and Tco89 preferentially when bound to GTP (Binda et al., 2009). The interaction involves the 3rd and 4th HEAT repeats of Kog1 and the C-terminal half of Tco89. Gtr2 can interact as well with Kog1 but is a weak binding partner for Tco89. In vitro pull-down experiments have shown that Kog1 has more affinity for Gtr2 than Gtr1 (Sekiguchi et al., 2014). E62 is a key residue for Gtr2 - Kog1 binding since mutation in lysine (E62K) almost abolished the interaction (Kira et al., 2014). Intriguingly, E62 is also involved in Mg^{2+} binding in $Gtr2^{GTP}$ and is relocated away from the nucleotide binding site in $Gtr2^{GDP}$ (Jeong et al., 2012).

The following table recapitulates the important residues for Gtr1 and Gtr2 described in the text (Tab.2).

Protein	Residue	Function	Mutation	Source
Gtr1	S15	Impairs intrinsic GTP hydrolysis	N.D.	(Jeong et al., 2012)
Gtr1	S20	Mg^{2+} coordination	S20L	(Nakashima et al., 1999)
Gtr1	L38	N.D.	N.D.	(Jeong et al., 2012)
Gtr1	Q65	Stabilizes the transition state	Q65L	(Nakashima et al., 1999)
Gtr1	L207	Dimerization	L207P	(Sekiguchi et al., 2014)
Gtr2	R18	Stabilizes the transition state	N.D.	(Jeong et al., 2012)
Gtr2	S23	Mg^{2+} coordination	S23L	(Gao and Kaiser, 2006)
Gtr2	T44	Mg^{2+} coordination	N.D.	(Jeong et al., 2012)
Gtr2	E62	Mg^{2+} coordination	E62K	(Jeong et al., 2012; Kira et al., 2014)
Gtr2	Q66	Stabilizes the transition state	Q66 L	(Gao and Kaiser, 2006)
Gtr2	L207	Dimerization	L207P	(Sekiguchi et al., 2014)
Gtr2	I214	G domain stabilization		(Jeong et al., 2012)

Table 2 Summary of the important Gtr1 and Gtr2 residues described in the thesis.

3.2.2 Regulators of Rag GTPases

Rag GTPases are key to regulate TORC1 depending on amino acid availability. However, propagation of a finely tuned signal requires the involvement of many players. Several studies have explained some of the mechanisms by which Rag GTPases sense availability of a specific amino acid. The following paragraph will describe the best-known Rag GTPase regulators in budding yeast and mammals.

3.2.2.1 The Ego1–Ego2–Ego3 ternary complex (EGO-TC)

In *S. cerevisiae*, the Gtr1-Gtr2 heterodimer is recruited to the vacuole via the Ego1-Ego2-Ego3 ternary complex (EGO-TC) (Fig.12) (Binda et al., 2009; Dubouloz et al., 2005; Gao and Kaiser, 2006; Powis et al., 2015). The EGO-TC together with Gtr1 and Gtr2 define the Exit from rapamycin-induced GrOwth arrest (EGO) complex. The name originates from the observation that mutants missing any of the complex subunits cannot recover after rapamycin treatment (Dubouloz et al., 2005). In higher eukaryotes, a complex called Ragulator has similar functions to the EGO-TC (Sancak et al., 2010). Ragulator is a pentameric complex composed of: LAMTOR1/p18, LAMTOR2/ p14, LAMTOR3/MP1, LAMTOR4/C7orf59 and LAMTOR5/HBXIP (Bar-Peled et al., 2012). The sequence similarity between Ragulator and EGO-TC subunits is low but they can be considered structurally equivalent. The roadblock domain organization of LAMTOR4 and LAMTOR5 consists of a β-sheet flanked by one α-helix on one side that is similar to Ego2. In comparison, LAMTOR2 and LAMTOR3 have one additional α-helix on the upper side, which is a fold reminiscent of the one of Ego3 (Powis et al., 2015). LAMTOR1 is tethered to the lysosomal surface via N-terminal palmitoylation and myristoylation and functions as a scaffold for the other subunits (Bar-Peled et al., 2012; Nada et al., 2009). Similarly to LAMTOR1, Ego1 is tethered to the vacuolar membrane because of its N-terminal myristoylation and palmitoylation (Ashrafi et al., 1998; Roth et al., 2006). The EGO-TC is considered as a platform that recruits the Gtr1-Gtr2 heterodimer at vacuolar membrane (Powis et al., 2015). Ragulator is functionally similar to the EGO-TC. Indeed, it is required for the recruitment of Rag GTPases to the lysosomal surface (Sancak et al., 2010). However, Ragulator also functions as a GEF for RagA/B sensing the amino acid stimuli thanks to the conserved vacuolar H^+-ATPase (v-ATPase) that also localizes at the lysosomal surface. During amino acid deprivation, the v-ATPase, Ragulator and Rags form a complex that does not recruit and activate mTORC1. Amino acid re-feeding increases the lysosomal amino acidic pool, generating a v-ATPase-dependent activating signal that will stimulate the Ragulator GEF activity toward RagA/B (Bar-Peled et al., 2012). The EGO-TC only serves as scaffold for Gtr1-Gtr2 heterodimer. As a matter of fact, artificial tethering of Gtr1 and Gtr2 at the vacuole is sufficient to have normal

TORC1 activity in the absence of the EGO-TC (Powis et al., 2015). The following table recapitulates the Ragulator subunits and the equivalent proteins in the EGO-TC (Tab.3).

Ragulator	EGO-TC
LAMTOR1	Ego1
LAMTOR2 LAMTOR3	Ego3
LAMTOR4 LAMTOR5	Ego2

Table 3 Summary of the Ragulator subunits and their respective functional homologs in the *S. cerevisiae* EGO-TC.

3.2.2.2 Vam6

Vam6 is a component of the HOmotypic fusion and vacuole Protein Sorting (HOPS/Class C-vps) complex, which is involved in vesicle fusion (Nakamura et al., 1997; Ostrowicz et al., 2008). The HOPS complex, together with the CORVET complex, is required for proper TORC1 signaling (Kingsbury et al., 2014; Zurita-Martinez et al., 2007). In higher eukaryotes, Ragulator functions as a GEF for RagA/B in response to amino acid stimulation (Bar-Peled et al., 2012). Conversely, in *S. cerevisiae* Vam6 is a GEF for Gtr1. Vam6 is necessary for proper TORC1 signaling, it localizes at the vacuole, interacts with Grt1 and stimulates guanine nucleotide release from Gtr1 *in vitro* (Binda et al., 2009) (Fig.12). Additional data in *S. pombe* indicated that Vam6 activates Gtr1 and is essential for TORC1 activation (Valbuena et al., 2012). In higher eukaryotes, two Vam6 homologs were initially found in hVps39–1 (or hVam6) and hVps39–2 (Caplan et al., 2001; Felici et al., 2003; Messler et al., 2011). However, Vps39-2 was later characterized as the homolog of the yeast Vam3 protein, a specific subunit of the CORVET complex (Lachmann et al., 2014). Knockdown of hVps39-1 blocks early/late endosome conversion and reduces mTORC1 activity. However, hVps39-1 does not function as a GEF for RagA/B, since it does not stimulate GDP or GTP dissociation from RagB *in vitro* and does not bind to RagA *in vivo* (Bar-Peled et al., 2012).

3.2.2.3 SEACAT, SEACIT and GATOR complexes

The octameric vacuolar Seh1-associated complex (SEAC) is a protein complex with structural characteristics similar to the membrane coating complexes and, in particular, HOPS and CORVET complexes. SEAC can be divided in two sub complexes. SEACIT (for SEAC inhibiting TORC1) is composed of Iml1, Npr2 and Npr3. SEACIT localizes at the vacuolar membrane and negatively regulates TORC1 during leucine starvation by functioning as a GAP for Gtr1, and thereby increasing its GDP-bound fraction (Fig.12). SEACAT (for SEAC activating TORC1) is a positive regulator of TORC1 composed of Seh1, Sec13, Sea2, Sea3, and Sea4. It is not clear the mechanism by which SEACAT regulates TORC1 but it is thought to interfere with the SEACIT inhibitory function (Fig.12) (Panchaud et al., 2013). SEACAT and SEACIT members are conserved in higher eukaryotes and are part of the two functionally similar complexes GATOR1 and GATOR2, respectively. GATOR1 is made up of DEPDC5, NPRL2 and NPRL3. Like SEACIT, GATOR1 localizes at the lysosomal surface and functions as a GAP for RagA/B, thereby inactivating mTORC1 during amino acid starvation. GATOR2 contains Seh1L, Sec13, Wdr24, Wdr59 and Mios. Similarly to SEACAT, GATOR2 positively regulates mTORC1, likely by repressing GATOR1 (Bar-Peled et al., 2013).

A group of proteins called Sestrins (Sestrins 1–3) was recently involved in mTORC1 regulation (Chantranupong et al., 2014; Kim et al., 2015b; Parmigiani et al., 2014; Peng et al., 2014). Sestrins do not seem to have sequence homologs in *S. cerevisiae*. Sestrins were proposed to negatively regulate mTORC1. However, how Sestrins regulate mTORC1 is still under debate. Some reports support the idea that Sestrin2 (and to a lesser extent Sestrins 1 and 3) interacts with GATOR2, and this binding is increased during amino acid deprivation (Chantranupong et al., 2014; Parmigiani et al., 2014). The Sestrin2-GATOR2 interaction is abolished by leucine re-addition (Wolfson et al., 2015). Furthermore, the leucine-bound Sestrin2 crystal structure (holo-structure) revealed a leucine-binding pocket and, in close proximity, a highly conserved GATOR2 binding site (Saxton et al., 2015). Several attempts to obtain the leucine unbound Sestrin2 structure (apo-structure) failed, although the protein purification procedure was performed without addition of leucine (Saxton et al., 2016b). A second group published the Sestrin2 apo-structure and made a comparison with the holo-structure, concluding that

leucine binding does not cause a substantial conformational change in Sestrin2 (Kim et al., 2015a; Lee et al., 2016). However, further characterization of the above mentioned apo-structure revealed the presence of a ligand (presumably leucine) (Saxton et al., 2016b).

Since inactivation of mTORC1 by Sestrins is mediated by GATOR1, a possible model would place Sestrins as upstream regulator of GATOR2.

Another report proposed Sestrins as GDIs for RagA/B. Sestrins have a conserved GDI motif within their amino acid sequence that is necessary and sufficient for mTORC1 inhibition. Furthermore, Sestrins can directly bind RagA/B and prevent GDP dissociation (Peng et al., 2014). In the leucine-bound Sestrin2 structure, the GDI motif is buried into the protein and, in principle, not accessible for protein-protein interactions (Saxton et al., 2015). In support of the GDI model, it could be speculated that the GDI motif is instead accessible when Sestrin2 is not leucine-bound.

Similarly to Sestrins, CASTOR1 is another negative regulator of the mTORC1 pathway. CASTOR1 can homodimerize or heterodimerize with CASTOR2. During amino acid or arginine deprivation CASTOR1 homodimer or CASTOR1-CASTOR2 heterodimer binds to GATOR2, likely inhibiting it. Arginine refeeding causes disruption of the CASTOR1-GATOR2 interaction and downstream mTORC1 activation (Chantranupong et al., 2016). Indeed, arginine binding to CASTOR1 modifies the position and exposure of close residues necessary for GATOR2 interaction (Saxton et al., 2016a). In *S. cerevisiae*, homologs of CASTOR proteins have not been found (Chantranupong et al., 2016).

3.2.2.4 Leucyl-tRNA synthetase

The tRNA charging enzyme Leucyl-tRNA synthetase (LeuRS) is a TORC1 regulator both in budding yeast and mammals. In *S. cerevisiae*, LeuRS (also called Cdc60) specifically interacts via its nonessential amino acid-editing domain with Gtr1 in a leucine-dependent manner, causing downstream TORC1 activation. Thus, LeuRS acts as a leucine sensor and likely favors the GTP-loading state of Gtr1 (Fig.12) (Bonfils et al., 2012). In mammals as well, LeuRS positively regulates mTORC1. Strikingly, LeuRS binds specifically to RagD and increases its GTP hydrolysis *in vitro*. Therefore, mammalian LeuRS has been proposed to function as a GAP for RagD (Han et al., 2012). However, this

topic is still under debate because a second report from a different group could not reproduce the in vitro GAP activity of LeuRS toward RagC/D (Tsun et al., 2013).

3.2.2.5 The FNIP–FLCN complex

RagC/D is required to be in its GDP-loading state to support, together with RagA/B, proper mTORC1 activation (Sancak et al., 2008). In mammals, the FNIP/FLCN complex functions as a GAP for RagC/D. During amino acid starvation, FNIP/FLCN complex is recruited to the lysosome membrane and it binds to the inactive Rag heterodimer. Following amino acid refeeding, the GAP complex stimulates RagC/D GTP hydrolysis (Tsun et al., 2013). In the first chapter of the results section I will describe the identification and characterization of the *S. cerevisiae* orthologs of FNIP1/2 and FLCN, termed Lst4 and Lst7.

3.2.2.6 Additional modulators

More modulators of Rag GTPases and thereby TORC1 pathway are known, but they have been mainly discovered and characterized only in higher eukaryotes (Powis and De Virgilio, 2016). For example, lysosomal membrane-localized transporters such as SLC38A9 and SLC36A1 were implicated in amino acid-dependent activation of TORC1, likely via Rag GTPases (Ögmundsdóttir et al., 2012; Wang et al., 2015). Regarding the TORC1 pathway, it would be interesting to understand if these additional modulators are functionally conserved in *S. cerevisiae*.

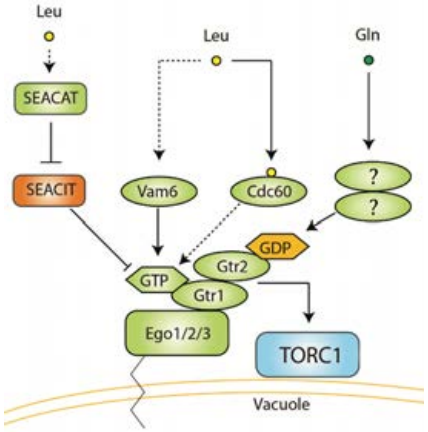

Figure 12 Known regulators for Gtr1 and Gtr2 in budding yeast. Scheme summarizing the above discussed regulators of Rag GTPases in *S. cerevisiae*. Question marks define two new regulators for Gtr2 described in the results chapter number 1. Figure adapted from (Shimobayashi and Hall, 2015).

Aims and Outline

Aim and outline

The general aim of this thesis is to gain more insight into how the Rag GTPases Gtr1 and Gtr2 regulate TORC1 and how they are themselves regulated in response to changing nutrient conditions. Recent studies have demonstrated that Vam6 acts as a GEF and the Iml1-Npr2-Npr3 complex (SEACIT) as a GAP for Gtr1 (Binda et al., 2009; Panchaud et al., 2013). Furthermore, the leucyl-tRNA synthetase (LeuRS) Cdc60 interacts with Gtr1 in a leucine-dependent manner and has a positive impact on TORC1 activation (Bonfils et al., 2012). While regulators for Gtr1 have been identified, possible GEFs, GAPs or GDIs for Gtr2 have remained instead elusive. Thus, the more specific goal of this thesis was to identify new regulators of Gtr2. To achieve this purpose, we have chosen three different approaches.

In the first chapter of this thesis, we present a targeted approach that was based on extensive data in the literature and that allowed me to identify *a bona* fide GAP for Gtr2. Accordingly, this GAP consists of Lst4 and Lst7 that form a heterodimer. Interestingly, the Lst4-Lst7 complex is recruited to and released from the vacuolar membrane following amino acid deprivation and refeeding, respectively. In parallel, this complex interacts well, but transiently, with Gtr2 only when cells were re-fed with amino acids. Thus, these results indicate that the Lst4-Lst7 complex mediates the presence of amino acids to activate TORC1 downstream of Gtr2.

In the second chapter of the thesis, we present a genetic screen that was aimed to identify novel regulators of Gtr1/Gtr2 and/or TORC1. The reasoning of this screen is conceptually based on a brilliant study in mammalian cells where the Rag heterodimer is involved in TSC complex recruitment, Rheb inactivation, and consequent TORC1 downregulation in response to amino acid starvation (Demetriades et al., 2014). In analogy to these observations, we previously found that over-production of a nucleotide-free form of Gtr1 ($Gtr1^{S20L}$) also causes downregulation of TORC1 and impairs growth in budding yeast. This negative effect on TORC1 could theoretically also involve a functional TSC complex homolog that impinges on the budding yeast Rheb ortholog Rhb1, or alternatively involve some hitherto undescribed new regulators of Rag GTPases and/or TORC1. The screening protocol laid out in this chapter therefore

aimed to identify suppressor mutations that alleviated the growth inhibitory phenotype caused by Gtr1^{S20L} over-expression. Most of the mutations isolated in this screen were located in genes whose products were previously known to play a role in the TORC1 signaling network. We present in this chapter an initial analysis of the respective mutants (including the assessment of their TORC1-related phenotypes) and discuss the data in the context of the current literature.

In the third chapter of this thesis, we describe our attempt to investigate the role of the Mrs6 protein as a regulator for Gtr2. The Rab escort protein Mrs6 is necessary for prenylation of the small GTPase Ypt1 and is one of the few proteins in yeast that bears a GDI motif. Mrs6 has been shown to function as a positive regulator of TORC1 activity (Lempiäinen et al., 2009). Additionally, Mrs6 was found to influence two nodes of TORC1 regulation that depend, or not, on the zinc-finger protein Sfp1 (Lempiäinen et al., 2009; Singh and Tyers, 2009). In this chapter, we focus on the Sfp1-independent regulatory role of Mrs6 in the TORC1 pathway. Accordingly, we investigated a potential role of Mrs6 as a GDI for Gtr2. Since Mrs6 positively regulates TORC1, we speculated that it could favor the Gtr2 GDP-bound form. Indeed, Gtr2 is predicted to have low affinity for GDP, supporting a model in which a GDI is needed to keep Gtr2 in its active form. However, we could not demonstrate such a role for Mrs6 in controlling Gtr2. Nevertheless, we found Mrs6 to bind Gtr2 and Gtr2^{Q66L} (GTP-locked), but not Gtr1, in exponentially growing and glucose starved cells, while glucose refeeding weakened the Mrs6-Gtr2 interaction. Our data indicate a functional link between Mrs6 and Rag GTPases that remain to be studied in more detail in the future.

CHAPTER I:

Amino Acids Stimulate TORC1 through Lst4-Lst7, a GTPase-Activating Protein Complex for the Rag Family GTPase Gtr2

Report

Cell Reports

Amino Acids Stimulate TORC1 through Lst4-Lst7, a GTPase-Activating Protein Complex for the Rag Family GTPase Gtr2

Graphical Abstract

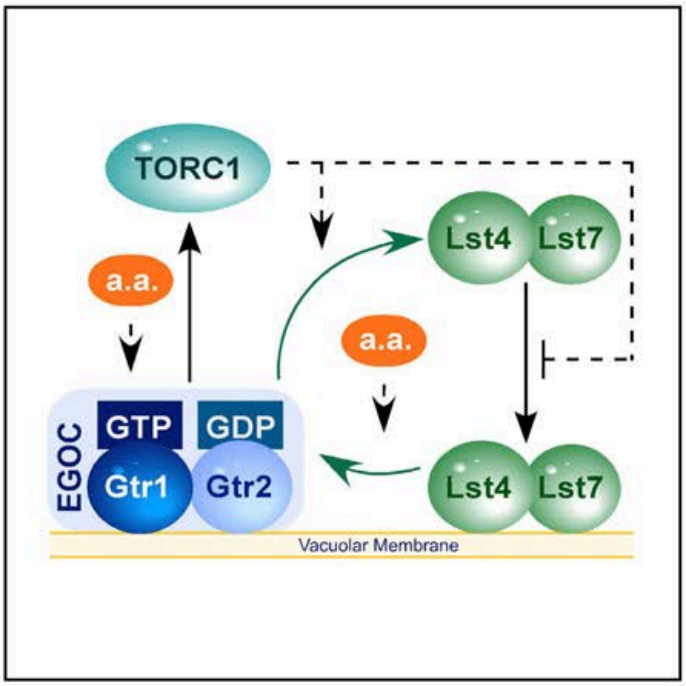

Authors

Marie-Pierre Péli-Gulli, Alessandro Sardu, Nicolas Panchaud, Serena Raucci, Claudio De Virgilio

Correspondence

claudio.devirgilio@unifr.ch

In Brief

Amino acids represent primordial signals that modulate TORC1 and, consequently, eukaryotic cell growth through conserved Rag GTPases. Here, Péli-Gulli et al. show that the Lst4-Lst7 complex in yeast functions as a GAP for the Rag family GTPase Gtr2 to mediate amino-acid-dependent activation of TORC1.

Highlights

- The Lst4-Lst7 complex in yeast is necessary for TORC1 activation by amino acids
- Rag GTPases associate with Lst4-Lst7 in response to amino acid stimulation
- The Lst4-Lst7 complex functions as a GAP for the Rag family GTPase Gtr2
- A TORC1-dependent feedback mechanism attenuates Lst4-Lst7 function

Péli-Gulli et al., 2015, Cell Reports *13*, 1–7
October 6, 2015 ©2015 The Authors
http://dx.doi.org/10.1016/j.celrep.2015.08.059

Please cite this article in press as: Péli-Gulli et al., Amino Acids Stimulate TORC1 through Lst4-Lst7, a GTPase-Activating Protein Complex for the Rag Family GTPase Gtr2, Cell Reports (2015), http://dx.doi.org/10.1016/j.celrep.2015.08.059

Cell Reports
Report

OPEN ACCESS
CellPress

Amino Acids Stimulate TORC1 through Lst4-Lst7, a GTPase-Activating Protein Complex for the Rag Family GTPase Gtr2

Marie-Pierre Péli-Gulli,[1,3] Alessandro Sardu,[1,3] Nicolas Panchaud,[1,2] Serena Raucci,[1] and Claudio De Virgilio[1,*]
[1]Department of Biology, University of Fribourg, 1700 Fribourg, Switzerland
[2]Present address: Novartis Institutes for Biomedical Research, NIBR, Novartis Pharma AG, 4002 Basel, Switzerland
[3]Co-first author
*Correspondence: claudio.devirgilio@unifr.ch
http://dx.doi.org/10.1016/j.celrep.2015.08.059

SUMMARY

Rag GTPases assemble into heterodimeric complexes consisting of RagA or RagB and RagC or RagD in higher eukaryotes, or Gtr1 and Gtr2 in yeast, to relay amino acid signals toward the growth-regulating target of rapamycin complex 1 (TORC1). The TORC1-stimulating state of Rag GTPase heterodimers, containing GTP- and GDP-loaded RagA/B/Gtr1 and RagC/D/Gtr2, respectively, is maintained in part by the FNIP-Folliculin RagC/D GAP complex in mammalian cells. Here, we report the existence of a similar Lst4-Lst7 complex in yeast that functions as a GAP for Gtr2 and that clusters at the vacuolar membrane in amino acid-starved cells. Refeeding of amino acids, such as glutamine, stimulated the Lst4-Lst7 complex to transiently bind and act on Gtr2, thereby entailing TORC1 activation and Lst4-Lst7 dispersal from the vacuolar membrane. Given the remarkable functional conservation of the RagC/D/Gtr2 GAP complexes, our findings could be relevant for understanding the glutamine addiction of mTORC1-dependent cancers.

INTRODUCTION

The target of rapamycin complex 1 (TORC1) plays a pivotal role in the control of eukaryotic cell growth by adjusting anabolic and catabolic processes to the nutritional status of organisms and of individual cells (Albert and Hall, 2015; Laplante and Sabatini, 2012). Amino acids represent primordial signals that modulate TORC1 activity through the conserved Rag family of GTPases (Jewell et al., 2013; Sancak and Sabatini, 2009), which assemble into heterodimeric complexes consisting of RagA or RagB and RagC or RagD in higher eukaryotes, or Gtr1 and Gtr2 in yeast (Binda et al., 2009; Kim et al., 2008; Sancak et al., 2008). The functionally active TORC1-stimulating state of these heterodimers contains guanosine 5′-triphosphate (GTP)-loaded RagA/B/Gtr1 and GDP-loaded RagC/D/Gtr2 and is maintained by an intricate interplay between distinct guanine nucleotide exchange factor (GEF) and GTPase-activating (GAP) protein complexes. In mammalian cells, these include (1) the pentameric Ragulator complex that tethers Rag heterodimers to the lysosomal membrane and acts as RagA/B GEF (Bar-Peled et al., 2012), (2) the heterotrimeric GATOR1 complex with RagA/B GAP activity (Bar-Peled et al., 2013), and (3) the heterodimeric FNIP-Folliculin complex that functions as RagC/D GAP (Petit et al., 2013; Tsun et al., 2013). The amino-acid-sensitive events upstream of these Rag GTPase regulators are currently poorly understood, but likely involve both lysosomal amino acid sensors, such as the v-ATPase and lysosomal amino acid transporter(s) (Rebsamen et al., 2015; Wang et al., 2015; Zoncu et al., 2011), and cytoplasmic amino acid sensors, such as the leucyl-tRNA synthetase (LeuRS) (Bonfils et al., 2012; Han et al., 2012).

Some of the regulatory mechanisms impinging on Rag GTPases have been remarkably conserved throughout evolution. Accordingly, yeast cells express a protein complex, coined the EGO complex (EGOC), that is structurally related to the Ragulator complex and that tethers Gtr1-Gtr2 to the vacuolar/lysosomal membrane, although it remains unknown whether it also exhibits Gtr1 GEF activity (Binda et al., 2009; Panchaud et al., 2013a, 2013b; Zhang et al., 2012b). In addition, the Gtr1 GAP complex termed SEACIT is functionally equivalent to GATOR1 and both GAP complexes are presumably inhibited in a similar manner by the yeast SEACAT and mammalian GATOR2 orthologous multi-subunit complexes (Bar-Peled et al., 2013; Panchaud et al., 2013a, 2013b). A Gtr2 GAP, however, has hitherto remained elusive.

Here, we report on our discovery that the heterodimeric Lst4-Lst7 complex in yeast functions as a GAP for Gtr2 to activate TORC1 following amino acid stimulation of cells. Like the functionally orthologous mammalian complex containing FNIP and Folliculin (Petit et al., 2013; Tsun et al., 2013), the Lst4-Lst7 complex is recruited to and released from the vacuolar surface upon amino acid starvation and refeeding, respectively. Our study suggests a model in which amino acids promote the Lst4-Lst7 complex to associate with and stimulate the GAP activity of the vacuolar membrane-resident fraction of Gtr2 in amino acid-starved cells, thereby triggering the activation of TORC1 and the release of Lst4-Lst7 from the vacuolar membrane.

OPEN ACCESS
CellPress

Please cite this article in press as: Péli-Gulli et al., Amino Acids Stimulate TORC1 through Lst4-Lst7, a GTPase-Activating Protein Complex for the Rag Family GTPase Gtr2, Cell Reports (2015), http://dx.doi.org/10.1016/j.celrep.2015.08.059

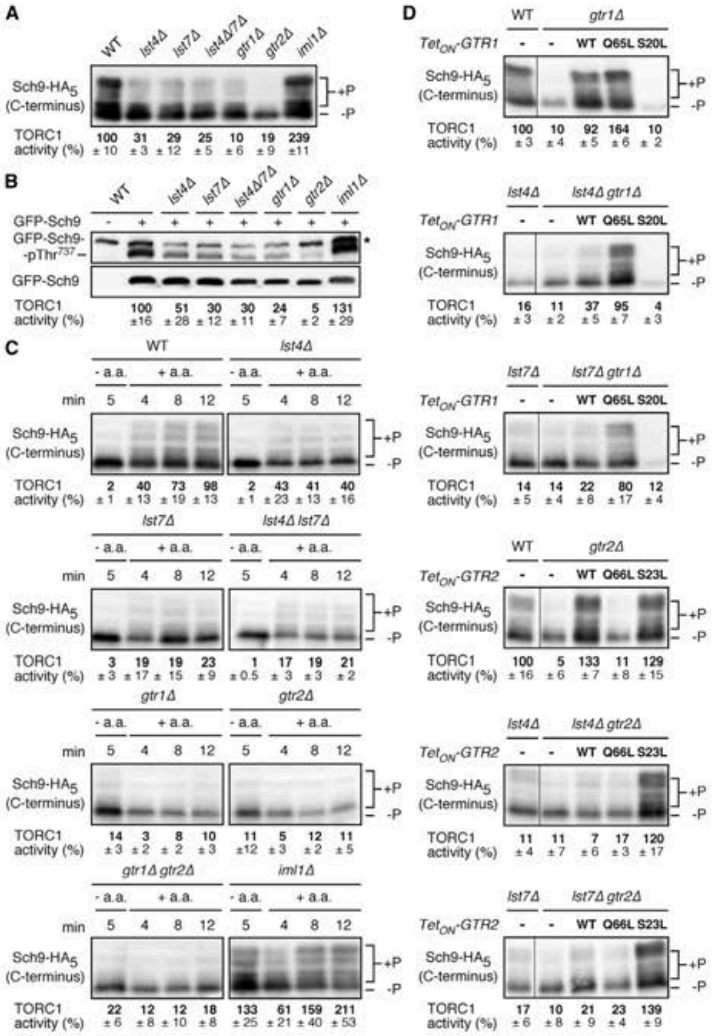

Figure 1. Lst4 and Lst7 Regulate Amino Acid Signaling to TORC1 through Gtr2

(A and B) Loss of Lst4 and/or Lst7 causes a decrease in TORC1 activity. In (A), indicated strains expressing Sch9^{T570A}-HA$_5$ were grown exponentially in synthetic dropout (SD) medium. A representative anti-HA immunoblot of NTCB-treated extracts is shown. The respective TORC1 activities were assessed as the ratio of hyperphosphorylated (+P)/hypophosphorylated (−P) Sch9 C terminus and normalized to that of wild-type (WT) cells (set to 100%). In (B), similar results for TORC1 activities were obtained by using specific antibodies recognizing the phosphorylated Thr^{737} (pThr^{737}) of Sch9, a key target of TORC1 in yeast (Urban et al., 2007). Indicated strains expressing (+) or not (−) GFP-Sch9 were grown as in (A). Representative anti-pThr^{737} and anti-GFP immunoblots are shown together with respective TORC1 activities calculated as the ratio of pThr^{737} GFP-Sch9/total GFP-Sch9 and normalized to the TORC1 activity in exponentially growing WT cells (set to 100%). *, cross-reacting band. See also Figure S1 for further phenotypes associated with loss of Lst4 and/or Lst7.

(C) Loss of Lst4 and/or Lst7 renders TORC1 less responsive to amino acid stimulation. Strains (genotypes indicated) were grown to exponential phase in a synthetic complete medium devoid of ammonium sulfate, but containing a mixture of all amino acids as nitrogen source (SC w/o AS). TORC1 activities (normalized to the one in exponentially growing WT cells; set to 100%) were monitored as in (A) following starvation (− aa; 5 min) and readdition (+ aa; times indicated) of amino acids.

(D) Overproduction of signaling competent Gtr2^{S23L} fully rescues the TORC1 activity defects caused by loss of Lst4 or Lst7. Gtr1 or Gtr2 variants were overexpressed under the control of the *Tet$_{ON}$* promoter in the indicated mutants grown exponentially in SD medium. TORC1 activities were assayed as in (A) and normalized to the TORC1 activity in exponentially growing WT cells (set to 100%). Numbers in (A)–(D) are means ± SD from three independent experiments.

RESULTS AND DISCUSSION

Lst4 and Lst7 Are Necessary for TORC1 Activation via the Rag GTPase Gtr2

Recent studies employing highly sensitive methods for structural homology detection (e.g., HHpred) identified *Saccharomyces cerevisiae* Lst4 and Lst7 as potential orthologs of FNIP and Folliculin, respectively (Levine et al., 2013; Zhang et al., 2012a). Lst4 and Lst7 have been originally identified in a genetic screen designed to identify mutations, which exhibit synthetic lethality when combined with *sec13-1* (Roberg et al., 1997). Surprisingly, in addition to being part of both the nuclear pore complex and the outer shell of coatmer complex II coated vesicles (Hoelz et al., 2011), Sec13 is also a component of the SEACAT complex that is required for normal TORC1 activity (Panchaud et al., 2013a). Together with the observation that the presumed Lst7/Folliculin ortholog in *Schizosaccharomyces pombe* (i.e., BHD) reportedly stimulates TORC1 by unknown means (van Slegtenhorst et al., 2007), the current literature therefore suggests that Lst4 and Lst7 may, like FNIP and Folliculin, control TORC1 function via Rag GTPases. In support of this assumption, we found that loss of Lst4 or of Lst7, like loss of Gtr1 or of Gtr2, resulted in decreased TORC1 activity (Figures 1A and 1B). The

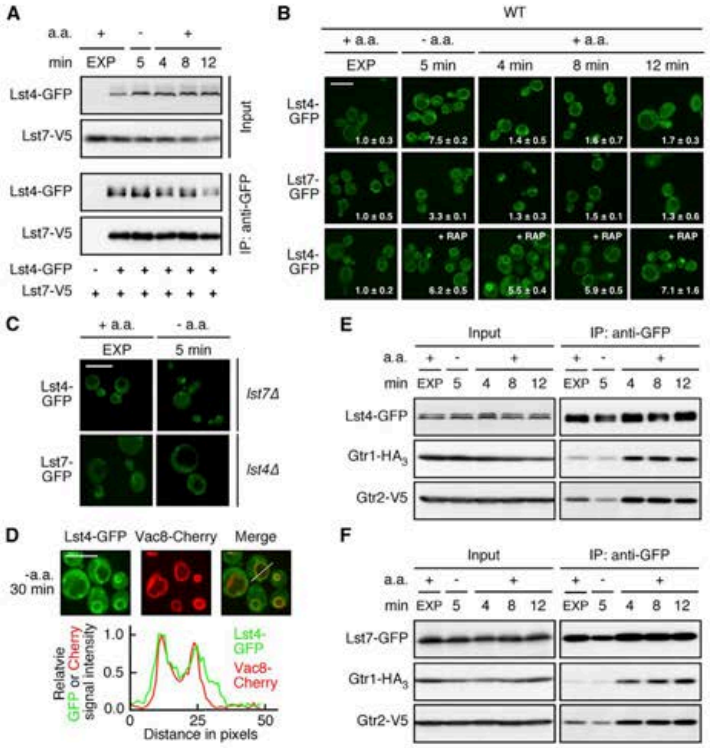

Figure 2. Lst4 and Lst7 Form a Complex that Assembles at the Vacuolar Membrane upon Amino Acid Starvation and Interacts with Rag GTPases in Response to Amino Acid Refeeding

(A) Lst4 stably binds Lst7 in the presence (aa: +) or absence (aa: −) of amino acids. Lst7-V5 cells co-expressing (+) or not (−) Lst4-GFP were grown as in Figure 1C. Lysates (input) and anti-GFP immunoprecipitates (IP: anti-GFP) were analyzed by immunoblotting with anti-GFP and anti-V5 antibodies.

(B) Amino acid starvation and readdition promote Lst4 and Lst7 recruitment to and redistribution from the vacuolar membrane, respectively. Representative pictures of GFP-tagged Lst4- or Lst7-expressing cells, cultured as in Figure 1C, are shown. Rapamycin (+ RAP) was also added to Lst4-GFP-expressing cells at the beginning of the amino acid starvation and maintained throughout the amino acid restimulation period. Numbers represent fold increases in the vacuolar membrane GFP signal intensity, normalized to respective signal in exponentially growing (EXP) cells (set to 1.0). Data are means ± SD from three independent experiments. Scale bar for all panels (white; top left), 5 μm.

(C) Lst4-GFP and Lst7-GFP depend on each other for their recruitment to the vacuolar membrane in both exponentially growing (+ aa; EXP) and amino-acid-starved (− aa; 5 min) cells. Scale bar for all panels (white; top left), 5 μm.

(D) Lst4-GFP colocalizes with the vacuolar membrane resident Vac8-Cherry. The lower graph shows the combined fluorescence intensity profiles of Lst4-GFP and Vac8-Cherry that were measured in an amino-acid-starved (30 min) cell along the defined line in the merged panel. Scale bar (white; first panel), 5 μm.

(E and F) Amino acids stimulate the interaction between Lst4-Lst7 and Gtr1-Gtr2 in amino-acid-starved cells. Lst4-GFP (E) or Lst7-GFP (F) were IPed in extracts from cells that co-expressed Gtr1-HA_3 and Gtr2-V5 and that were grown as in Figure 1C. Cell lysates (input) and anti-GFP immunoprecipitates (IP: anti-GFP) were analyzed by immunoblotting using anti-GFP, anti-HA, and anti-V5 antibodies.

See also Figure S2.

concomitant loss of Lst4 and Lst7 decreased TORC1 activity (and caused rapamycin sensitivity and a mild defect in recovery from rapamycin treatment) to a similar extent to the individual loss of Lst4 or Lst7 (Figures 1A, 1B, and S1), indicating that Lst4 and Lst7 may share a common biological function in TORC1 stimulation. Next, we studied the effect of amino acid readdition to wild-type, *lst4Δ*, *lst7Δ*, *lst4Δ lst7Δ*, *gtr1Δ*, *gtr2Δ*, *gtr1Δ gtr2Δ*, and *iml1Δ* cells that had been subjected to amino acid starvation (for 5 min), following which all strains exhibited very low TORC1 activity (except the *iml1Δ* control strain that is defective in SEACIT/Gtr1 GAP activity; Panchaud et al., 2013b). Readdition of amino acids strongly elicited TORC1 activity in wild-type cells within 4–12 min, while this effect was significantly reduced in the absence of Lst4 and/or Lst7 and virtually undetectable in the absence of Gtr1 and/or Gtr2 (Figure 1C). Thus, Lst4 and Lst7 are important for proper amino acid stimulation of TORC1, possibly through regulation of the Gtr1-Gtr2 heterodimer. Consistent with this idea, the reduced TORC1 activity in exponentially growing *lst4Δ* and *lst7Δ* cells could be suppressed by expression of either the GTP-locked $Gtr1^{Q65L}$ or the $Gtr2^{S23L}$ variant (which has low affinity for nucleotides; Figure 1D). Since TORC1 activity remained to some extent sensitive to the loss of Lst4 or Lst7 in the presence of the $Gtr1^{Q65L}$, but not in the presence of the $Gtr2^{S23L}$ form, our genetic data suggested that Lst4 and Lst7 specifically act upstream of Gtr2.

Lst4 and Lst7 Form a Complex that Interacts with Rag GTPases in Response to Amino Acid Stimulation of Cells

Our genetic epistasis analyses led us to examine next whether Lst4 interacted with Lst7 in cells using co-immunoprecipitation (coIP) assays. Lst4 specifically and stably bound Lst7 in exponentially growing cells, as well as in cells that were starved for and subsequently restimulated with amino acids (Figure 2A). Our analyses of functional GFP-fused Lst4 and Lst7 further indicated that both proteins were mainly present in the cytoplasm in exponentially growing cells with minor fractions being localized to the vacuolar membrane (Figure 2B), where EGOC and TORC1 primarily reside in yeast (Binda et al., 2009; Sturgill

OPEN ACCESS CellPress

Please cite this article in press as: Péli-Gulli et al., Amino Acids Stimulate TORC1 through Lst4-Lst7, a GTPase-Activating Protein Complex for the Rag Family GTPase Gtr2, Cell Reports (2015), http://dx.doi.org/10.1016/j.celrep.2015.08.059

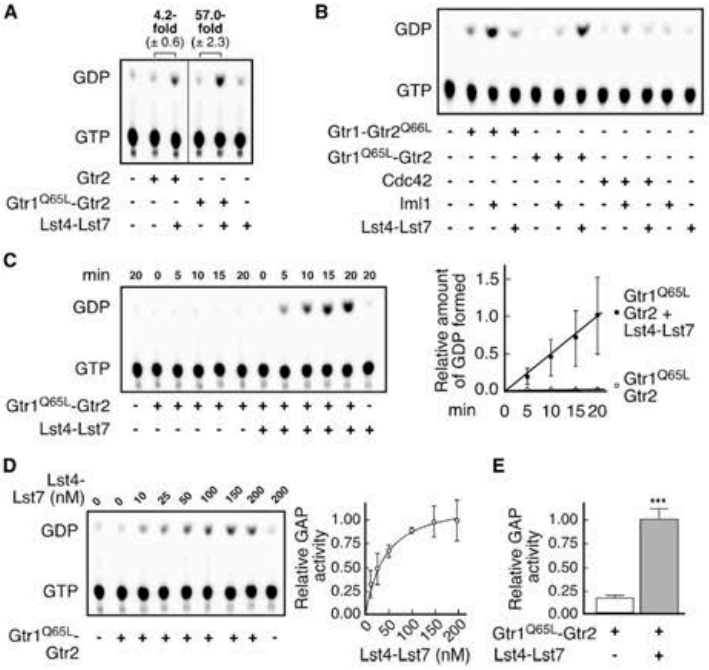

Figure 3. The Lst4-Lst7 Complex Functions as a GAP for Gtr2

(A) The Lst4-Lst7 complex stimulates the GTP hydrolysis activity by Gtr2 particularly within the Gtr1^{Q65L}-Gtr2 heterodimer. Purified Gtr2 and Gtr1^{Q65L}-Gtr2 were pre-loaded with [α-^{32}P] GTP. Following a 20-min incubation in the absence (–) or presence (+) of purified Lst4-Lst7, the extent of [α-^{32}P] GTP hydrolysis to [α-^{32}P] GDP was examined. One representative thin-layer chromatography (TLC) autoradiograph is shown. Numbers represent fold increases ± SD from three independent experiments. GTP was incubated either alone (first lane) or with the Lst4-Lst7 complex solely (last lane) in control experiments.

(B) The GAP activities of the Lst4-Lst7 complex and of Iml1 are specific for Gtr2 and Gtr1, respectively. GAP specificity was determined by comparing the GAP activities of the Lst4-Lst7 complex and of Iml1 toward Gtr1^{Q65L}-Gtr2 (with Gtr1 in its GTP-locked state), Gtr1-Gtr2^{Q66L} (with Gtr2 in its GTP-locked state), and the unrelated Rho GTPase Cdc42. Control experiments were as in (A).

(C and D) The Lst4-Lst7 complex stimulates GTP hydrolysis by Gtr1^{Q65L}-Gtr2 in a time- (C) and concentration- (D) dependent manner. GAP assays were performed as in (A) with indicated reaction times (C) or increasing concentrations of Lst4-Lst7 (D). Representative TLC autoradiographs and quantifications (± SD from three independent experiments) are shown.

(E) Single-turnover GAP assays on Gtr1^{Q65L}-Gtr2 in the absence (–) or presence (+) of Lst4-Lst7. Data are means ± SD from three independent experiments. ***$p < 0.003$, compared to the control assay without Lst4-Lst7 using an unpaired Student's t test.

et al., 2008). Provided that each of the two proteins was present, amino acid starvation rapidly provoked an enrichment of Lst4-GFP and Lst7-GFP at the vacuolar membrane, which was promptly reversed upon readdition of amino acids (Figures 2B–2D). Together with our genetic and biochemical data, these cell biological analyses suggested that Lst4 and Lst7 assemble into a complex that mediates amino acid regulation of TORC1 via Gtr2, within the Gtr1-Gtr2 module. In support of this notion, Gtr2 and Gtr1 colPed with Lst4-GFP and Lst7-GFP in exponentially growing cells (Figures 2E and 2F). Moreover, amino acid starvation (for 5 min and up to 50 min) slightly weakened the interactions between Gtr1-Gtr2 and Lst4 or Lst7, while subsequent stimulation of starved cells with amino acids substantially strengthened the respective interactions (Figures 2E, 2F, and S2). Thus, amino acid starvation triggers the recruitment of the Lst4-Lst7 complex to the vacuolar membrane, where it is adjacent to, but not directly associated with Gtr1-Gtr2, while subsequent stimulation of cells with amino acids promotes the interaction between the Lst4-Lst7 complex and Gtr1-Gtr2, as well as the release of Lst4-Lst7 from the vacuolar membrane.

The Lst4-Lst7 Complex Is a GAP for Gtr2

Combined, our data suggested that the Lst4-Lst7 complex activates TORC1 following amino acid stimulation of cells indirectly, possibly by functioning as a GAP for Gtr2. To verify this assumption, we performed in vitro GAP assays with purified Lst4-Lst7 and Gtr2 alone or within a heterodimer containing GTP-locked Gtr1^{Q65L} (Binda et al., 2009). Lst4-Lst7 stimulated the rate of GTP hydrolysis by monomeric Gtr2 and heterodimeric Gtr1^{Q65L}-Gtr2 by factors of 4.2 and 57.0, respectively (Figure 3A). A control experiment with purified Lst4-Lst7 and free GTP showed minimal GTP hydrolysis, excluding the possibility that the observed GTP hydrolysis was due to contaminating phosphatases (Figure 3A). In addition, unlike the Gtr1 GAP Iml1 (Panchaud et al., 2013b), Lst4-Lst7 did not noticeably stimulate the rate of GTP hydrolysis by Gtr1 (within a Gtr1-Gtr2^{Q66L} complex containing the GTP-locked form of Gtr2) (Figure 3B). Conversely, Iml1, unlike Lst4-Lst7, only marginally affected the rate of GTP hydrolysis by Gtr2 (within the Gtr1^{Q65L}-Gtr2 complex), and both Iml1 and Lst4-Lst7 had little impact on the rate of GTP hydrolysis by the unrelated Rho GTPase Cdc42 (Figure 3B). Finally, in addition to stimulating the GTP hydrolysis by Gtr2 in a time- and dose-dependent manner in steady-state GAP assays (Figures 3C and 3D), Lst4-Lst7 also significantly accelerated the catalytic rate of Gtr2-mediated GTP hydrolysis in single-turnover GAP assays (Figure 3E). The Lst4-Lst7 complex therefore functions as a bona fide GAP for Gtr2, specifically within the context of the Gtr1-Gtr2 heterodimer.

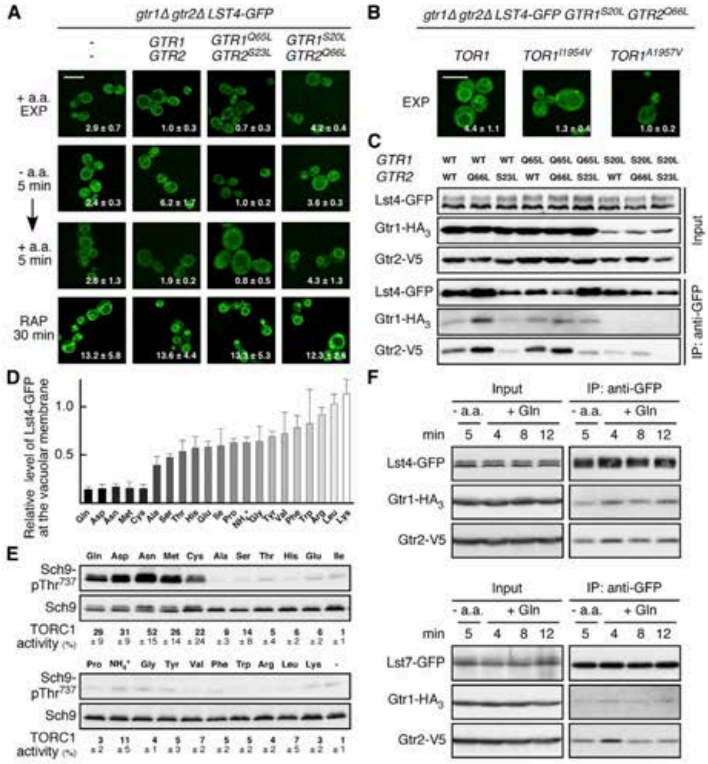

Figure 4. Amino Acids Act Upstream of the Lst4-Lst7 Complex

(A and B) Enrichment of Lst4-GFP at the vacuolar membrane does not depend on Rag GTPases and is antagonized by TORC1. The *gtr1Δ gtr2Δ LST4-GFP* strain carrying either empty plasmids (−/−) or the indicated combinations of plasmid-encoded alleles of *GTR1* and *GTR2* in the absence (A) or presence of a copy of the indicated *TOR1* alleles (B) were analyzed by fluorescence microscopy during exponential growth (+ aa; EXP), following amino acid starvation (− aa; 5 min) and subsequent amino acid replenishment (+ aa; 5 min) and following rapamycin treatment (+ RAP; 30 min). Numbers represent fold increases in the vacuolar membrane GFP-signal intensity, normalized to respective signal (set to 1.0) in control cells (i.e., exponentially growing *gtr1Δ gtr2Δ LST4-GFP* cells expressing WT *GTR1* and *GTR2* from plasmids). The scale bar (white; 5 μm) in the top left panel in (A) and in (B) applies to all panels in (A) and in (B), respectively.

(C) Lst4-GFP preferentially binds Gtr2 and $Gtr2^{Q66L}$. Lst4-GFP was IPed in extracts from exponentially growing cells that co-expressed the indicated variants of Gtr1-HA_3 and Gtr2-V5. Cell lysates (input) and anti-GFP immunoprecipitates (IP: anti-GFP) were analyzed by immunoblotting using anti-GFP, anti-HA, and anti-V5 antibodies.

(D and E) Glutamine (Gln), aspartate (Asp), asparagine (Asn), methionine (Met), and cysteine (Cys) are highly competent in displacing Lst4-GFP from the vacuolar membrane (D) and reactivating TORC1 (E) in amino-acid-starved cells. Lst4-GFP-expressing WT cells were starved for 5 min for all amino acids, restimulated for 12 min with individual amino acids (each at a final concentration of 3 mM) or NH_4^+ (37.7 mM), and then analyzed for Lst4-GFP localization and TORC1 activity. The Lst4-GFP signal at the vacuolar membrane was expressed relative to a control sample (set to 1.0) that received no amino acids and TORC1 activities (i.e., Sch9-$pThr^{737}$/total Sch9) were normalized to the ones of untreated exponentially growing cells (set to 100%). −aa, no amino acids added (E). All data are means ± SD from three independent experiments. See also Figure S3A.

(F) Glutamine transiently stimulates the interaction between Lst4 and Gtr2 in amino-acid-starved cells. Cells co-expressing Lst4-GFP, Gtr1-HA_3, and Gtr2-V5 were starved for amino acids (− aa; 5 min) and then restimulated with 3 mM glutamine (+ Gln) for the indicated times. Cell lysates (input) and anti-GFP immunoprecipitates (IP: anti-GFP) were analyzed by immunoblotting with anti-GFP, anti-HA, and anti-V5 antibodies.

See also Figures S3B and S3C.

TORC1 Antagonizes the Vacuolar Membrane Enrichment of the Lst4-Lst7 Complex

The mammalian FNIP-Folliculin complex preferentially associates with and docks to the lysosomal membrane via the inactive form of the Rag GTPase heterodimer that prevails under amino acid starvation conditions (Petit et al., 2013; Tsun et al., 2013). We were therefore surprised to find that the Lst4-Lst7 complex, despite its recruitment to the vacuolar membrane, appeared to be slightly compromised for Gtr1-Gtr2 binding in amino-acid-starved cells (Figures 2E and 2F). We therefore considered the possibility that the vacuolar membrane recruitment of the Lst4-Lst7 complex may not require the presence of Rag GTPases. This was indeed the case, as loss of Gtr1 and Gtr2 per se prompted the enrichment of Lst4-GFP at the vacuolar membrane in exponentially growing cells (Figure 4A). Conspicuously, expression of the active $Gtr1^{Q65L}$-$Gtr2^{S23L}$ heterodimer not only reduced the level of vacuolar membrane-resident Lst4-GFP in exponentially growing cells, but also prevented the accumulation of Lst4-GFP at the vacuolar membrane in amino-acid-starved cells (Figure 4A). Expression of the inactive $Gtr1^{S20L}$-$Gtr2^{Q66L}$ heterodimer, in contrast, resulted in constitutively high levels of Lst4-GFP recruitment to the vacuolar membrane, independently of whether the cells were starved for or fed with amino acids. An interpretation that fits well with all of these results is that the Rag GTPases in yeast regulate the vacuolar membrane localization of the Lst4-Lst7 complex indirectly via TORC1. Two sets of additional observations support this assumption. First, addition of rapamycin stimulated the accumulation of Lst4-GFP at the vacuolar membrane in exponentially growing cells (even in the presence of the active $Gtr1^{Q65L}$-$Gtr2^{S23L}$ heterodimer; Figure 4A) and precluded the redistribution of Lst4-GFP to the cytoplasm upon refeeding of

Please cite this article in press as: Péli-Gulli et al., Amino Acids Stimulate TORC1 through Lst4-Lst7, a GTPase-Activating Protein Complex for the Rag Family GTPase Gtr2, Cell Reports (2015), http://dx.doi.org/10.1016/j.celrep.2015.08.059

amino acids in starved cells (Figure 2B). Second, the expression of the hyperactive *TOR1*^{I1954V} and *TOR1*^{A1957V} alleles (Reinke et al., 2006), unlike wild-type *TOR1*, fully suppressed the constitutive vacuolar membrane-enrichment of Lst4-GFP in *gtr1Δ gtr2Δ* cells expressing *GTR1*^{S20L}/*GTR2*^{Q66L} (Figure 4B). Thus, the enrichment of Lst4-Lst7 at the vacuolar membrane does not require Rag GTPases and is antagonized by TORC1, which is apparently not the case for FNIP-Folliculin in mammalian cells (Petit et al., 2013; Tsun et al., 2013). Not surprisingly, therefore, the affinity of Lst4 to the different combinations of Rag GTPase alleles also did not recapitulate the reported preference of the FNIP-Folliculin module for the GDP-free RagA allele (Petit et al., 2013; Tsun et al., 2013). Accordingly, Lst4 only weakly bound Gtr1 or the rather unstable GDP-free Gtr1^{S20L} allele, but associated well with Gtr2, specifically in its GTP-locked state, which is a property that it shares with many other GAPs and their cognate GTPases (Figure 4C).

Our findings predicted that the Lst4-Lst7 complex, once tethered to the vacuolar membrane in amino-acid-starved cells, requires an amino-acid-dependent signal to activate TORC1 via Gtr2 and be released from the vacuolar membrane. To begin to study the respective mechanism(s), we asked whether the Lst4-Lst7 complex responds to certain amino acids more specifically. Interestingly, most amino acids (and NH_4^+) were, to some extent, able to displace Lst4-GFP from the vacuolar membrane (Figures 4D and S3A). However, glutamine (as well as aparagine and aspartate, which both can be specifically deaminated and readily be converted to glutamate/glutamine) and methionine (as well as cysteine, which can serve as precursor for methionine biosynthesis) (Ljungdahl and Daignan-Fornier, 2012) were exclusively potent in both displacing Lst4-GFP from the vacuolar membrane and reactivating TORC1 in amino-acid-starved cells (Figures 4D and 4E). Since glutamine plays an essential role in anabolic metabolism (e.g., in purine and pyrimidine synthesis) and is under homeostatic control by, and plays a pivotal role in, TORC1 regulation in yeast (Laxman et al., 2014; Ljungdahl and Daignan-Fornier, 2012), we specifically studied the effects of glutamine addition to amino-acid-starved cells. Accordingly, glutamine transiently reinforced the interaction between Lst4-Lst7 and Gtr2 and reactivated TORC1 in an Lst4-, Lst7-, and Gtr1-Gtr2-dependent manner when added to amino-acid-starved cells (Figures 4F, S3B, and S3C). All together, these data are best explained in a model in which glutamine (and presumably also other amino acids, such as methionine) stimulates the Lst4-Lst7 complex to act on the vacuolar membrane-resident fraction of Gtr2, thereby entailing its subsequent release into the cytoplasm. In this model, Rag GTPase-dependent activation of TORC1 is part of a feedback inhibitory loop that favors Lst4-Lst7 removal from or prevents Lst4-Lst7 docking to Gtr2-proximal sites at the vacuolar membrane. This could also elegantly explain the previously reported transient nature of the rapid Rag GTPase-dependent response of TORC1 to glutamine addition (Stracka et al., 2014).

Glutamine and glutamine-derived metabolite(s) activate TORC1 via Rag GTPase-dependent and/or Rag GTPase-independent ways (Durán et al., 2012; Jewell et al., 2015; Nicklin et al., 2009; Stracka et al., 2014), although the underlying mechanisms remain largely to be discovered. In this context, our present study pinpoints the Lst4-Lst7 complex as an important node that likely channels (among others) glutamine signals via the Rag GTPases to TORC1. Given the surprising functional conservation of the Lst4-Lst7 complex, it will therefore be interesting to determine whether the glutamine addiction of certain mTORC1-dependent cancers (Wise and Thompson, 2010) may in part be mediated by the FNIP-Folliculin complex.

EXPERIMENTAL PROCEDURES

Strains, Growth Conditions, and Plasmids

Unless stated otherwise, prototrophic strains were pre-grown overnight in synthetic dropout (SD) medium (0.17% yeast nitrogen base, 0.5% ammonium sulfate, 0.2% dropout mix [USBiological], and 2% glucose) to maintain plasmids. Before each experiment, cells were harvested by centrifugation and diluted to an OD_{600} (optical density at 600 nm) of 0.2 and further grown at 30°C in synthetic complete medium without ammonium sulfate (SC w/o AS; 0.17% yeast nitrogen base, 0.2% of the complete mix of all amino acids [i.e., dropout mix complete (USBiological)], and 2% glucose) until they reached an OD_{600} of 0.8. For amino acid deprivation experiments, cells were filtered and transferred to amino acid starvation medium (SM, which is SC w/o AS, but lacking all amino acids). For restimulation by all amino acids, cells in SM medium were filtered and transferred back to SC w/o AS. For restimulation with single compounds, cells in SM medium were supplemented with a final concentration of 37.7 mM ammonium sulfate or of 3 mM of the indicated amino acid. The *S. cerevisiae* strains and plasmids used in this study are listed in Tables S1 and S2, respectively.

TORC1 Activity Assays

TORC1 activity was quantified by assessing the phosphorylation of the C-terminal part of hemagglutinin (HA) -tagged Sch9^{T570A}, which contains five bona fide TORC1 phosphorylation sites and a mutation in the Pkh1/2-dependent activation loop residue Thr^{570}, as previously described (Urban et al., 2007). Alternatively, TORC1 activity was assessed as the ratio between the phosphorylation on Thr^{737} of full-length Sch9 (or GFP-Sch9) compared to the total abundance of Sch9 (or GFP-Sch9) using phosphospecific anti-pThr^{737}-Sch9 produced by GenScript and anti-Sch9 (or anti-GFP) antibodies, respectively.

GTP Hydrolysis Assays

GAP assays were performed as previously described (Panchaud et al., 2013b). Briefly, 100 nM of purified GTPase were incubated for 30 min at room temperature in loading buffer (20 mM Tris-HCl [pH 8.0], 2 mM EDTA, and 1 mM DTT) in the presence of 40 nM [α-^{32}P]-GTP (Hartman Analytic; 3,000 Ci/mmol). Unless otherwise indicated, 200 nM of His_6-Lst4/His_6-Lst7 or Iml1-His_6 were then added to the mix, together with 10 mM $MgCl_2$ to initialize the reaction. Reactions were stopped after 20 min of incubation at room temperature by the addition of elution buffer (1% SDS, 25 mM EDTA, 5 mM GDP, and 5 mM GTP), and samples were then heat denatured for 2 min at 65°C. Single turnover GAP assays were performed as described above, except that 1.7 mM unlabeled GTP was added at the same time as $MgCl_2$. The concentration of His_6-Lst4/His_6-Lst7 was constant (200 nM), and samples were taken at times 0 and 30 min. [α-^{32}P]-GTP and [α-^{32}P]-GDP were separated by thin-layer chromatography (TLC) on PEI Cellulose F Plates (Merck) with buffer containing 1.0 M acetic acid and 0.8 M LiCl. Results were visualized using a phosphorimager and quantified with ImageQuant software.

SUPPLEMENTAL INFORMATION

Supplemental Information includes Supplemental Experimental Procedures, three figures, and two tables and can be found with this article online at http://dx.doi.org/10.1016/j.celrep.2015.08.059.

AUTHOR CONTRIBUTIONS

M.-P.P.-G., A.S., N.P., and C.D.V. are responsible for the conception and design of the study. M.-P.P.-G., A.S., N.P., and S.R. performed all the

experiments. C.D.V. directed the project, prepared all the figures, and wrote the manuscript. All authors discussed and interpreted the data together.

ACKNOWLEDGMENTS

We thank Robbie Loewith and Ted Powers for plasmids, Floriane Jaquier and Malika Jaquenoud for technical assistance, and Katie Powis for insightful input. This research was supported by the Canton of Fribourg and the Swiss National Science Foundation (C.D.V.).

Received: May 7, 2015
Revised: July 21, 2015
Accepted: August 20, 2015
Published: September 17, 2015

REFERENCES

Albert, V., and Hall, M.N. (2015). mTOR signaling in cellular and organismal energetics. Curr. Opin. Cell Biol. *33*, 55–66.

Bar-Peled, L., Schweitzer, L.D., Zoncu, R., and Sabatini, D.M. (2012). Ragulator is a GEF for the rag GTPases that signal amino acid levels to mTORC1. Cell *150*, 1196–1208.

Bar-Peled, L., Chantranupong, L., Cherniack, A.D., Chen, W.W., Ottina, K.A., Grabiner, B.C., Spear, E.D., Carter, S.L., Meyerson, M., and Sabatini, D.M. (2013). A Tumor suppressor complex with GAP activity for the Rag GTPases that signal amino acid sufficiency to mTORC1. Science *340*, 1100–1106.

Binda, M., Péli-Gulli, M.P., Bonfils, G., Panchaud, N., Urban, J., Sturgill, T.W., Loewith, R., and De Virgilio, C. (2009). The Vam6 GEF controls TORC1 by activating the EGO complex. Mol. Cell *35*, 563–573.

Bonfils, G., Jaquenoud, M., Bontron, S., Ostrowicz, C., Ungermann, C., and De Virgilio, C. (2012). Leucyl-tRNA synthetase controls TORC1 via the EGO complex. Mol. Cell *46*, 105–110.

Durán, R.V., Oppliger, W., Robitaille, A.M., Heiserich, L., Skendaj, R., Gottlieb, E., and Hall, M.N. (2012). Glutaminolysis activates Rag-mTORC1 signaling. Mol. Cell *47*, 349–358.

Han, J.M., Jeong, S.J., Park, M.C., Kim, G., Kwon, N.H., Kim, H.K., Ha, S.H., Ryu, S.H., and Kim, S. (2012). Leucyl-tRNA synthetase is an intracellular leucine sensor for the mTORC1-signaling pathway. Cell *149*, 410–424.

Hoelz, A., Debler, E.W., and Blobel, G. (2011). The structure of the nuclear pore complex. Annu. Rev. Biochem. *80*, 613–643.

Jewell, J.L., Russell, R.C., and Guan, K.L. (2013). Amino acid signalling upstream of mTOR. Nat. Rev. Mol. Cell Biol. *14*, 133–139.

Jewell, J.L., Kim, Y.C., Russell, R.C., Yu, F.X., Park, H.W., Plouffe, S.W., Tagliabracci, V.S., and Guan, K.L. (2015). Metabolism. Differential regulation of mTORC1 by leucine and glutamine. Science *347*, 194–198.

Kim, E., Goraksha-Hicks, P., Li, L., Neufeld, T.P., and Guan, K.L. (2008). Regulation of TORC1 by Rag GTPases in nutrient response. Nat. Cell Biol. *10*, 935–945.

Laplante, M., and Sabatini, D.M. (2012). mTOR signaling in growth control and disease. Cell *149*, 274–293.

Laxman, S., Sutter, B.M., Shi, L., and Tu, B.P. (2014). Npr2 inhibits TORC1 to prevent inappropriate utilization of glutamine for biosynthesis of nitrogen-containing metabolites. Sci. Signal. *7*, ra120.

Levine, T.P., Daniels, R.D., Gatta, A.T., Wong, L.H., and Hayes, M.J. (2013). The product of C9orf72, a gene strongly implicated in neurodegeneration, is structurally related to DENN Rab-GEFs. Bioinformatics *29*, 499–503.

Ljungdahl, P.O., and Daignan-Fornier, B. (2012). Regulation of amino acid, nucleotide, and phosphate metabolism in *Saccharomyces cerevisiae*. Genetics *190*, 885–929.

Nicklin, P., Bergman, P., Zhang, B., Triantafellow, E., Wang, H., Nyfeler, B., Yang, H., Hild, M., Kung, C., Wilson, C., et al. (2009). Bidirectional transport of amino acids regulates mTOR and autophagy. Cell *136*, 521–534.

Panchaud, N., Péli-Gulli, M.P., and De Virgilio, C. (2013a). SEACing the GAP that nEGOCiates TORC1 activation: evolutionary conservation of Rag GTPase regulation. Cell Cycle *12*, 2948–2952.

Panchaud, N., Péli-Gulli, M.P., and De Virgilio, C. (2013b). Amino acid deprivation inhibits TORC1 through a GTPase-activating protein complex for the Rag family GTPase Gtr1. Sci. Signal. *6*, ra42.

Petit, C.S., Roczniak-Ferguson, A., and Ferguson, S.M. (2013). Recruitment of folliculin to lysosomes supports the amino acid-dependent activation of Rag GTPases. J. Cell Biol. *202*, 1107–1122.

Rebsamen, M., Pochini, L., Stasyk, T., de Araújo, M.E., Galluccio, M., Kandasamy, R.K., Snijder, B., Fauster, A., Rudashevskaya, E.L., Bruckner, M., et al. (2015). SLC38A9 is a component of the lysosomal amino acid sensing machinery that controls mTORC1. Nature *519*, 477–481.

Reinke, A., Chen, J.C., Aronova, S., and Powers, T. (2006). Caffeine targets TOR complex I and provides evidence for a regulatory link between the FRB and kinase domains of Tor1p. J. Biol. Chem. *281*, 31616–31626.

Roberg, K.J., Bickel, S., Rowley, N., and Kaiser, C.A. (1997). Control of amino acid permease sorting in the late secretory pathway of *Saccharomyces cerevisiae* by *SEC13*, *LST4*, *LST7* and *LST8*. Genetics *147*, 1569–1584.

Sancak, Y., and Sabatini, D.M. (2009). Rag proteins regulate amino-acid-induced mTORC1 signalling. Biochem. Soc. Trans. *37*, 289–290.

Sancak, Y., Peterson, T.R., Shaul, Y.D., Lindquist, R.A., Thoreen, C.C., Bar-Peled, L., and Sabatini, D.M. (2008). The Rag GTPases bind raptor and mediate amino acid signaling to mTORC1. Science *320*, 1496–1501.

Stracka, D., Jozefczuk, S., Rudroff, F., Sauer, U., and Hall, M.N. (2014). Nitrogen source activates TOR (target of rapamycin) complex 1 via glutamine and independently of Gtr/Rag proteins. J. Biol. Chem. *289*, 25010–25020.

Sturgill, T.W., Cohen, A., Diefenbacher, M., Trautwein, M., Martin, D.E., and Hall, M.N. (2008). TOR1 and TOR2 have distinct locations in live cells. Eukaryot. Cell *7*, 1819–1830.

Tsun, Z.Y., Bar-Peled, L., Chantranupong, L., Zoncu, R., Wang, T., Kim, C., Spooner, E., and Sabatini, D.M. (2013). The folliculin tumor suppressor is a GAP for the RagC/D GTPases that signal amino acid levels to mTORC1. Mol. Cell *52*, 495–505.

Urban, J., Soulard, A., Huber, A., Lippman, S., Mukhopadhyay, D., Deloche, O., Wanke, V., Anrather, D., Ammerer, G., Riezman, H., et al. (2007). Sch9 is a major target of TORC1 in *Saccharomyces cerevisiae*. Mol. Cell *26*, 663–674.

van Slegtenhorst, M., Khabibullin, D., Hartman, T.R., Nicolas, E., Kruger, W.D., and Henske, E.P. (2007). The Birt-Hogg-Dube and tuberous sclerosis complex homologs have opposing roles in amino acid homeostasis in *Schizosaccharomyces pombe*. J. Biol. Chem. *282*, 24583–24590.

Wang, S., Tsun, Z.Y., Wolfson, R.L., Shen, K., Wyant, G.A., Plovanich, M.E., Yuan, E.D., Jones, T.D., Chantranupong, L., Comb, W., et al. (2015). Metabolism. Lysosomal amino acid transporter SLC38A9 signals arginine sufficiency to mTORC1. Science *347*, 188–194.

Wise, D.R., and Thompson, C.B. (2010). Glutamine addiction: a new therapeutic target in cancer. Trends Biochem. Sci. *35*, 427–433.

Zhang, D., Iyer, L.M., He, F., and Aravind, L. (2012a). Discovery of novel DENN proteins: implications for the evolution of eukaryotic intracellular membrane structures and human disease. Front. Genet. *3*, 283.

Zhang, T., Péli-Gulli, M.P., Yang, H., De Virgilio, C., and Ding, J. (2012b). Ego3 functions as a homodimer to mediate the interaction between Gtr1-Gtr2 and Ego1 in the ego complex to activate TORC1. Structure *20*, 2151–2160.

Zoncu, R., Bar-Peled, L., Efeyan, A., Wang, S., Sancak, Y., and Sabatini, D.M. (2011). mTORC1 senses lysosomal amino acids through an inside-out mechanism that requires the vacuolar H(+)-ATPase. Science *334*, 678–683.

Cell Reports

Supplemental Information

Amino Acids Stimulate TORC1 through Lst4-Lst7, a GTPase-Activating Protein Complex for the Rag Family GTPase Gtr2

Marie-Pierre Péli-Gulli, Alessandro Sardu, Nicolas Panchaud, Serena Raucci, and Claudio De Virgilio

Supplemental Figures

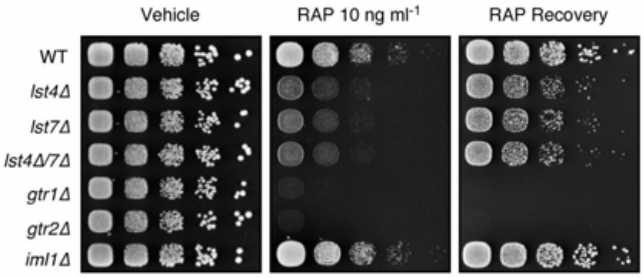

Figure S1. Loss of Lst4 and/or Lst7 Causes Rapamycin-Sensitivity and a Mild Defect in Recovery from a Rapamycin-Induced Growth Arrest, Related to Figure 1

Wild-type and isogenic mutant cells (genotypes indicated) were grown exponentially in YPD (standard rich medium with 2% glucose) and spotted as 10-fold serial dilutions on YPD plates containing no rapamycin (vehicle) or 10 ng ml^{-1} rapamycin (RAP). To assay the ability of cells to recover from a rapamycin-induced growth arrest, exponentially growing cells were treated for 6 h with rapamycin (200 ng ml^{-1}), washed twice, and then spotted as 10-fold serial dilutions on YPD plates (RAP Recovery).

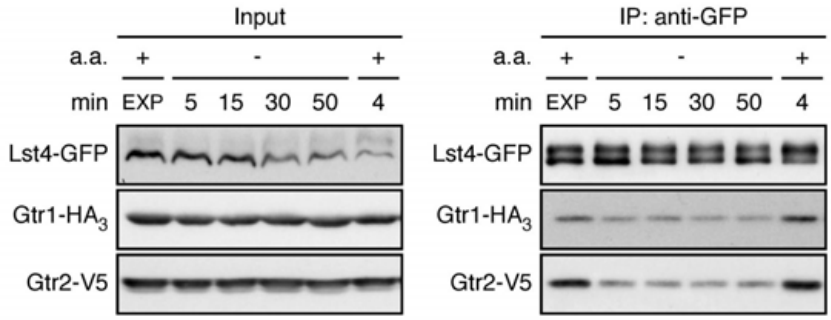

Figure S2. Short or Prolonged Amino Acid Starvation and Subsequent Refeeding Reduces and Re-Stimulates, Respectively, the Interaction Between Lst4 and Gtr1-Gtr2, Related to Figure 2

Lst4-GFP was IP-ed in extracts from cells that co-expressed Gtr1-HA_3 and Gtr2-V5. Cells were grown as in Figure 2E, but were harvested following 5, 15, 30, and 50 min of amino acid starvation (a.a.; -), and after 4 min of amino acid refeeding (a.a.; +; 4 min) to 50 min-starved cells.

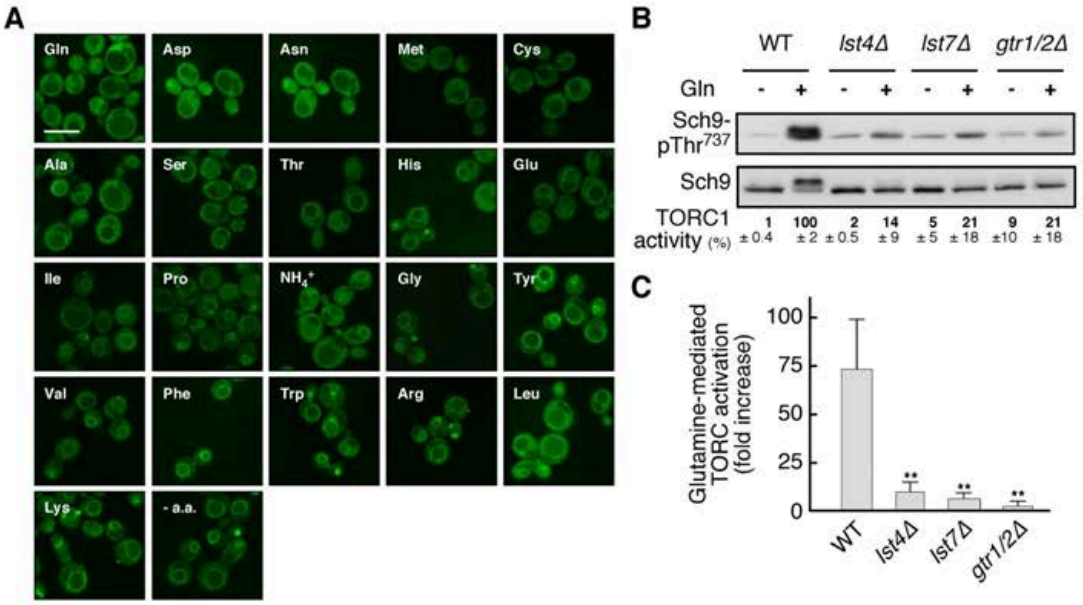

Figure S3. Amino Acids Such as Glutamine Stimulate TORC1 in an Lst4-, Lst7-, and Gtr1/2-Dependent Manner, Related to Figure 4

(A) Glutamine (Gln), aspartate (Asp), asparagine (Asn), methionine (Met), and cysteine (Cys) are highly competent in displacing Lst4-GFP from the vacuolar membrane. Lst4-GFP-expressing cells were starved for 5 min for all amino acids, re-stimulated for 12 min with individual amino acids (3 mM) or NH_4^+ (37.7 mM), and then analyzed for Lst4-GFP localization. One representative image is shown for each condition and the quantification data are presented in Figure 4D. The scale bar (white; top left panel) represents 5 μm and applies to all panels.

(B and C) Glutamine stimulates TORC1 activity in amino acid-starved cells in an Lst4-, Lst7- and Gtr1/2-dependent manner. In (B), TORC1 activity (*i.e.* Sch9-pThr^{737}/total Sch9) was assayed in exponentially growing cells with the indicated genotypes that were deprived for 5 min of all amino acids (Gln; -) and subsequently stimulated for 12 min with 3 mM glutamine (Gln; +). TORC1 activities (means ± SD from three independent experiments) were normalized to the value of glutamine-stimulated WT cells (set to 100%). The respective glutamine (Gln) -mediated fold-increase in TORC1 activity (*i.e.* the ratio of the TORC1 values between glutamine-stimulated and amino acid-starved cells) for each strain is shown in (C). Significance was estimated by Student's t-test (**$P < 0.01$).

Supplemental Tables

Table S1. Strains Used in This Study

Strain	Genotype	Source	Figure
YL515	[BY4741/2] *MATα; his3Δ1, leu2Δ0, ura3Δ0*	(Binda et al., 2009)	1A-D; S1
MP347-4A	[YL515] *MATα; lst4Δ::KanMX*	This study	1A-D; S1
MP348-3C	[YL515] *MATα; lst7Δ::KanMX*	This study	1A-D; S1
MP354-9A	[YL515] *MATα; lst4Δ::KanMX, lst7Δ::KanMX*	This study	1A-C; S1
MB36-4B	[YL515] *MATα; gtr1Δ::kanMX*	This study	1A-C; S1
MB33	[YL515] *MATa; gtr2Δ::kanMX*	(Binda et al., 2009)	1A-C; S1
NP04-C4	[YL515] *MATα; iml1Δ::KanMX*	(Panchaud et al., 2013b)	1A-C; S1
MP06-8B	[YL515] *MATα; gtr1Δ::kanMX, gtr2Δ::kanMX*	(Binda et al., 2009)	1C
MB27	[YL515] *MATα; gtr1Δ::HIS3*	(Binda et al., 2009)	1D
MP359-5A	[YL515] *MATα; lst4Δ::KanMX gtr1Δ::HIS3*	This study	1D
MP360-2C	[YL515] *MATα; lst7Δ::KanMX gtr1Δ::HIS3*	This study	1D
MB28	[YL515] *MATα; gtr2Δ::HIS3*	(Binda et al., 2009)	1D
MP361-7D	[YL515] *MATα; lst4Δ::KanMX gtr2Δ::HIS3*	This study	1D
MP362-4A	[YL515] *MATα; lst7Δ::KanMX gtr2Δ::HIS3*	This study	1D
KT1961	*MATa; his3, leu2, ura3-52, trp1*	(Pedruzzi et al., 2003)	S3B, C
KP09	[KT1961] *MATa; lst4Δ::KanMX*	This study	S3B, C
KP10	[KT1961] *MATa; lst7Δ::KanMX*	This study	2A; S3B, C
MP409-2A	[KT1961] *MATa; LST4-GFP::HIS3MX*	This study	2B, D; 4D, E; S3A
MP410-5B	[KT1961] *MATa; LST7-GFP::HIS3MX*	This study	2B
MP374-1C	[KT1961] *MATa; LST4-GFP::HIS3MX, lst7Δ::KanMX*	This study	2A, C
MP372-2D	[KT1961] *MATa; LST7-GFP::HIS3MX, lst4Δ::KanMX*	This study	2C
MP406-8A	[KT1961] *MATa; LST4-GFP::HIS3MX, gtr1Δ::natMX, gtr2Δ::natMX*	This study	2E; 4A-C, F; S2
MP405-3D	[KT1961] *MATa; LST7-GFP::HIS3MX, gtr1Δ::natMX, gtr2Δ::natMX*	This study	2F; 4F
MP268-2B	[KT1961] *MATa; gtr1Δ::natMX, gtr2Δ::natMX*	This study	S3B, C

Table S2. Plasmids Used in This Study

Plasmid	Genotype	Source	Figure
pRS413	CEN, ARS, *HIS3*	(Brachmann et al., 1998)	1A-D; 2A, E, F; S3B, C
pRS414	CEN, ARS, *TRP1*	(Brachmann et al., 1998)	2A-D; 4A, C-E; S2; S3A-C
pRS415	CEN, ARS, *LEU2*	(Brachmann et al., 1998)	1A-D; 2A-C, E, F; 4A, D-F; S3A-C
pRS416	CEN, ARS, *URA3*	(Brachmann et al., 1998)	1D; 2A-D; 4A, D, E; S3A-C
pJU1030	[pRS416] *SCH9p-SCH9^{T570A}-HA$_5$*	(Urban et al., 2007)	1A, C, D
pJU793	[pRS416] *SCH9p-GFP-SCH9*	(Urban et al., 2007)	1B
pJU1058	[pRS415] *SCH9p-SCH9^{T570A}-HA$_5$*	(Urban et al., 2007)	1D
YCplac33	CEN, ARS, *URA3*	(Gietz and Sugino, 1988)	
pMB1393	[YCplac33] *TetON-GTR1*	(Binda et al., 2009)	1D
pMB1394	[YCplac33] *TetON-GTR1^{Q65L}*	(Binda et al., 2009)	1D
pMB1395	[YCplac33] *TetON-GTR1^{S20L}*	(Binda et al., 2009)	1D
YCplac111	CEN, ARS, *LEU2*	(Gietz and Sugino, 1988)	
pPM1621	[YCplac111] *TetON-GTR2*	(Binda et al., 2009)	1D
pPM1622	[YCplac111] *TetON-GTR2^{Q66L}*	(Binda et al., 2009)	1D
pPM1623	[YCplac111] *TetON-GTR2^{S23L}*	(Binda et al., 2009)	1D
pMP2562	[pRS414] *LST7p-LST7-V5-HIS$_6$*	This study	2A
pYM2847	[YCplac111] *VAC8p-VAC8-Cherry*	This study	2D
pMPG2177	[pRS414] *GTR2p-GTR2-V5-HIS$_6$*	This study	2E, F; 4F
pNP2055	[YCplac111] *ADH1p-IML1- HIS$_6$-TEV-ProtA*	(Panchaud et al., 2013b)	3B
pNP2035	[pET-24d] *GST-TEV-GTR1*	(Panchaud et al., 2013b)	3B
pNP2038	[pET-24d] *GST-TEV-GTR2*	(Panchaud et al., 2013b)	3A-E
pJU1046	[pGEX-6P] *GST-TEV-GTR1^{Q65L}-HIS$_6$*	R. Loewith	3A-E
pJU1048	[pGEX-6P] *GST-TEV-GTR2^{Q66L}-HIS$_6$*	(Panchaud et al., 2013b)	3B
pMP2101	[pGEX-4T] *GST-CDC42*	(Panchaud et al., 2013b)	3B
pAS2570	[pET28b$^+$] *HIS$_6$-LST4*	This study	3A-E
pAS2571	[pET15b$^+$] *HIS$_6$-LST7*	This study	3A-E
pJU650	[pRS416] *GTR1p-GTR1*	R. Loewith	4A
pJU652	[pRS416] *GTR1p-GTR1^{S20L}*	R. Loewith	4A, B
pJU653	[pRS416] *GTR1p-GTR1^{Q65L}*	R. Loewith	4A
pMP2337	[pRS416] *GTR1p-GTR1-HA$_3$*	This study	2E, F; 4A, C, F; S2
pMP2338	[pRS416] *GTR1p-GTR1^{S20L}-HA$_3$*	This study	4C
pMP2339	[pRS416] *GTR1p-GTR1^{Q65L}-HA$_3$*	This study	4C
pJU661	[pRS415] *GTR2p-GTR2*	R. Loewith	4A
pJU658	[pRS415] *GTR2p-GTR2^{S23L}*	R. Loewith	4A
pJU659	[pRS415] *GTR2p-GTR2^{Q66L}*	R. Loewith	4A
pMP2136	[pRS415] *GTR2p-GTR2-V5-HIS$_6$*	This study	4C, S2
pMP2777	[pRS415] *GTR2p-GTR2^{S23L}-V5-HIS$_6$*	This study	4C
pMP2778	[pRS415] *GTR2p-GTR2^{Q66L}-V5-HIS$_6$*	This study	4C
pMP2782	[pRS414] *GTR2p-GTR2^{Q66L}-V5-HIS$_6$*	This study	4B
pPL132	CEN, ARS, *LEU2*, *HA$_3$-TOR1*	(Reinke et al., 2006)	4B
pPL155	CEN, ARS, *LEU2*, *HA$_3$-TOR1^{A1957V}*	(Reinke et al., 2006)	4B
pPL156	CEN, ARS, *LEU2*, *HA$_3$-TOR1^{I1954V}*	(Reinke et al., 2006)	4B

Supplemental Experimental Procedures

Coimmunoprecipitation

Yeast cells expressing the indicated fusion proteins were harvested by filtration. Filters were immediately snap-frozen in liquid nitrogen and stored at -80°C. Cells were then resuspended in lysis buffer (50 mM Tris HCl, pH 7.5, 150 mM NaCl, 10 mM $MgCl_2$, 0.1% NP-40, and 1x protease and phosphatase inhibitor cocktails [Roche]) and lysed with glass beads using the Precellys cell disruptor. Lysates were clarified by two successive centrifugations for 10 min at 13'000 rpm. For input samples, aliquots of cleared lysates were concentrated by precipitation with ice-cold methanol, resuspended in 6x concentrated loading buffer, and denatured for 10 min at 65°C. For coimmunoprecipitations, cleared lysates were incubated for 2 hours at 4°C with prewashed GFP-Trap® Magnetic-Agarose beads (Chromotek). After three washes with the lysis buffer, beads were resuspended in 6x concentrated loading buffer and denatured for 10 min at 65°C. Inputs and pull-down samples were analyzed by SDS-PAGE immunoblot with anti-GFP (Roche), anti-HA (HA.11; SantaCruz), and anti-V5 (Lubio).

Fluorescence microscopy and image quantification

Images were captured with an inverted Spinning Disk Confocal Microscope (VisiScope CSU-W1) equipped with an Evolve 512 (Photometrics) EM-CCD camera and a 100x 1.3 NA oil immersion Nikon CFI series objective. Quantification of the signal intensity at the vacuolar membrane was performed using the ImageJ software as follows: For each cell the median intensity value of the total GFP-signal was measured and subtracted from the respective median intensity value of the GFP-signal at the vacuolar membrane. Quantifications were performed on three independent experiments (with at least 9 cells analyzed in each experiment).

Protein purification

Iml1-His_6 was purified from *Saccharomyces cerevisiae* as previously described (Panchaud et al., 2013b). GST-Gtr2, GST-Gtr1^{Q65L}-His_6/Gtr2-His_6, Gtr1-His_6/GST-Gtr2^{Q66L}-His_6, GST-Cdc42 and His_6-Lst4/His_6-Lst7 were produced in the *Escherichia coli* Rosetta strain (Novagen) after induction with 0.5 mM IPTG during 5 hours at 18°C (GST-Gtr2, GST-Gtr1^{Q65L}-His_6/Gtr2-His_6, Gtr1-His_6/GST-Gtr2^{Q66L}-His_6), or at 37°C (GST-Cdc42) or overnight at 16°C (His_6-Lst4/His_6-Lst7). Cells were collected by centrifugation and lysed with a microfluidizer in the appropriate buffer. Purification of GST-tagged proteins was done using Glutathione-Sepharose beads (GE Healthcare) in Buffer A (50 mM Tris-HCl, pH 7.5, 200 mM NaCl, 1.5 mM $MgCl_2$, 5% glycerol, 1 mM DTT, 0.1% NP40, and 0.1 mM GDP) and proteins were finally eluted with Buffer A + 10 mM reduced glutathione. His_6 purification (His_6-Lst4/His_6-Lst7) was performed using Ni-NTA agarose beads (Qiagen) in Buffer B (50 mM NaH_2PO_4 pH 8.0, 300 mM NaCl, 0.1% NP40, and 50 mM imidazole) and elution was achieved in Buffer B + 250 mM imidazole. Glycerol was added to a final concentration of 20% and proteins were stored at -80°C.

Supplemental References

Binda, M., Péli-Gulli, M.P., Bonfils, G., Panchaud, N., Urban, J., Sturgill, T.W., Loewith, R., and De Virgilio, C. (2009). The Vam6 GEF controls TORC1 by activating the EGO complex. Mol. Cell *35*, 563-573.

Brachmann, C.B., Davies, A., Cost, G.J., Caputo, E., Li, J., Hieter, P., and Boeke, J.D. (1998). Designer deletion strains derived from *Saccharomyces cerevisiae* S288C: a useful set of strains and plasmids for PCR-mediated gene disruption and other applications. Yeast *14*, 115-132.

Gietz, R.D., and Sugino, A. (1988). New yeast-*Escherichia coli* shuttle vectors constructed with *in vitro* mutagenized yeast genes lacking six-base pair restriction sites. Gene *74*, 527-534.

Panchaud, N., Péli-Gulli, M.P., and De Virgilio, C. (2013b). Amino acid deprivation inhibits TORC1 through a GTPase-activating protein complex for the Rag family GTPase Gtr1. Sci. Signal. *6*, ra42.

Pedruzzi, I., Dubouloz, F., Cameroni, E., Wanke, V., Roosen, J., Winderickx, J., and De Virgilio, C. (2003). TOR and PKA signaling pathways converge on the protein kinase Rim15 to control entry into G_0. Mol. Cell *12*, 1607-1613.

Reinke, A., Chen, J.C., Aronova, S., and Powers, T. (2006). Caffeine targets TOR complex I and provides evidence for a regulatory link between the FRB and kinase domains of Tor1p. J. Biol. Chem. *281*, 31616-31626.

Urban, J., Soulard, A., Huber, A., Lippman, S., Mukhopadhyay, D., Deloche, O., Wanke, V., Anrather, D., Ammerer, G., Riezman, H., *et al.* (2007). Sch9 is a major target of TORC1 in *Saccharomyces cerevisiae*. Mol. Cell *26*, 663-674.

CHAPTER II:

Genetic screen for suppressors of the growth inhibitory phenotype caused by Gtr1^{S20L} overexpression

2.1 Introduction

GTPases are often described as "molecular switches", being active and signaling competent in their GTP-bound form and inactive when GDP-bound (Bourne et al., 1990). However, this archetype does not properly fit with our knowledge of Rag GTPases. In mammals, the RagA/B^{GDP}-RagC/D^{GTP} heterodimer was previously defined as the "inactive form", but actually it participates in the propagation of an inhibitory signal toward TORC1. The RagA/B^{GDP}-RagC/D^{GTP} heterodimer interacts with the TSC1-TSC2-TBC1D7 complex leading to its recruitment at the lysosomal membrane (Demetriades et al., 2014). There, TSC2 can function as a GAP for Rheb (Inoki et al., 2003a; Tee et al., 2003). In *S. cerevisiae*, the expression of the nucleotide free form of Gtr1 (Gtr1^{S20L}), or a GTP-locked form of Gtr2 (Gtr2^{Q66L}), has a negative effect on TORC1 activity, but the mechanism by which they inactivate TORC1 is still not known (Binda et al., 2009). Could this involve a TSC/Rheb branch? Orthologs of TSC1 and TSC2 in budding yeast have not been discovered yet. Instead, a Rheb ortholog has been found and named Rhb1, but experimental data that could link it to the TORC1 signaling pathway are missing. Interestingly, in budding yeast, Gtr1^{S20L} overexpression causes growth inhibition. This phenotype was specifically caused by the Gtr1 mutation since deletion of *GTR1* did not show such a defect. Remarkably, growth inhibition could be suppressed by deletion of *TCO89* (encoding a TORC1 component), suggesting its involvement as mediator of this signal. It could therefore be speculated that Gtr1^{S20L} binds to TORC1 and inactivates it via Tco89. However, deletion of *TCO89* did not abolish the interaction between wild-type Gtr1 and the other TORC1 component Kog1 (Binda, 2009). Furthermore, Gtr1^{S20L} did not show any interaction with Tco89 in a membrane-based split ubiquitin yeast two-hybrid system (Binda et al., 2009). Strikingly, we found that the growth defect could be occasionally rescued by spontaneous suppressor mutations. We therefore undertook, on a small-scale, the identification and characterization of few of these mutations as a proof of concept for a potential suppressor screening.

In this chapter a genetic selection to identify the mutations responsible for the suppression of the growth inhibition mediated by Gtr1^{S20L} overexpression will be described. Ideally, this project could lead to the discovery of novel TORC1 regulators. In *S. cerevisiae*, possible functional orthologs of TSC complex or Rheb might be involved in causing growth inhibition during Gtr1^{S20L} overexpression. The analysis of these

suppressor colonies might also help uncover the Rheb-TSC signaling branch in budding yeast.

2.2 Results and Discussion

2.2.1 Overexpression of Gtr1^{S20L} causes growth inhibition

To confirm the growth inhibition observed in cells overexpressing Gtr^{S20L}, we compared the growth rate of *gtr1Δ* cells overproducing the different forms of Gtr1 by drop spot assay. All cells grew at similar rates when incubated at 30°C without doxycycline. (Fig.2.1). Overexpression of doxycycline-inducible Gtr1^{S20L}, but not Gtr1 wild-type or Gtr1^{Q65L}, resulted in growth inhibition and this defect could be suppressed by deletion of *TCO89* (Fig.2.1). These results confirmed the previously seen growth defect provoked by Gtr^{S20L} overexpression (Binda et al., 2009).

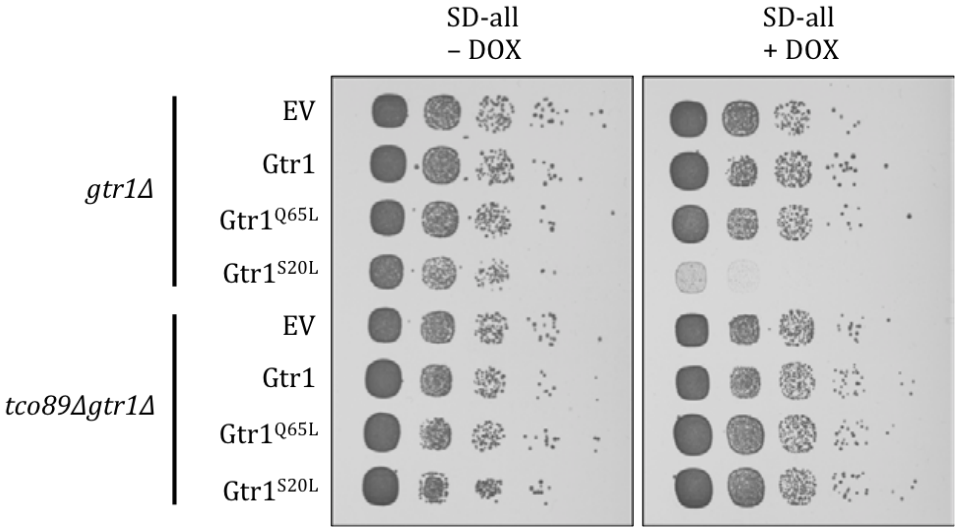

Figure 2.1 Overexpression of Gtr1^{S20L} causes Tco89-dependent growth inhibition. Prototrophic *gtr1Δ* or *gtr1Δ tco89Δ* cells were transformed with an empty vector (EV) or vectors overexpressing Gtr1, Gtr1^{Q65L}, or Gtr1^{S20L} from the doxycycline-inducible *Tet$_{ON}$* promoter. Cells were grown on SD with ammonium sulfate as nitrogen source and without amino acids (SD-all) until they reached an OD_{600} of 0.8. Serial 10-fold dilutions were spotted on plates containing (+ DOX), or not (-DOX), doxycycline (5 µg/ml). Pictures were taken after two days of incubation at 30°C.

2.2.2 Genetic selection of suppressors of the Gtr1^{S20L} growth inhibition phenotype

Occasionally, after 2-3 days of incubation at 30°C, we noticed spontaneous colonies growing despite the Gtr1^{S20L} overexpression (data not shown). We speculated that the initial growth inhibition could be suppressed by spontaneous mutations impinging on one or more theoretical effectors of Gtr1^{S20L} signaling. Thus, we planned a small-scale screening to select more of these hypothetical suppressors and, at a later time, to identify them via whole genome sequencing. Since false positive suppressors may arise due to genetic rearrangements of the plasmid leading to loss of Gtr1^{S20L} overexpression (*i.e.* mutation in the *GTR1^{S20L}* open reading frame), we planed a "double selection" approach to exclude this event. We also decided to use a *gtr1Δ* background to avoid any interference from an endogenous wild-type copy of Gtr1. Furthermore, overproduction of Gtr1^{S20L} in a *gtr1Δ* background causes stronger growth inhibition (Binda, 2009). As first step of the screening procedure, we co-transformed *gtr1Δ* cells with two different inducible plasmids that could overexpress Gtr1^{S20L}: one allowed the expression of Gtr1^{S20L} from the doxycycline-inducible *Tet$_{ON}$* promoter while the other from the galactose-inducible *GAL1* promoter (Fig.2.2).

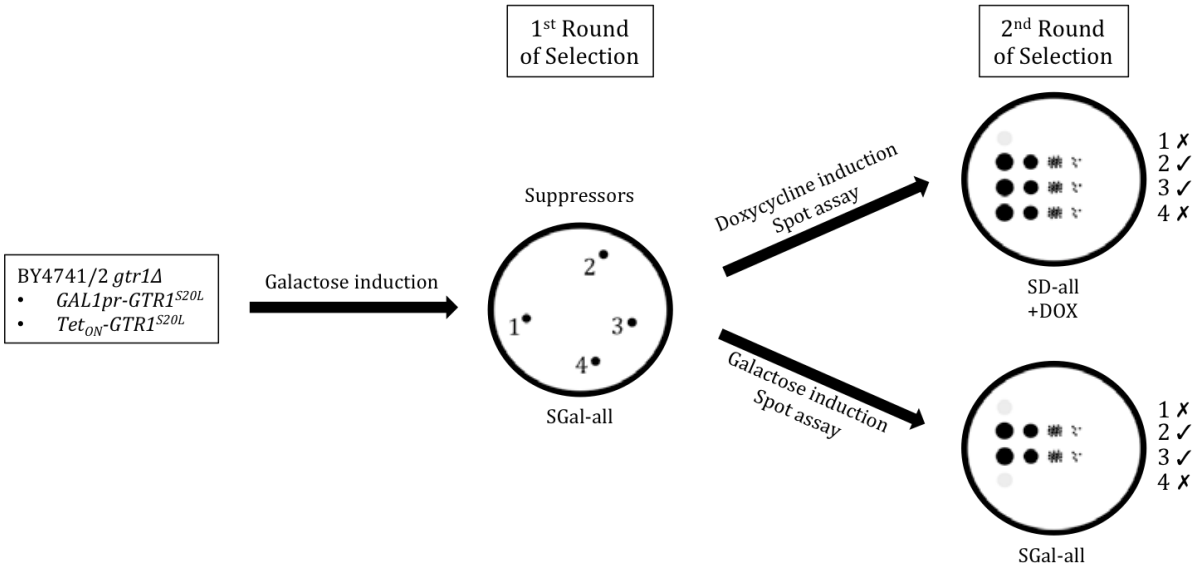

Figure 2.2 Outline of the selection procedure. Prototrophic *gtr1Δ* cells were transformed with the *GAL1pr-GTR1^{S20L}* and the *Tet$_{ON}$-GTR1^{S20L}* plasmids. During the first round of selection, cells were plated on synthetic medium with 2% galactose as only carbon source and without addition of amino acids (SGal-all). In the second round of selection, the resulting suppressors were collected, cultured again and spotted on SGal-all and SD-all containing doxycycline. Suppressors that failed to grow in SD-all +DOX and/or SGal-all were considered false positive and therefore discarded.

Our protocol required a first round of suppressor selection by overexpressing Gtr1^{S20L} only via the *GAL1* promoter. The suppressors obtained could then be further tested for growth during Gtr1^{S20L} overexpression from the *Tet$_{ON}$* promoter and the *GAL1* promoter. We reasoned that suppressors not growing during the second round of selection could be considered as false positive and therefore discarded. To obtain single suppressor colonies, cells were grown on SD-all until they reached an OD_{600} of 0.8, and 0.6 x 10^6 cells were plated on synthetic medium with 2% galactose as the only carbon source and without amino acids. This procedure has been performed for a total of two independent plates (overall, 1.2 x 10^6 cells were used). After two days of incubation at 30°C, a total of three colonies grew. Following one more day of incubation at 30°C, six additional colonies arose. The nine suppressors were therefore cultured on SD-all and spotted on SGal-all and SD-all doxycycline containing plates (2nd round of selection) (Fig.2.3).

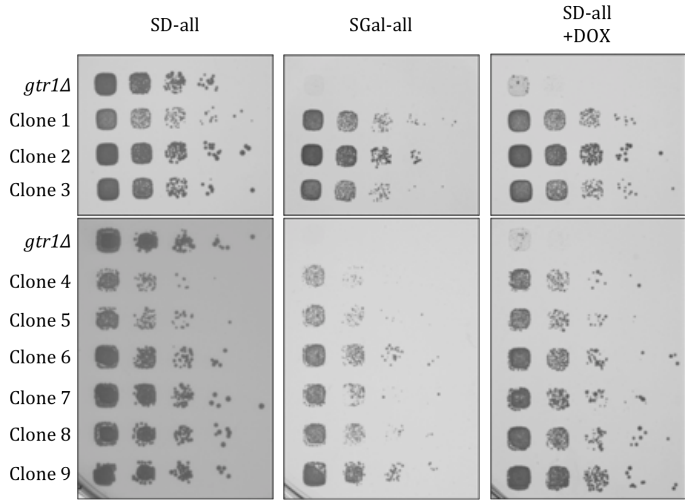

Figure 2.3 Exclusion of suppressors still sensitive to Gtr1^{S20L} growth inhibition. Candidates obtained during the first round of selection were tested again for their suppressor phenotype. All strains carried the *GAL1pr-GTR1^{S20L}* and the *Tet$_{ON}$-GTR1^{S20L}* expressing plasmids. Prototrophic cells were spotted on SD-all, SGal-all, and SD-all containing doxycycline plates as described in figure 2.1. The nine suppressors were numbered sequentially. The strain used to obtain the suppressors (*gtr1Δ*) was used as a positive control for Gtr1^{S20L} growth inhibition.

Although the suppressors grew at different rates, they did not show Gtr1^{S20L}-mediated growth inhibition comparable to the *gtr1Δ* control strain. Since it was not likely that both Gtr1^{S20L} expressing plasmids were not functional, we thought that the suppression of the phenotype could be caused by mutations into the genome. At this point of the screening, the resulting suppressors were cultured on YPD to facilitate loss of

previously transformed plasmids. The plasmid-free suppressors were then stored at -80°C and tested in the following assays, restricting the *GTR1*^{S20L} expression to the *GAL* inducible system. From here on, I will refer to the absence of growth inhibition caused by Gtr1^{S20L} overexpression as "suppressor phenotype".

It was already known that *TCO89* deletion was sufficient to suppress Gtr1^{S20L}-mediated growth inhibition (Binda et al., 2009). Thus, it was possible as well that the suppressors obtained from the screening harbor mutations in the *TCO89* gene. Therefore, we transformed the nine suppressors plus the *gtr1Δ* control strain with a plasmid allowing expression of a *TCO89* wild-type gene from its own promoter. We then checked if this wild-type copy of the *TCO89* gene was sufficient to restore sensitivity to Gtr1^{S20L} overexpression (Fig.2.4).

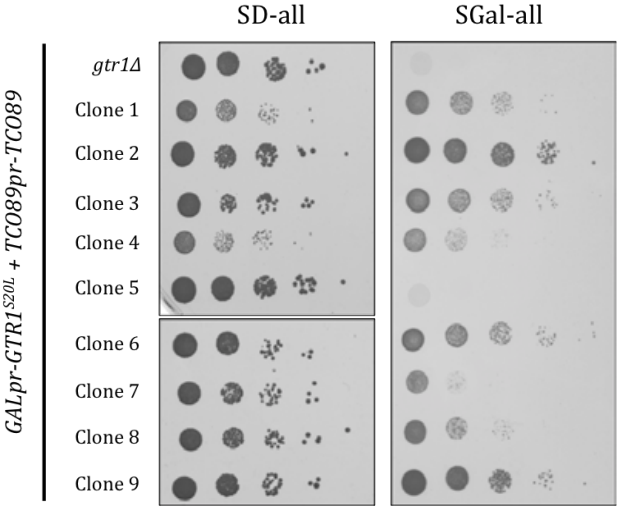

Figure 2.4 Exclusion of suppressors containing mutations in *TCO89* gene. The *gtr1Δ* control and suppressor strains were transformed with the *GALpr-GTR1*^{S20L} and *TCO89pr-TCO89* expressing plasmids. Prototrophic cells were spotted in SD-all and SGal-all as described in figure 2.1.

Under these conditions, only clone 5 was again affected by Gtr1^{S20L} overexpression while the other suppressors were not, thus we speculated that suppression of the phenotype in clone 5 was likely caused by *TCO89* mutation. Although characterization of a hypothetical *TCO89* mutation would be useful to better understand the role of this TORC1 subunit, it was not the main goal of the screening. Therefore, clone 5 was not taken into account for further analysis in this chapter. However, we planed to sequence the *TCO89* gene from clone 5 to confirm, and in positive case, annotate its mutation.

Finally, genomic DNA from the remaining eight suppressor candidates was extracted and sent for whole genome sequencing. The resulting data (analyzed by Dr. Falquet,

University of Fribourg) allowed the identification of genomic variants in comparison to the wild-type reference strain. All sequenced genomes presented at least one genomic variation, with only two different strains harboring different mutations in the same gene. Mutations found in the eight analyzed suppressors are summarized in table 2.1.

Clone	Gene	Mutation	Amino acid substitution
1	*VPS33*	cTa/cCa	L18P
2	*EGO1*	Aga/Tga	R9*
	VID27	aAg/aCg	K513T
3	*RSC1*	cCc/cTc	P387L
4	*DPB11*	Aat/Cat	N92H
	PEP5	Caa/Taa	Q76*
6	*VAM6*	Caa/Taa	Q391*
7	*APL6*	aTg/aGg	M613R
8	*APL6*	Atg/Gtg	M1V
9	*GTR2*	tgC/tgG	C231W

Table 2.1 Mutations found in suppressor strains. Genetic variants identified after whole genome sequencing are recapitulated. The mutation column shows the wild-type sequence and the corresponding mutation found in the suppressor strain (differences are in capital letters). In the amino acid substitution column, the asterisk is used to define a nonsense mutation (stop codon).

Ego1 and Gtr2, two components of the EGO complex, have been extensively described in the introduction of the thesis. Vps33, Pep5/Vps11 and Vam6/Vps39 are components of the class C Vps family and are important for protein sorting, vesicle docking, and fusion at the vacuole (Balderhaar and Ungermann, 2013). Apl6 is a component of the AP-3 complex, which mediates protein transport to the vacuole (Odorizzi et al., 1998). Rsc1 is a component of the RSC nucleosome-remodeling complex and is required for expression of genes involved in sporulation (Bungard et al., 2004). Dpb11 is an essential protein that functions as DNA replication initiation protein (Masumoto et al., 2000). Finally, Vid27 is the last characterized protein and is possibly involved in vacuolar protein degradation (Regelmann et al., 2003). From here on, I will refer to the suppressors by indicating the gene name and the relative amino acid substitution. The identified genes are all known proteins already linked to specific processes and will be discussed in the next paragraphs in more detail.

2.2.3 Gtr1 vacuolar localization is compromised in most of the suppressor strains

The Gtr1-Gtr2 heterodimer needs to be at the vacuolar membrane to activate TORC1. Furthermore, $Gtr1^{S20L}$ still interacts with Gtr2 even though to a lesser extent compared to $Gtr1^{WT}$ or $Gtr1^{Q65L}$ (Powis et al., 2015). Finally, $Gtr1^{S20N}$ binds to Ego1 and Ego3 in yeast two hybrid system (Sekiguchi et al., 2014). It can be reasoned that $Gtr1^{S20L}$ needs to be at the vacuolar membrane to start propagation of the growth inhibitory signal, which likely has TORC1 as final target. Therefore, we decided to check Gtr1 localization in all suppressor mutants. A functional N-terminal tagged GFP-Gtr1 was used together with the vacuolar marker FM4-64 to verify Gtr1 localization and vacuolar morphology (Fig.2.5).

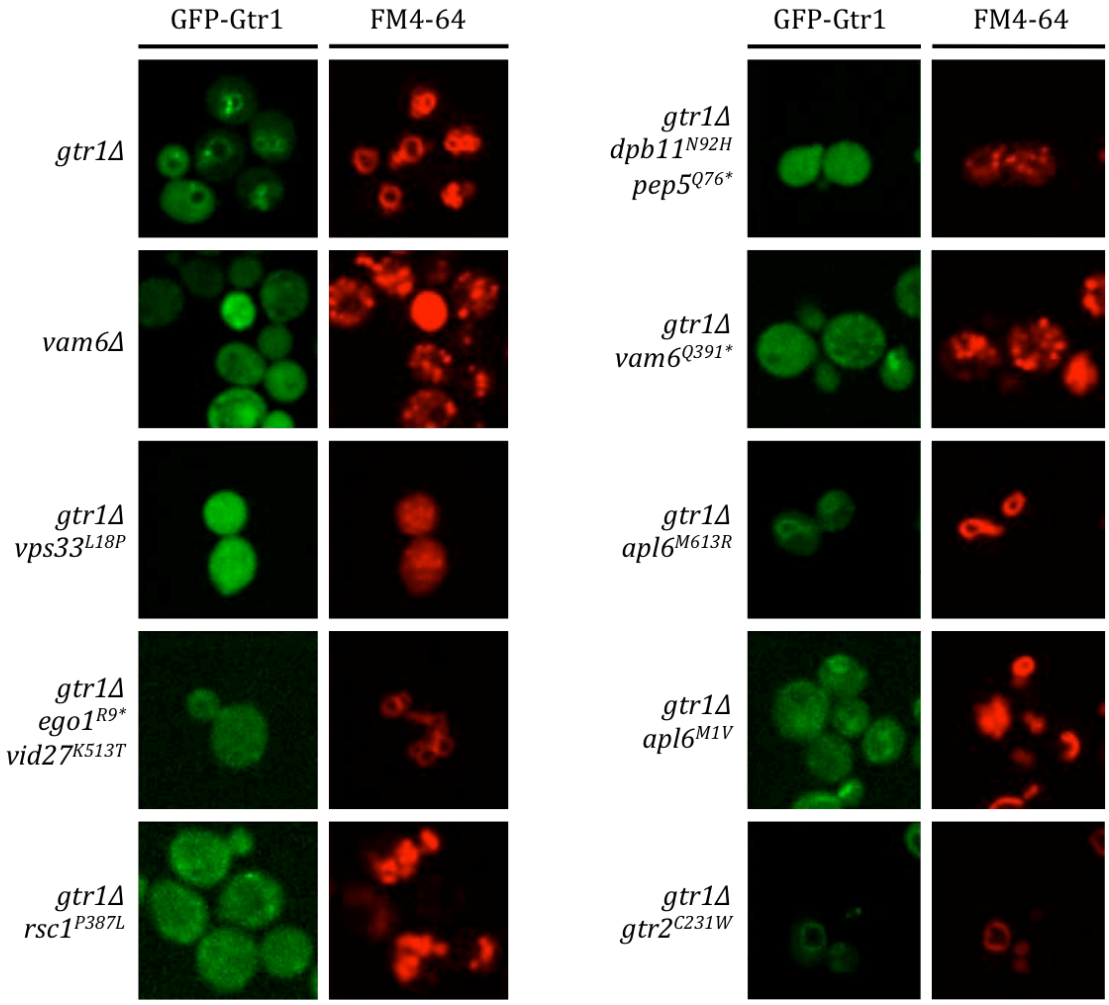

Figure 2.5 GFP-Gtr1 localization in suppressor strains. Exponentially growing cells expressing a plasmid-encoded GFP-Gtr1 from its own promoter were specifically stained at the vacuolar membrane with the lipophilic styryl dye FM4-64. The *gtr1Δ* and *vam6Δ* strains were used as positive and negative controls, respectively. SD medium lacking histidine (SD-His) was used for plasmid selection.

GFP-Gtr1 vacuolar localization was compromised in all suppressor strains except in Gtr2^{C231W} and partially in the *apl6*^{M613R} and *vam6*^{Q391*}. Vacuoles were highly fragmented in all suppressor strains except in *ego*^{R9*} *vid27*^{K513T}, *gtr2*^{C231W} and *apl6*^{M613R} strains.

2.2.4 All suppressor mutants, but not *gtr2*^{C231W}, exhibit sensitivity to rapamycin and an EGO phenotype

Strains missing any component of the EGO complex are sensitive to rapamycin and fail to recover after exposure to rapamycin. The latter phenotype is also called "EGO phenotype". (Binda et al., 2009; Dubouloz et al., 2005). We thought that the improper GFP-Gtr1 localization could be connected to a partially defective TORC1 signaling. Therefore, we tested the ability of the suppressor strains to grow in presence of sub-inhibitory concentrations of rapamycin (Fig.2.6).

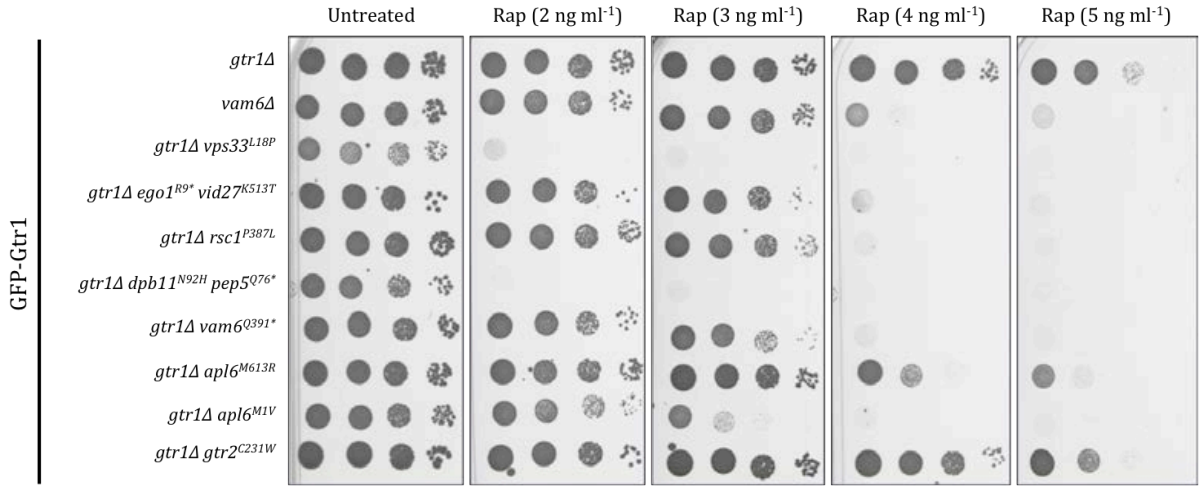

Figure 2.6 Sensitivity of suppressor strains to rapamycin. Strains were the same as in figure 2.5. Exponentially growing cells were spotted on SD-His containing 0, 2, 3, 4, or 5 ng/ml rapamycin as described in figure 2.1. The *vam6Δ* strain was used as positive control for rapamycin treatment.

Both the double *dpb11*^{N92H} *pep5*^{Q76*} and the *vps33*^{L18P} strains presented strong sensitivity to low concentration of rapamycin (2 ng/ml). The two *apl6* mutants behaved differently already at 3 ng/ml of rapamycin, *apl6*^{M1V} being more sensitive than *apl6*^{M613R} to the treatment. At 5 ng/ml rapamycin only *gtr2*^{C231W} presented a comparable growth rate to the control strain.

To further characterize the suppressors, we tested if they presented an EGO phenotype (Fig 2.7). Except *gtr2*^{C231W} and *apl6*^{M613R} strains, all suppressors failed to recover from a prolonged rapamycin exposure (6 hours).

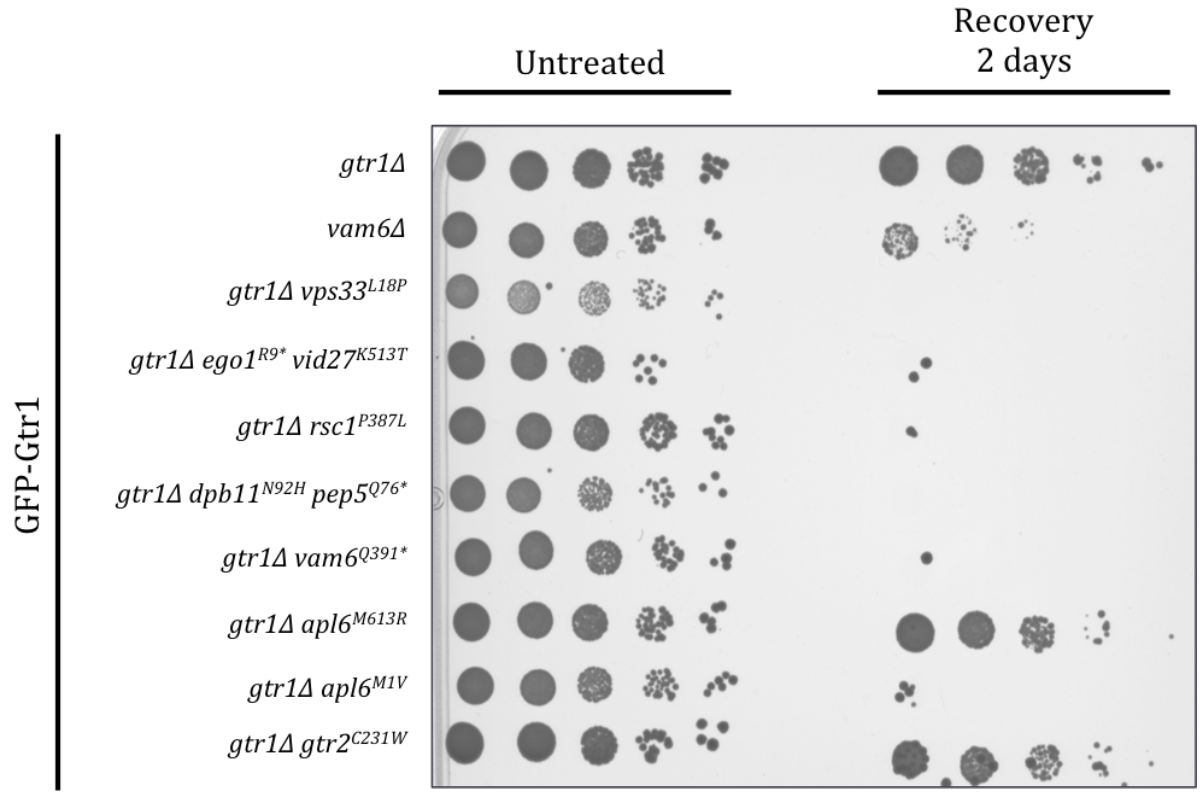

Figure 2.7 Recovery of suppressor strains from rapamycin treatment. Strains were the same as in figure 2.5. Cells were grown exponentially in SD-His, treated for six hours with rapamycin (200 ng ml^{-1}), washed twice, and spotted on SD-His plates as in figure 2.1.

2.2.5 All suppressor mutants except *gtr2*^{C231W} have reduced TORC1 activity

Rapamycin sensitivity and EGO phenotype are common indicators of impaired TORC1 signaling. Therefore, we assessed the activation state of TORC1 by analyzing the phosphorylation state of its target Sch9 in all suppressors (Fig.2.8). The *gtr2*^{C231W} strain was the only suppressor with TORC1 activity levels similar to the *gtr1Δ* GFP-Gtr1 control strain. The *apl6*^{M1V} and *apl6*^{M613R} mutants showed slightly reduced TORC1 activity. Instead, all the other strains presented reduced TORC1 activity similarly to the *vam6Δ* control strain. These results were in line with previous observations regarding sensitivity to and recovery from rapamycin treatment.

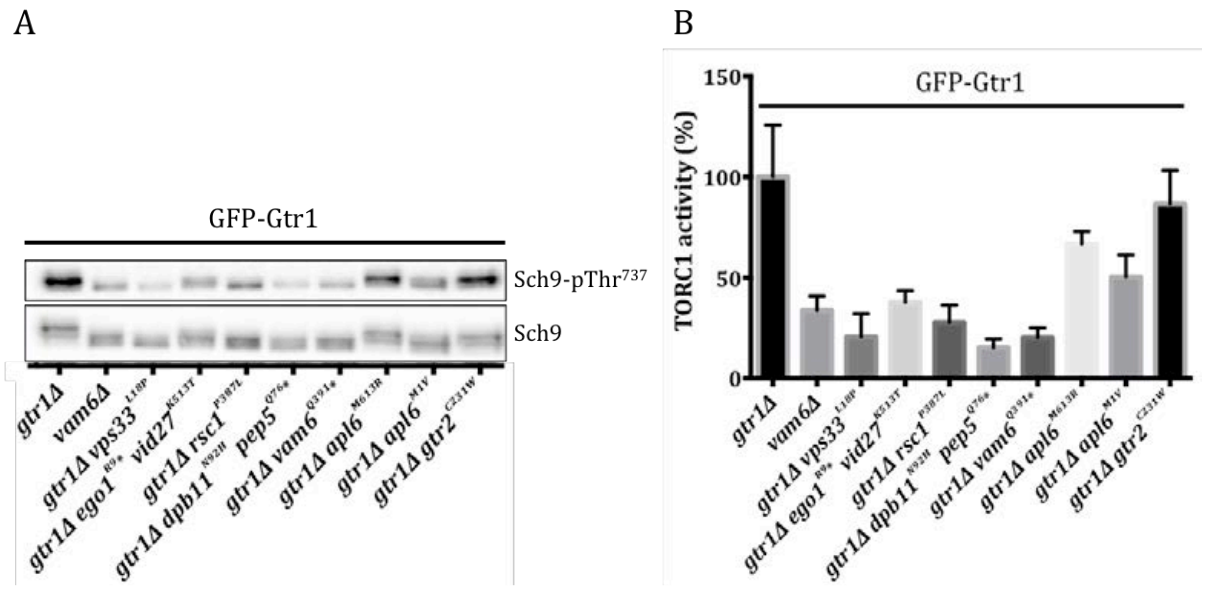

Figure 2.8 TORC1 activity in suppressor strains. A) Strains were the same as in figure 2.5. Exponentially growing cells were collected at an OD_{600} of 0.8 for whole protein extraction. The *vam6Δ* strain was used as a control for decreased TORC1 activity. Specific antibodies recognizing the phosphorylated Thr737 (pThr737) of Sch9 and the total Sch9 were used to assay TORC1 activity. Representative immunoblots for both antibodies are shown. B) Histogram representative of the TORC1 activity in suppressor strains and controls assessed in A. TORC1 activity was calculated as the ratio of $pThr^{737}$ Sch9/total Sch9 and normalized to the TORC1 activity in *gtr1Δ GFP-GTR1* cells (set to 100%). Data are means ± SD from three independent experiments.

Taken all of the above listed observations together, it seems that some of the mutant alleles recovered in our screen prevent $Gtr1^{S20L}$ from inactivating TORC1 simply by abrogating its proper subcellular localization. For instance, **Ego1** is a subunit of the EGO ternary complex (EGO-TC). This protein is N-terminally myristoylated and palmitoylated and is necessary to anchor the EGO-TC to the membrane of the vacuole (Dubouloz et al., 2005; Powis et al., 2015). The *ego1*^{R9*} mutation results in a short peptide of 9 amino acids because of a premature stop codon. By comparison with the EGO-TC crystal structure, the $Ego1^{R9*}$ protein would likely miss the necessary regions to interact with both Ego2 and Ego3, therefore it should not form the EGO-TC (Powis et al., 2015). As a consequence, the Gtr1-Gtr2 heterodimer could not be recruited at the vacuolar membrane (Dubouloz et al., 2005; Powis et al., 2015). Our data suggest that growth inhibition mediated by $Gtr1^{S20L}$ requires a functional EGO ternary complex. Notably, the *ego1*^{R9*} *vid27*^{K513T} suppressor strain bears two different mutations. **Vid27** is a cytoplasmic protein of unknown function that could be involved in vacuolar protein

degradation (Regelmann et al., 2003). Large-scale studies did not find any interesting phenotype that could be connected to the TORC1 pathway. It would be interesting to test the effects of *vid27*^{K513T} in an *EGO1* wild-type background. The two mutations could be separated by crossing *ego1*^{R9*} *vid27*^{K513T} strain to a wild-type. Dissection of the resulting tetrads would allow the selection of the *ego1*^{R9*} and *vid27*^{K513T} single mutants. Alternatively, if the *ego1*^{R9*} mutation is not dominant, a plasmid expressing *EGO1* wild-type could suppress the phenotypes dependent on *ego1*^{R9*}. This would allow the study just of the *vid27*^{K513T} mutation.

Similar to loss of Ego1 function, loss of **Vps33** and **Pep5/Vps11** function could prevent Gtr1^{S20L} from being properly localized at the vacuolar membrane. Of note, Vps33 and Pep5/Vps11 are components of the class C Vps family. Two Vps-C complexes, called CORVET and HOPS, are important for protein sorting via regulation of vesicle docking and fusion both at the endosome (mediated by the CORVET complex) and between the endosome and the vacuole (mediated by the HOPS complex). Vps33 and Pep5 are shared subunits between the two complexes (Balderhaar and Ungermann, 2013). The two proteins were already known to be involved in TORC1 regulation (Binda et al., 2009; Kingsbury et al., 2014; Zurita-Martinez et al., 2007). Deletion of any of these genes causes increased rapamycin sensitivity and inability to recover from a rapamycin treatment. Mutants missing components of the Vps-C complexes have low concentrations of intracellular amino acids, therefore suggesting an important role of the two complexes in keeping proper amino acid homeostasis for functional TORC1 signaling (Kingsbury et al., 2014; Zurita-Martinez et al., 2007). Similarly to the respective deletions, the double *dpb11*^{N92H} *pep5*^{Q76*} and the *vps33*^{L18P} mutant strains showed sensitivity to rapamycin treatment, an EGO phenotype, and had reduced TORC1 activity. The *pep5*^{Q76*} mutation results in a premature stop codon, generating a 75 amino acid protein instead of the normal 1029 amino acids. The strain harboring the *pep5*^{Q76*} mutation also has the N92H mutation in *dpb11*. This gene encodes an essential protein involved in DNA replication. More interestingly, the *vps33*^{L18P} mutation falls in the region encoding an α-helix part of an interacting domain with SNARE proteins, which are involved in the membrane fusion process (Baker et al., 2013). Proline mutations often result in destabilization of protein-protein interactions because proline restricts the conformation of the following residue in the protein sequence and it is incapable of forming hydrogen-bonds (Bajaj et al., 2007).

How the mutation in **Rsc1** suppress the effect of Gtr1^{S20L} overproduction cannot be readily explained based on the current results, but the GFP-Gtr1 localization data indicate that the respective mutation in *RSC1* may indirectly also prevent Gtr1^{S20L} from being properly localized within cells. Rsc1 is a component of the RSC chromatin-remodeling complex. It is important, together with its paralog Rsc2, for expression of mid-late sporulation-specific genes (Bungard et al., 2004). Furthermore, the Rsc1-containing RSC complex (Rsc1-RSC) is also required for autophagy induction and TORC1 inactivation during nitrogen starvation. It has been proposed that TORC1 is negatively regulated through Rsc1-dependent Rho1 GTPase-Kog1 binding (Yu et al., 2015). Thus, it remains to be studied, whether the latter effect is indirectly due to a mis-localization of Gtr1 within *rsc1* mutant cells.

Finally, a couple of suppressor mutations (including *vam6^{Q391*}*, *apl6^{M613R}*, *apl6^{M1V}* and *gtr2^{C231W}*) may suppress the growth-inhibitory effect of Gtr1^{S20L} overproduction by means that may not, or not solely, relate to the mislocalization of Gtr1. These are therefore studied in more detail in the following sections.

2.2.6 The *vam6^{Q391*}* mutation, but not *VAM6* deletion, is sufficient to suppress growth inhibition caused by Gtr1^{S20L} overexpression

The *vam6^{Q391*}* mutation results in defective TORC1 signaling because of its reduced TORC1 activity and higher sensitivity to rapamycin compared to a wild-type strain. Furthermore, the mutation causes vacuolar fragmentation (but GFP-Gtr1 seems still to localize to some extent to these fragmented vacuoles). Those results are reminiscent of *VAM6* deletion. However, it was previously published that overexpression of Gtr1^{S20L} results in a synthetic growth defect when combined with *vam6Δ* (Binda et al., 2009). Thus, we set out to overexpress Gtr1^{S20L} in *gtr1Δ* Vam6^{Q391*} and *gtr1Δvam6Δ* strains to compare them side-by-side. Differently from *gtr1Δ vam6Δ*, which behaved like the *gtr1Δ* control, *vam6^{Q391*}* strain was confirmed to be insensitive to growth inhibition caused by Gtr1^{S20L} overexpression (Fig 2.9).

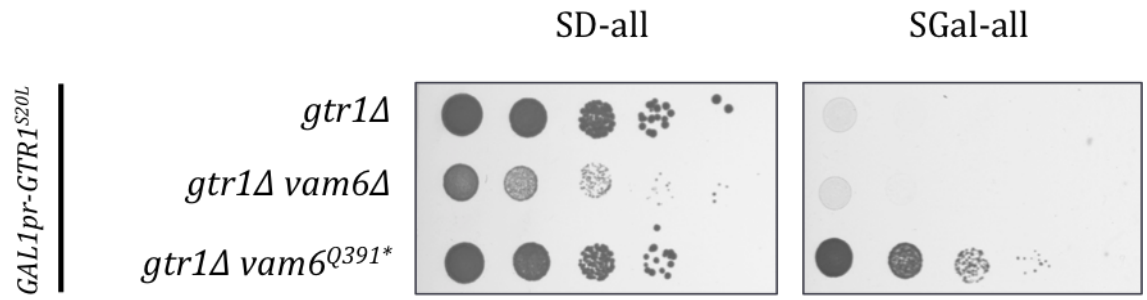

Figure 2.9 Gtr1^{S20L}-induced growth inhibition is suppressed by *vam6^{Q391*}*, but not *VAM6* deletion. The *gtr1Δ*, *gtr1Δvam6Δ* and *gtr1Δ - vam6^{Q391*}* strains were transformed with the *GALpr-GTR1^{S20L}* plasmid. Prototrophic cells were spotted on SD-all and SGal-all as described in figure 2.1.

Vam6/Vps39 is a member of the class C Vps family and a subunit of the HOPS complex (Balderhaar and Ungermann, 2013). Similarly to Vps33 and Pep5, Vam6 is involved TORC1 regulation. Vam6 functions as a GEF for Gtr1 and is likely important in regulation of amino acid homeostasis (Binda et al., 2009; Kingsbury et al., 2014; Zurita-Martinez et al., 2007). A *vam6Δ* strain, similarly to *vam6^{Q391*}*, is characterized by reduced TORC1 activity, rapamycin sensitivity and inability to recover from a rapamycin treatment. However, the *vam6^{Q391*}* mutant differs from the *vam6Δ* strain because the former can grow upon Gtr1^{S20L} overexpression. This result would suggest a possible function for *vam6^{Q391*}* in TORC1 regulation. It could be possible that the first 400 amino acids in Vam6 still have GEF activity toward Gtr1, resulting in a constitutive active GEF no longer responsive to amino acid levels. Our results show how this mutant has defective TORC1 signaling but it could be argued that Vam6 is both required for amino acid homeostasis via the HOPS complex and as a GEF for Gtr1. As described in the previous paragraph, both functions are fundamental for proper TORC1 activation. A nucleotide-exchange assay would be required to test *vam6^{Q391*}* GEF activity toward wild-type Gtr1 *in vitro*.

2.2.7 GFP-Gtr2^{C231W} properly localizes at the vacuolar membrane and it still displays impaired TORC1 activity upon Gtr1^{S20L} overexpression.

The *gtr2^{C231W}* mutation is in an important region necessary for the Gtr1-Gtr2 heterodimer formation (Gong et al., 2011). We reasoned that Gtr2^{C231W} vacuolar localization might be altered in case of problems in Gtr1-Gtr2 interaction. For this

reason we compared GFP-Gtr2^{C231W} and GFP-Gtr2 localization in the presence or absence of Gtr1 (Fig.2.10).

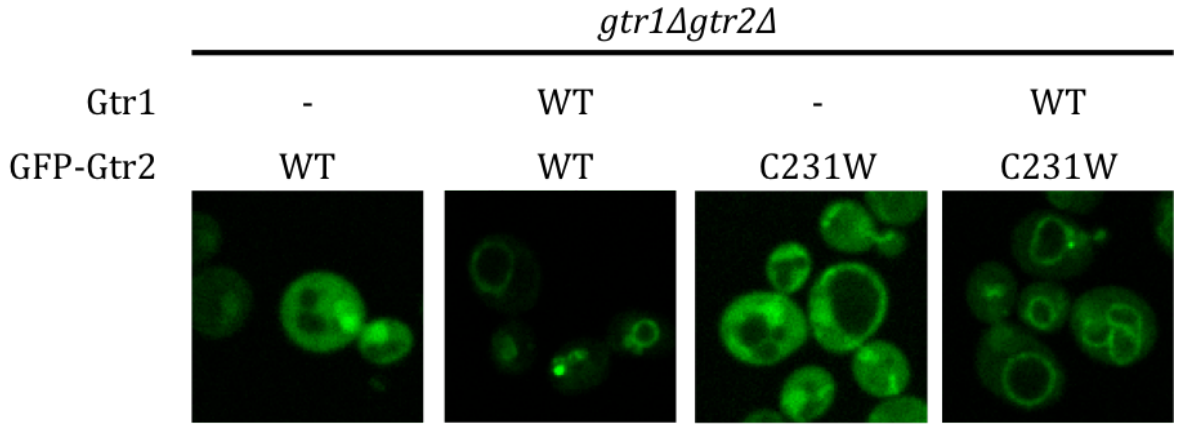

Figure 2.10 Localization of GFP-Gtr2 and GFP-Gtr2^{C231W} at the vacuolar membrane is Gtr1 dependent. Representative pictures of the *gtr1Δgtr2Δ* strain expressing plasmid encoded Gtr1 and GFP-Gtr2 by their own promoter. Cells were grown in SD lacking histidine and uracil (SD-HU).

GFP-Gtr2^{C231W} localized to the vacuolar membrane similarly to WT Gtr2. Furthermore, Gtr1 was still necessary for proper localization of GFP-Gtr2^{C231W}, since removal of the former caused vacuolar delocalization of the latter, as seen for GFP-Gtr2 wild-type. Strikingly, upon deletion of *GTR1* we noticed nuclear accumulation of both GFP-Gtr2 and GFP-Gtr2^{C231W}. It is unclear if this observation is biologically relevant and part of an unknown function of Gtr2, or it is an artifact resulting from *GTR1* deletion. However, nuclear accumulation of Gtr2 in a *gtr1Δ* strains has been already reported (Sekiguchi et al., 2001).

Short-term expression of the Gtr1^{S20L} allele causes drastic reduction of TORC1 activity (Binda et al., 2009). Since the Gtr2^{C231W} strain has normal TORC1 activity, we wondered if overexpression of Gtr1^{S20L} in this strain still resulted in impaired activation of TORC1. Overexpression of Gtr1^{S20L} in a *gtr1Δ GTR2* wild-type or *gtr1Δ gtr2^{C231W}* strain decreased TORC1 activity to a similar extent (Fig.2.11).

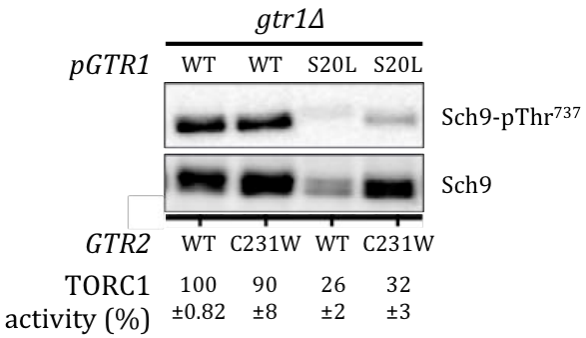

Figure 2.11 TORC1 activity in *gtr2*^{C231W} is still reduced upon over expression of Gtr1^{S20L}. *gtr1Δ* or *gtr1Δ gtr2*^{C231W} strains expressing either plasmid-encoded wild-type Gtr1 from its own promoter or Gtr1^{S20L} from a doxycycline-inducible promoter. Prototrophic cells were pre-cultured in SD-all over night. The following morning, cells were diluted in SD-all containing doxycycline (5 µg/ml) and further grown for ~5 hours until OD_{600} of 0.8. Cell were treated and analyzed as in figure 2.9 A. Representative immunoblots are shown. TORC1 activity was calculated as in figure 2.9 B. Data are means ± SD from three independent experiments.

Interestingly, we noticed that overexpression of Gtr1^{S20L} caused reduction of the Sch9 protein levels in a *gtr1Δ* strain, but not in a *gtr1Δ gtr2*^{C231W} strain. This decrease might be connected to the growth inhibition mediated by Gtr1^{S20L}, which is not observed in the *gtr1Δ gtr2*^{C231W} strain.

Regarding the TORC1 related phenotypes we tested, the *gtr2*^{C231W} strain always behaved like a wild-type strain albeit not showing growth inhibition caused by Gtr1^{S20L} overexpression. The C231W substitution lies in the α8-helix of the Gtr2 CTD domain, which is involved in interaction with Gtr1. This region is of key importance and mutations in the Gtr2 α8-helix are likely to disrupt the Gtr1-Gtr2 binding (Gong et al., 2011). However, in this suppressor strain, TORC1 activity is similar to a wild-type strain. Furthermore, both Gtr1 and Gtr2^{C231W} localize at the vacuolar membrane, while Gtr2^{C231W} does not if *GTR1* is deleted. Thus, we speculated that they correctly interact to form the heterodimer, although experiments such as co-immunoprecipitation between Gtr1 and Gtr2 are required to confirm this hypothesis. How the *gtr2*^{C231W} mutation makes cells resistant to Gtr1^{S20L} growth inhibition is still unknown and further experiments are required. A hypothetical model could be that Gtr1^{S20L}, and likely Gtr1^{GDP}, recruits an inhibitor together with Gtr2, which then causes growth inhibition. Analysis of Gtr2 and Gtr2^{C231W} interacting proteins during growth conditions that may mimic the phenotype caused by the *gtr1*^{S20L} allele (*i.e.* nitrogen or amino acid starvation) could identify binding partners specific to either Gtr2 or Gtr2^{C231W}.

Furthermore, co-immunoprecipitation of Gtr1 with either Gtr2 or Gtr2^{C231W} could reveal if the C231W mutation changes the interaction levels between the two GTPases.

2.2.8 Ego1 properly localizes at the vacuolar membrane in *apl6* mutants.

Apl6 is involved in cargo-selective transport to the yeast vacuole (Cowles et al., 1997). We reasoned that the two *apl6* mutants obtained from the screening could be defective in Ego1 vacuolar localization and hence in proper Gtr1-Gtr2 heterodimer positioning at the vacuolar membrane. We therefore looked at Ego1-GFP localization in *apl6^{M1V}* and *apl6^{M613R}*. Ego1-GFP localized at the vacuolar surface in *apl6^{M613R}* and likely in *apl6^{M1V}*, although vacuolar morphology was compromised in the latter mutant (Fig 2.12).

Figure 2.12 Ego1-GFP localizes at the vacuole in *apl6^{M613R}* and *apl6^{M1V}* mutants. Prototrophic cells expressing plasmid-encoded *EGO1-GFP* from its endogenous promoter were treated as in figure 2.6. SD-all was used to maintain plasmids.

Apl6 is a subunit of the AP-3 complex which functions in protein transport from the Golgi to the vacuole/lysosome (Odorizzi et al., 1998). In our screening, we found two different *apl6* mutants, one with a M1V mutation and the other with the M613R substitution. The *apl6^{M1V}* strain presented more sensitivity to rapamycin as well as less TORC1 activity compared to *apl6^{M613R}*. Furthermore, *apl6^{M1V}* has an EGO phenotype. A comparison between the *apl6^{M1V}* and *apl6Δ* strains would be needed to understand if the mutation is more similar to a deletion phenotype. Because of the M1V substitution, the *APL6* open reading frame is missing its canonical start codon. It could be speculated that *apl6^{M1V}* is either not expressed or expressed in one or more truncated variants. We initially thought that Apl6 could be involved in localization of the EGO-TC at the vacuolar membrane by regulating its transport to the vacuole. However Ego1 properly localized at the vacuolar surface in both *apl6* mutants. Instead, Gtr1 vacuolar localization was partially decreased. Deletion of *APL6* results in mislocalization of protein such as the vacuolar t-SNARE Vam3 and the alkaline phosphatase (ALP). Vam3

binds to Vps33 allowing membrane fusion at vacuoles mediated by the HOPS complex (Lürick et al., 2015). It is possible that the phenotypes caused by *apl6*^{M1V} mutation, and to a lesser extent by *apl6*^{M613R}, are a consequence of Vam3 delocalization and therefore reminiscent of what we have observed for v*ps33*^{L18P}.

2.2.9 Final remarks

At the end of the screening procedure, eight suppressors were selected and further assessed for their TORC1 related phenotypes, such as sensitivity to rapamycin and Sch9 phosphorylation. Table 2.2 summarizes the results obtained.

Mutant	Growth on rapamycin plates	EGO phenotype	Gtr1 vacuolar localization	TORC1 activity
vps33^{L18P}	-	Yes	-	-
ego1^{R9*} **-** ***vid27***^{K513T}	+/-	Yes	-	-
rsc1^{P387L}	+/-	Yes	-	-
dpb11^{N92H} **-** ***pep5***^{Q76*}	-	Yes	-	-
vam6^{Q391*}	+/-	Yes	-	-
apl6^{M613R}	+/-	No	+/-	+/-
apl6^{M1V}	-	Yes	-	+/-
gtr2^{C231W}	+	No	+	+

Table 2.2 Summary of the TORC1 related phenotypes for the suppressors. The following symbols in the table mean: (+) like wild-type; (+/-) slightly different from the wild-type; (-) highly different from the wild-type.

The small-scale screening here described was a proof of concept to show its potential for a more large-scale approach. Regarding the general characterization of the suppressors, some aspects can still be improved. First, every suppressor should be compared to its deletion mutant. As we have shown for *vam6*^{Q391*}, a point mutation could result in additional phenotypes not available by simply deleting the mutated gene. Second, every suppressor should be crossed with a *gtr1Δ* strain, and the resulting diploids should be tested again for growth during Gtr1^{S20L} overexpression. This would

allow understanding if the suppressor mutation has a dominant or recessive behavior. Furthermore, sporulation of these diploids, dissection of the resulting tetrads, and their analysis would state if the suppressor bears one or more mutations impinging on the suppression of the $Gtr1^{S20L}$-induced growth inhibition. Third, we only tested the localization of Gtr1 in the suppressors, but a more complete analysis would also inquire the localization of the other components of the EGO complex.

To summarize, this project shows the high potential for the described suppressor selection procedure. Saturation screenings, such as the one we described, are used to discover all genes involved in a specific phenotype. Usually, this type of screening is carried out until no new genes involved in the studied phenotype can be found. Among the eight candidate suppressors only two of them presented a mutation on the same gene. This observation suggests that many other candidate genes can be found before reaching saturation the screening. Many of the mutations found were in genes already involved in TORC1 regulation and they may be of valuable importance in further dissecting their molecular functions and gaining insight into TORC1 signaling pathway.

CHAPTER III:
Characterization of the Mrs6 protein as a regulator for Gtr2

3.1 Introduction

The Rab/Ypt GTPase family, which belongs to the Ras GTPase superfamily, controls vesicle docking and fusion events at all phases of intracellular transport (Rybin et al., 1996). As part of their regulation, Rab/Ypt proteins cycle between cytoplasm and membranes (Segev, 2011). Membrane anchorage is achieved via prenylation of the GTPase by the geranylgeranyl transferase II (GGTase II). The Rab escort protein (REP), which is structurally similar to the Rab/Ypt GDP dissociation inhibitor (RabGDI), forms a complex with the GGTase II. REP is necessary for recognition of the Rab/Ypt proteins by the GGTase II and, subsequently to prenylation, redirection of the modified GTPase to the correct membrane (Alexandrov et al., 1994). In *S. cerevisiae*, REP is encoded by the essential *MRS6/MSI4* gene (Fujimura et al., 1994). Mrs6 is necessary for prenylation of the two essential GTPases Ypt1 and Sec4 via the GGTase II subunits Bet2 (β subunit) and Bet4 (α subunit) (Fig.3.1) (Jiang and Ferro-Novick, 1994).

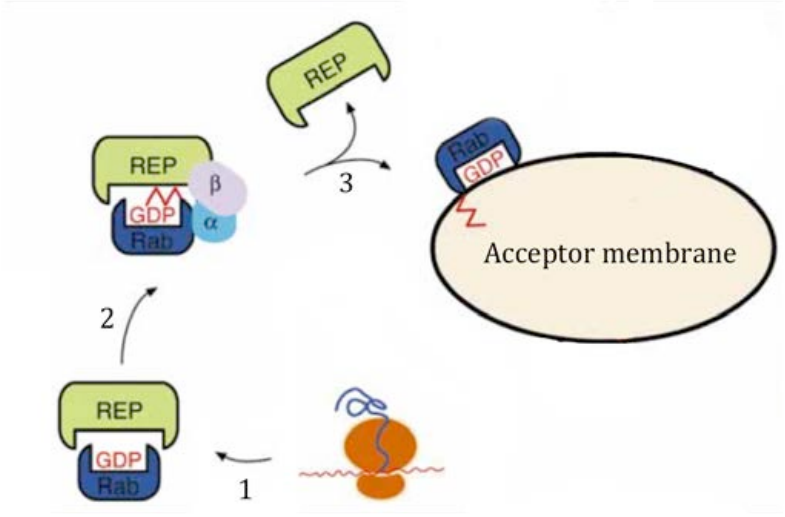

Figure 3.1 The Rab prenylation cycle. REP binds newly synthesized Rab in the cytosol (1) and delivers Rab to the GGTase II (complex composed of α and β subunits), which, in turn, it prenylates the Rab GTPase (2). Following prenylation, Rab is released from GGTase II and transferred to the acceptor membrane by REP (3). Figure adapted from (Alory and Balch, 2001).

The Mrs6 biological role is not limited to the Rab/Ypt regulation. Indeed, Mrs6 was found to influence two nodes of TORC1 regulation, one dependent on the zinc-finger protein Sfp1 and the other one independent (Lempiäinen et al., 2009; Singh and Tyers, 2009). Sfp1 is a member of the Cys_2His_2 zinc-finger family of DNA-binding proteins, and is predicted to be an RNA polymerase II transcription factor important for regulation of

cell size and activation of transcription of ribosomal protein genes (Blumberg and Silver, 1991; Fingerman et al., 2003; Jorgensen et al., 2004; Lempiäinen et al., 2009). TORC1 directly binds and phosphorylates Sfp1. These events are unaffected by either nutrient deprivation or osmotic stress. The Sfp1 phosphorylation by TORC1 and the Sfp1-Mrs6 interaction are necessary for Sfp1 nuclear localization. As part of a negative-feedback mechanism, the transcriptional activation function of Sfp1 causes a decrease in Sch9 phosphorylation by TORC1 (Lempiäinen et al., 2009). Controversially, another study proposed that Mrs6 negatively regulates Sfp1 by sequestering the transcription factor in the cytoplasm, thus preventing its nucleolar localization (Singh and Tyers, 2009). Besides this unclear aspect, Mrs6 is also required to positively regulate TORC1, since a temperature-sensitive allele of *MRS6* (*mrs6-2*) showed decreased Sch9 phosphorylation. Considering the above-mentioned negative feedback mediated by Sfp1, this function is predicted to be Sfp1-independent (Lempiäinen et al., 2009). Furthermore, mutation of the Mrs6 serine 335 (S335) to proline (S335P) and alanine (S335A) rendered the strain rapamycin resistant, while change to glutamate (S335E) resulted in sensitivity to and inability to recover from and rapamycin treatment (Singh and Tyers, 2009). How Mrs6 regulates TORC1 is still unknown.

Guanine nucleotide Dissociation Inhibitors (GDIs) are a class of proteins that preferentially bind the GDP-bound GTPase and inhibit spontaneous exchange of GDP for GTP. A recent study in mammals proposed the Sestrin proteins as negative regulators of mTORC1. Briefly, Sestrins function as GDIs for RagA/B, therefore keeping RagA/B GDP-bound and inhibiting mTORC1 relocation to the lysosome. Sestrins are characterized by a conserved amino acid motif, which is highly similar to the Rab GTPase-binding motif of Rab GDI. A peptide containing this motif is sufficient to inactivate mTORC1 (Peng et al., 2014). In *S. cerevisiae*, this GDI motif is found in only three proteins that are the monocarboxylate/proton symporter Jen1, the GDP dissociation inhibitor Gdi1, and Mrs6. Because of the connection with TORC1 signaling, this observation prompted us to test whether Mrs6 could be a GDI for Gtr2 by keeping the GTPase in its active GDP-bound state. Previous biochemical studies proposed that Gtr2 preferentially binds GTP instead of GDP (Jeong et al., 2012). A GDI protein would help to keep Gtr2 in its GDP-bound state when growing conditions, such as amino acid sufficiency, are compatible with TORC1 activation. Furthermore, *mrs6-2* was defective in TORC1 activity, and a similar result would be expected in the absence of a GDI favoring the $Gtr2^{GDP}$ form.

Finally, *mrs6*^{S335E} was characterized by its inability to recover from rapamycin treatment, a phenotype reminiscent of absence of any member of the EGO complex (Gtr1, Gtr2, Ego1, Ego2, and Ego3) (Singh and Tyers, 2009). In this chapter, I will describe our attempts to characterize Mrs6 as a regulator of Gtr2, and therefore of TORC1 signaling.

3.2 Results

3.2.1 The *mrs6-2* temperature sensitive mutant has impaired TORC1 activity already at the permissive temperature of 24°C

We initially sought to experimentally reproduce the previously published decreased TORC1 activity for the temperature sensitive form of Mrs6 (Lempiäinen et al., 2009). Therefore, we used the *mrs6-2* allele coming from our temperature sensitive (TS) collection of yeast mutants (Li et al., 2011). The *mrs6-2* strain has two point mutations, the replacement of glycine 227 by valine (G227V) and the replacement of serine 335 by proline (S335P) (Bialek-Wyrzykowska et al., 2000). We looked at *mrs6-2* TORC1 activity at the permissive temperature of 24°C and after 1 hour at 37°C. Phosphorylation of Sch9 was almost undetectable at both temperatures, confirming the involvement of Mrs6 in TORC1 regulation (Fig.3.2).

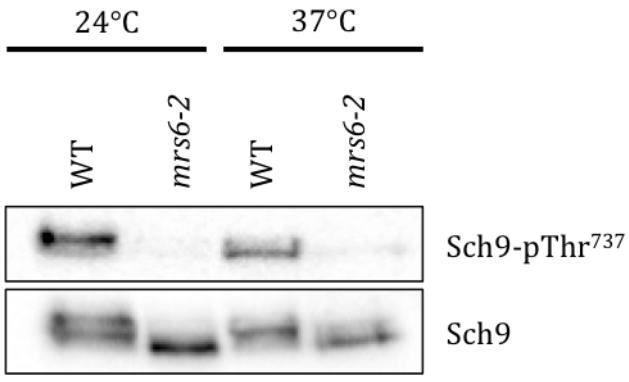

Figure 3.2 *mrs6-2* exhibits decreased TORC1 activity already at 24°C. Wild-type (WT) and *mrs6-2* cells were grown on YPD at 24°C until they reached an OD_{600} of 0.7. They were then grown at either 24 °C or 37 °C (to inactivate *mrs6-2*) for one additional hour before whole protein extraction. Specific antibodies recognizing the phosphorylated Thr737 (pThr737) of Sch9 and the total Sch9 were used to assay TORC1 activity. Representative immunoblots for both antibodies are shown.

3.2.2 The *mrs6*^{S335P} and *mrs6*^{S335E} strains have impaired TORC1 activity

The *mrs6*^{S335P} and *mrs6*^{S335E} mutants are known to cause increased resistance to rapamycin exposure, while the S335E causes sensitivity to and inability to recover from rapamycin treatment (EGO phenotype) (Singh and Tyers, 2009). Interestingly, the S335P mutation is also present in the *mrs6-2* strain (Bialek-Wyrzykowska et al., 2000). We made our own set of *mrs6* mutant alleles by inserting the desired point mutation in the genome and we characterized them for their growth rate, sensitivity to rapamycin treatment, EGO phenotype and TORC1 activity. The *mrs6*^{S335P} and *mrs6*^{S335E} mutations affected the growth of cells at 30°C, while *mrs6*^{S335A} had no obvious growth defect (Fig.3.3).

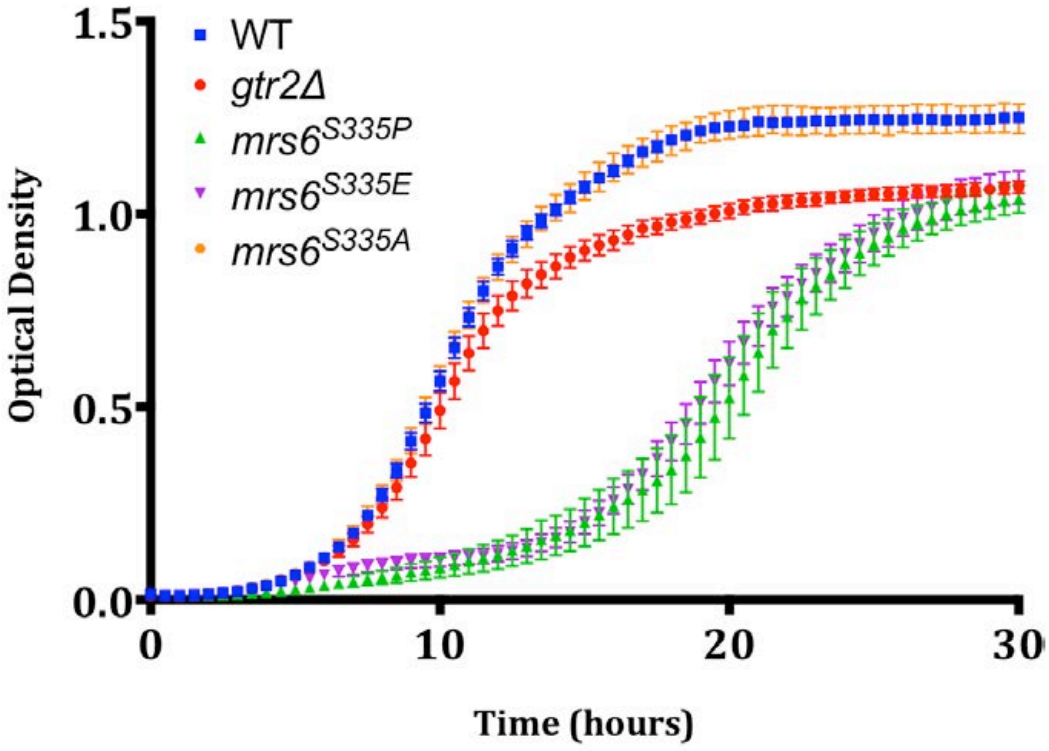

Figure 3.3 The *mrs6*^{S335P} and *mrs6*^{S335E} mutants have a slow growth phenotype. Wild-type (WT), *gtr2Δ* and *mrs6* mutant cells were grown on YPD at 30°C. Optical density for the indicated strains was measured every 30 minutes at 600 nm. Data are means ± S.D. from three independent experiments.

Concordantly with Singh and colleagues, *mrs6*^{S335P} showed a marginal rapamycin resistance (6 ng/ml). Conversely, the rapamycin resistance for *mrs6*^{S335A} and the rapamycin sensitivity for *mrs6*^{S335E} could not be confirmed. Moreover, we could not

reproduce the previously published EGO phenotype of *mrs6*^{S335E} (Singh and Tyers, 2009). The *mrs6*^{S335P} and *mrs6*^{S335E} strains presented a mild defect in recovery from rapamycin, which could be explained by their slower growth phenotype (Fig.3.4).

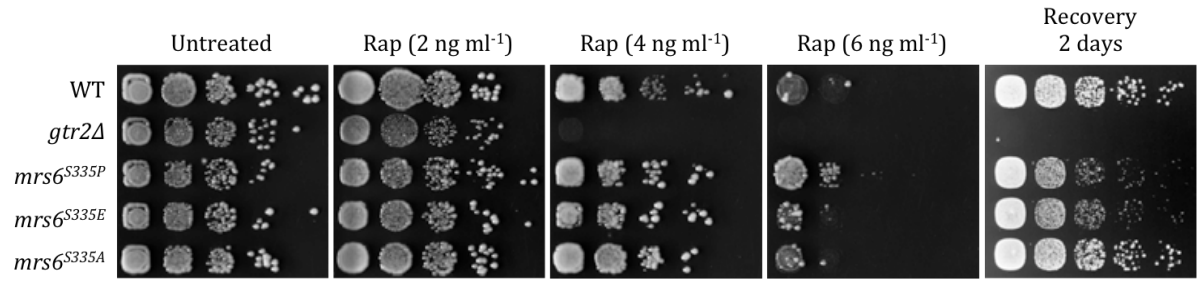

Figure 3.4 *mrs6*^{S335P} is slightly resistant to rapamycin. Wild-type (WT), *gtr2Δ* and *mrs6* mutant strains were grown on YPD until they reached an OD_{600} of 0.8. Serial 10-fold dilutions were spotted on YPD plates containing 0, 2, 4, or 6 ng/ml rapamycin. To test rapamycin recovery, cells were grown exponentially in YPD, treated for six hours with rapamycin (200 ng/ml), washed twice and spotted on YPD plates as described above. Pictures were taken after two days of incubation at 30°C.

The *mrs6*^{S335P} and *mrs6*^{S335E} strains presented reduced TORC1 activity compared to the wild-type strain. Instead, no obvious defect could be noticed in the *mrs6*^{S335A} strain (Fig.3.5).

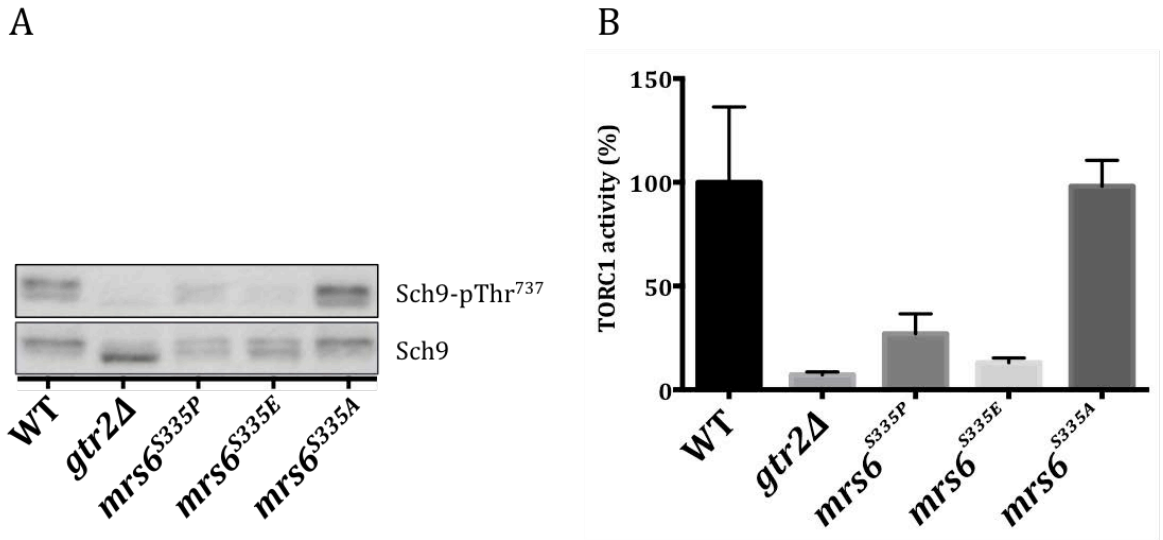

Figure 3.5 *mrs6*^{S335P} and *mrs6S*^{335E} have defective TORC1 activity. A) Prototrophic wild-type (WT), *gtr2Δ* and *mrs6* mutant strains were grown on SD without histidine, tryptophan, uracil, adenine and leucine (SD-HWUAL) at 30°C until they reached an OD_{600} of 0.8 before whole protein extraction. Immunoblot analysis was performed as in figure 3.2. B) Histogram representative of the TORC1 activity in *mrs6* mutants and controls assessed in A. TORC1 activity was calculated as the ratio of pThr^{737} Sch9/total Sch9 and normalized to the TORC1 activity of WT cells (set to 100%). Data are means ± SD from three independent experiments.

Since the S335A mutation did not differ from the wild-type regarding the tested phenotypes, it was not used for further experiments.

3.2.3 Gtr2^{S23L} overexpression cannot suppress the reduced TORC1 activity caused by S335P or S335E mutations in *MRS6*

In our prediction, if Mrs6 is an upstream positive regulator of Gtr2^{GDP}, overexpression of the nucleotide free Gtr2^{S23L} should suppress the reduced TORC1 activity in *mrs6^{S335P}* and *mrs6^{S335E}* strains. Conversely, TORC1 activity should remain sensitive to the S335P and E mutations during expression of GTP-locked Gtr1^{Q65L}. However, overexpression of either Gtr2^{S23L} or Gtr1^{Q65L} could not rescue the impaired TORC1 activity in *mrs6* mutants (Fig.3.6).

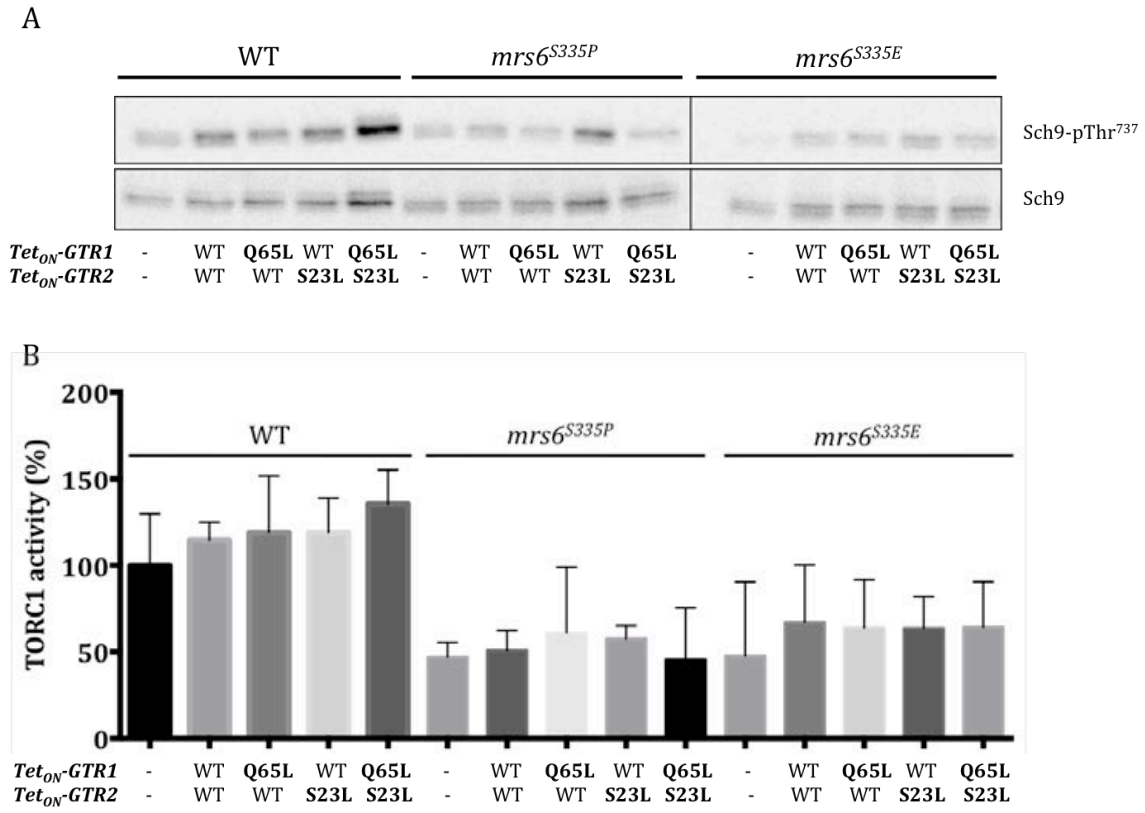

Figure 3.6 Gtr2^{S23L} does not suppress the reduced TORC1 activity of *mrs6^{S335P}* and *mrs6^{S335E}* strains. A) Prototrophic wild-type (WT), and *mrs6* mutant strains were expressing the indicated combination of plasmid-encoded Gtr1 and Gtr2 under the control of the doxycycline-inducible promoter *Tet$_{ON}$* (5 µg/ml for induction). Cells were grown and treated as in figure 3.5. Immunoblot analysis was performed as in figure 3.2. B) Histogram representative of the TORC1 activity in *mrs6* mutants and controls assessed in A. TORC1 activity was calculated as in figure 3.5. Data are means ± SD from three independent experiments.

Since the *mrs6*^{S335P} and *mrs6*^{S335E} strains used for this experiment were not deleted for the *GTR1* and *GTR2* genes, we speculated that the wild-type copies of *GTR1* and *GTR2* could interfere with the function of plasmid-encoded *GTR1* and *GTR2* alleles. Consequently, we deleted *GTR1* and *GTR2* in both *mrs6*^{S335P} and *mrs6*^{S335E} strains. Unfortunately, the resulting strains failed to show a reduced TORC1 activity when complemented by plasmid-encoded Gtr1^{WT} and Gtr2^{WT} (data not shown). We also tried to overexpress the *GTR1* and *GTR2* alleles in the *mrs6-2* mutant (TS). Again, after the required plasmid transformation steps, the *mrs6-2* control strain carrying empty vectors no longer showed reduced TORC1 activity, at both 24°C and 37°C (data not shown).

3.2.4 Mrs6 partially accumulates in the nucleus during nitrogen and glucose starvation

Although our genetic analysis could not clarify the role of Mrs6 in TORC1 regulation, we continued with the Mrs6 characterization thinking that other aspects, such as cellular localization, could help to better dissect its functions. Known Gtr1 regulators like Vam6 or the SEACIT localize to the vacuolar membrane (Binda et al., 2009; Panchaud et al., 2013). The Lst4-Lst7 complex, a GAP for Gtr2, also localizes to the vacuolar periphery upon amino acid starvation or rapamycin treatment (see Chapter 1, results section). Mrs6 has been visualized both in the cytoplasm and the nucleus, but not at the vacuolar membrane (Huh et al., 2003). However, it is still possible that vacuolar localization could be triggered by specific conditions such as deprivation of nutrients. Thus, we made a genomically-tagged *MRS6-GFP* strain to test its localization. The GFP tag did not alter the functionality of Mrs6, as assessed by TORC1 activity assay (data not shown). Mrs6 partially relocated to the nucleus during either nitrogen or glucose starvation, as confirmed by the nuclear marker Hhf2-TDimer. Nuclear relocalization seemed to be stronger during glucose starvation than during nitrogen starvation (Fig.3.7). Upon refeeding with the missing nutrients, Mrs6 appeared less concentrated in the nucleus. Mrs6 localization to the nucleus did not result in its exclusion from the cytoplasm.

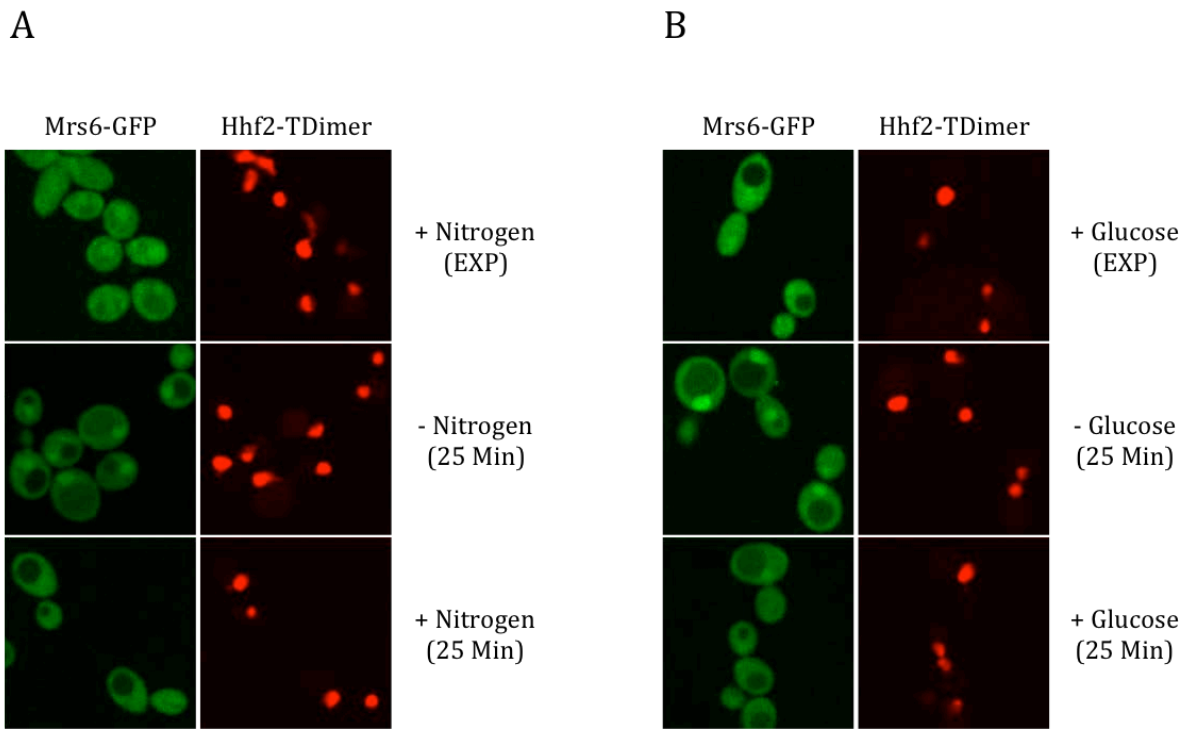

Figure 3.7 Mrs6 partially concentrates to the nucleus during nitrogen or glucose deprivation. Prototrophic cells expressing genomically-tagged Mrs6-GFP and Hhf2-TDimer (nuclear marker) were initially grown in SD with all amino acids (SC). Next, they were nitrogen (A) or glucose deprived (B) and refed for the indicated times. Samples were analyzed by fluorescence microscopy.

Since TORC1 could be the mediator of the partial Mrs6 relocalization following nutrient deprivation, we next treated cells using either rapamycin or cycloheximide, which inactivates or hyper-activates TORC1, respectively. However, neither treatment induced nuclear accumulation of Mrs6-GFP (Fig.3.8).

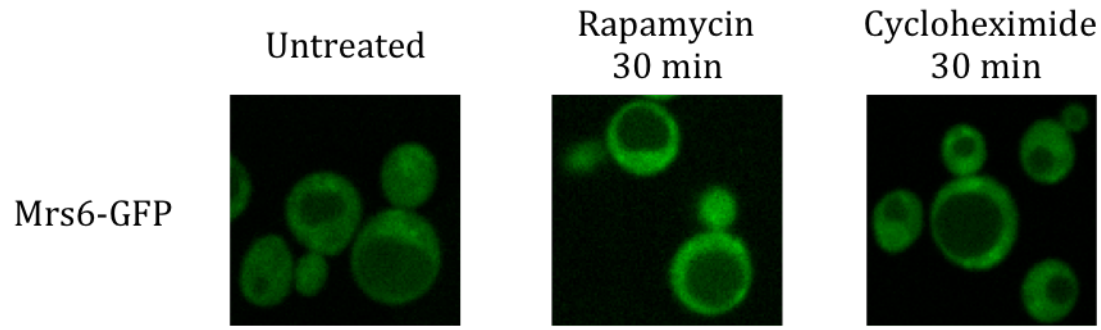

Figure 3.8 Subcellular distribution of Mrs6-GFP is not responsive to rapamycin/cycloheximide treatment. Prototrophic exponentially growing cells expressing genomically-tagged Mrs6-GFP were grown in SC. Cells were then threated with rapamycin (200 ng/ml), or cycloheximide (25 μg/ml), or left untreated for the indicated time. Samples were analyzed as in figure 3.7.

3.2.5 Two PKA consensus sites in the N-terminus of Mrs6 control its localization to the nucleus

Since Mrs6 accumulates in the nucleus under certain conditions, we reasoned that a nuclear localization signal (NLS) sequence could be responsible for Mrs6 localization. Accordingly, we used the SeqNLS tool to scan the Mrs6 amino acid sequence for putative NLSs (Lin et al., 2012). The SeqNLS tool predicted a putative NLS at the N-terminus of Mrs6 (Fig.3.8). Remarkably, the residues S3 (close to the predicted NLS) and S9 (within the predicted NLS) were found to be phosphorylated in large-scale studies (Albuquerque et al., 2008; Swaney et al., 2013). Furthermore, the predicted NLS sequence also presented two putative PKA target sites (RRXS), predicted to be phosphorylated by the PKA kinase on serines S9 and S16 (Singh and Tyers, 2009). PKA is a protein kinase that plays a fundamental role in the nutritional control of metabolism, cell cycle, growth, stress resistance, and transcription. Availability of nutrients, such as the presence of a rapidly fermentable sugar and amino acids, controls all these properties (Rubio-Texeira et al., 2010). Thus, we constructed a plasmid expressing *MRS6* with the residues S3, S9 and S16 mutated to alanine (*mrs6*^{AAA}) or to the phospho-mimetic glutamate (*mrs6*^{EEE}) (Fig.3.9).

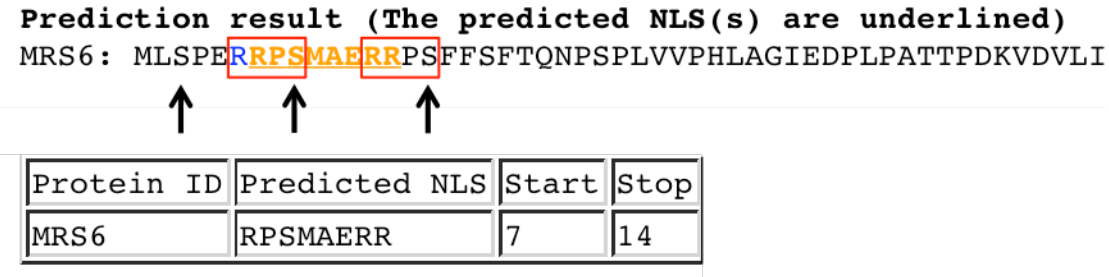

Figure 3.9 Mrs6 is predicted to have a nuclear localization signal at its N-terminus. The predicted NLS in Mrs6 amino acid sequence is colored in orange (only the first 50 amino acid residues of Mrs6 are shown). Red boxes define the two predicted PKA sites (RRXS motif). Black arrows define the serine residues that were mutated in alanine (A) or glutamate (E).

Mrs6^{AAA}-GFP partially concentrated in the nucleus already in exponentially growing cells (Fig.3.10C). Glucose starvation and readdition did not alter Mrs6^{AAA} nuclear accumulation. Noticeably, Mrs6^{EEE} localized similarly to Mrs6^{AAA} (Fig.3.10B). The similar behavior between the two mutants is likely caused by the glutamate mutations not behaving as phospho-mimetic residues.

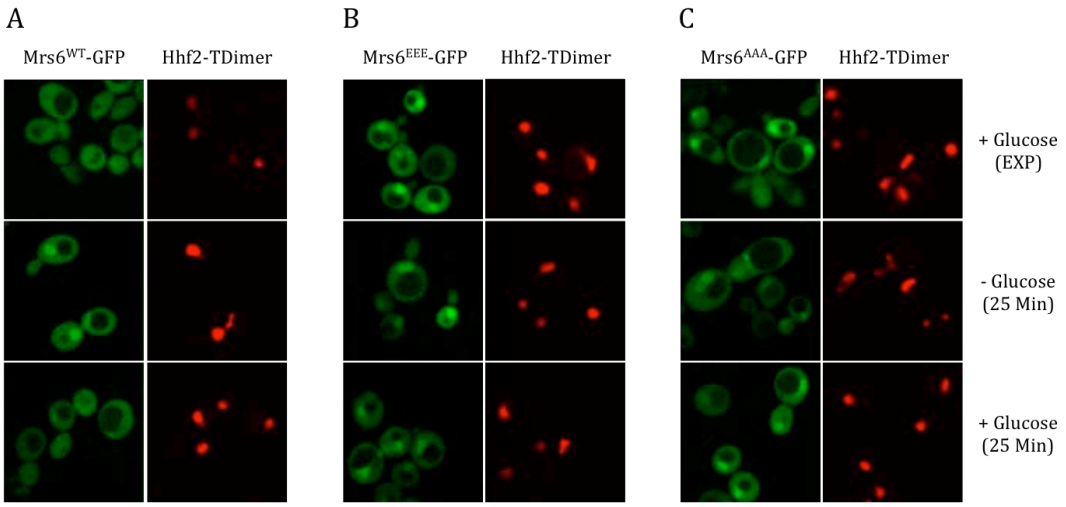

Figure 3.10 Mrs6^{AAA}-GFP and Mrs6^{EEE}-GFP partially localize to the nucleus independently of glucose availability. Prototrophic wild-type (WT) cells expressing plasmid encoded Hhf2-TDimer (nuclear marker) and Mrs6^{WT}-GFP (A), Mrs6^{EEE}-GFP (B), or Mrs6^{AAA}-GFP (C) were initially grown in SC, then starved and refed for glucose for the indicated times. Samples were analyzed as in figure 3.7.

3.2.6 Mrs6 specifically interacts with Gtr2 and Gtr2^{Q66L}, but not Gtr1

Next, we tested the interaction between Mrs6, Gtr1 and Gtr2 (Fig.3.11). We also checked the interaction between Mrs6, Gtr2^{Q66L} (GTP-locked allele) and Gtr2^{S23L} (nucleotide-free) by co-immunoprecipitation experiments (Fig.3.11).

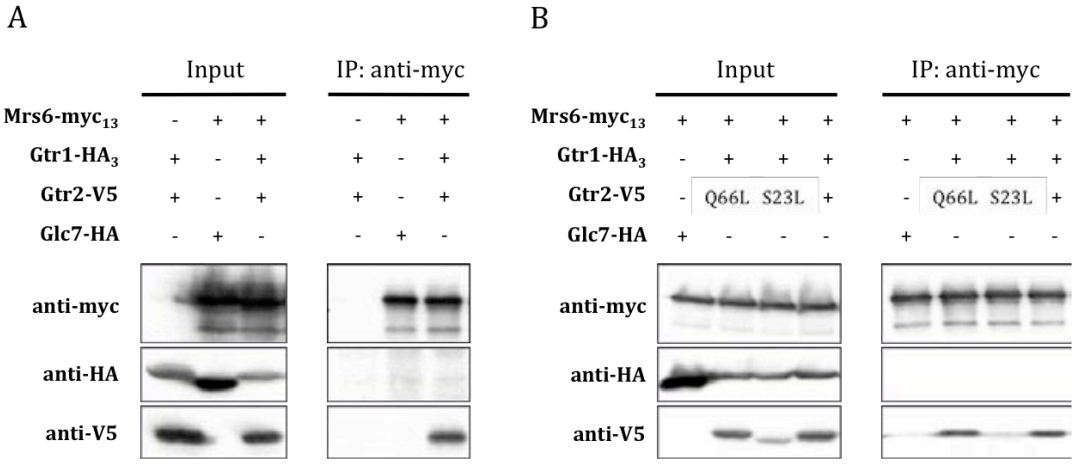

Figure 3.11 Mrs6 specifically interacts with Gtr2. A) Control experiment showing specific interaction of Mrs6-myc$_{13}$ with Gtr2-V5, but not with Glc7-HA. B) Mrs6-myc$_{13}$ interaction with Gtr2-V5 and Gtr2^{Q66L}-V5. Prototrophic exponentially growing *gtr1Δgtr2Δ* and *gtr1Δgtr2Δ MRS6-myc$_{13}$* cells carrying the indicated *GTR1* and *GTR2* expression plasmids were grown in YPD, and respective lysates were immunoprecipitated for Mrs6-Myc$_{13}$. Cells expressing Glc7-HA were used as control. Lysates (input) and anti-myc immunoprecipitates (IP: anti-myc) were analyzed by immunoblotting with anti-myc, anti-HA and anti-V5 antibodies.

Mrs6 did not interact with the control Glc7 or Gtr1 (Fig.3.11A). Conversely, Mrs6 could bind Gtr2 and $Gtr2^{Q66L}$ (Fig.3.11B). Finally, we could not visualize interaction between Mrs6 and $Gtr2^{S23L}$ (Fig.3.11B). This result could also be caused by the lower protein amount of $Gtr2^{S23L}$ compared to Gtr2 or Gtr^{Q66L} in the input blot.

3.2.7 Glucose refeeding, but not starvation, weakens the Mrs6-Gtr2 interaction

Mrs6 nuclear localization is increased by nutrient withdrawal such as glucose starvation. We reasoned that this could be a mechanism to avoid or limit the Mrs6-Gtr2 interaction, resulting in TORC1 inactivation. Therefore, we looked at the Mrs6-Gtr2 interaction during glucose starvation and readdition. Mrs6 similarly interacted with Gtr2 in the starting condition (EXP) and during glucose starvation (Fig.3.12). Intriguingly, the Mrs6-Gtr2 interaction weakened over time after glucose refeeding. Gtr1 and Gtr2 protein levels decreased upon glucose starvation and raised again following glucose readdition. This unexpected result could reflect a regulatory mechanism in which TORC1 is activated/inactivated also via fluctuation in the Gtr1/Gtr2 levels. Further experiments would be required to test this hypothesis.

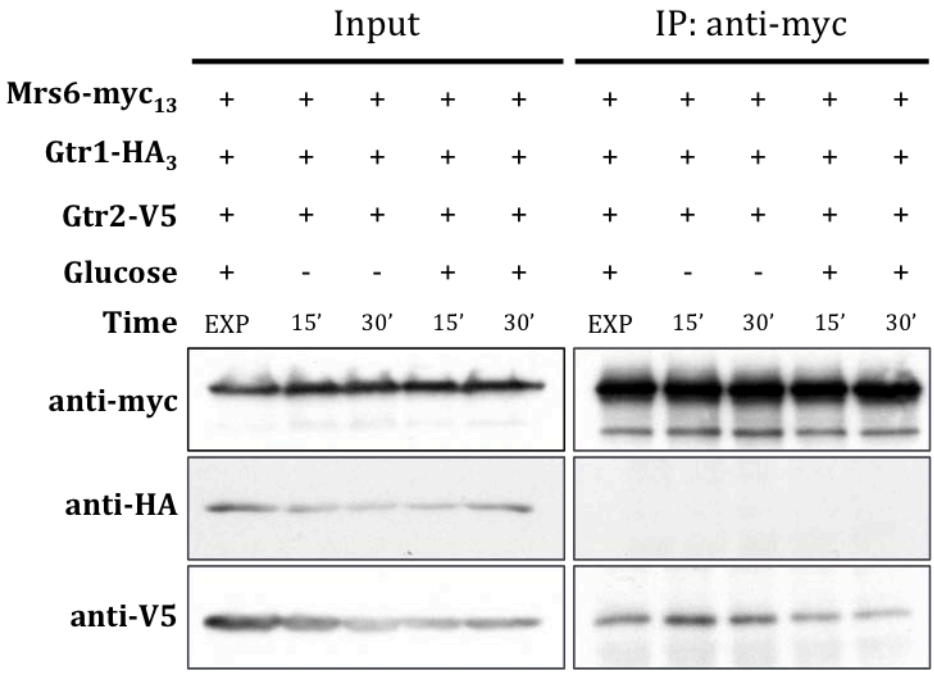

Figure 3.12 Mrs6-Gtr2 interaction is weakened during glucose readdition. Prototrophic *gtr1Δgtr2Δ MRS6-myc13* cells carrying the indicated Gtr1 and Gtr2 expressing plasmids were grown exponentially in YPD (EXP), then starved and refed for glucose at the indicated time points. Lysates (input) and anti-myc immunoprecipitates (IP: anti-myc) were analyzed as in figure 3.11.

3.2.8 Gtr2 cellular distribution is unaffected by changes in glucose availability

Since Mrs6 interacted better with Gtr2 during glucose starvation, we wondered whether Gtr2 could re-localize to the nucleus under such a condition. Unlike Mrs6, Gtr2 did not change its vacuolar localization following glucose starvation (Fig.3.13A). Gtr2 colocalized neither with Mrs6 nor with the Hhf2-TDimer nuclear marker (Fig.3.13A and B).

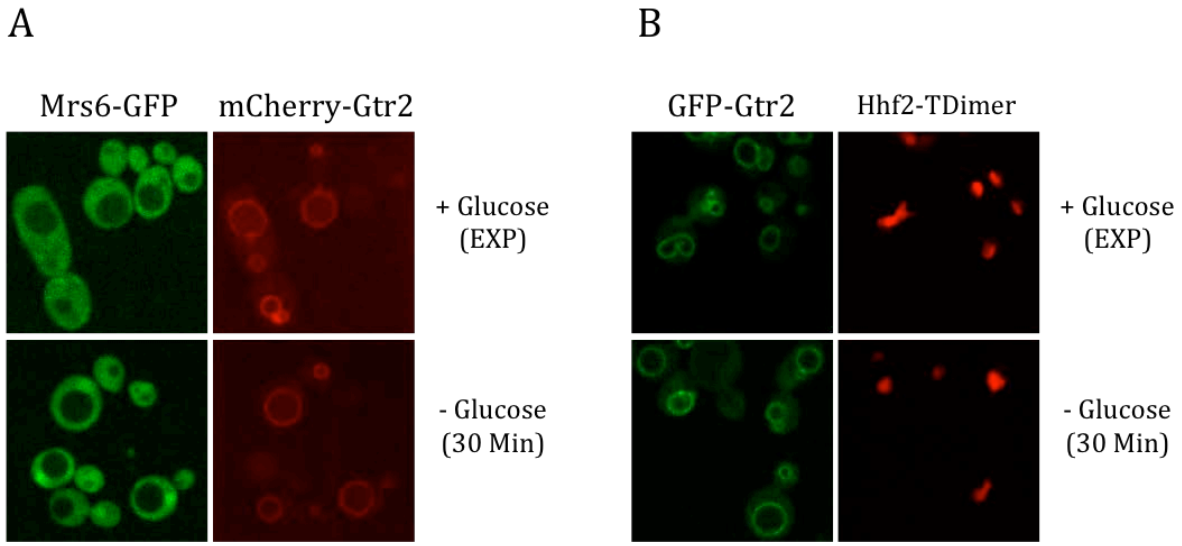

Figure 3.13 Mrs6 and Gtr2 do not colocalize during glucose starvation. A) Prototrophic genomically-tagged Mrs6-GFP cells expressing a plasmid-encoded mCherry-Gtr2 were initially grown in SC. Cells were then glucose deprived for the indicated time. B) Prototrophic *gtr2Δ* expressing plasmid-encoded GFP-Gtr2 and Hhf2-TDimer were grown and treated as in figure 3.12A. Samples were analyzed by fluorescence microscopy.

3.3 Discussion

In this chapter we have tried to better understand the role of Mrs6 in TORC1 signaling. Although we discovered that both S335P and S335E mutations caused decreased TORC1 activity, overexpression of the nucleotide free $Gtr2^{S23L}$ could not restore normal TORC1 activity. However, this result could be explained from two different perspectives. First, proper experimental settings would require a *gtr1Δgtr2Δ mrs6* mutated strain, since the endogenous Rag GTPases could interfere with the plasmid-encoded ones. Unfortunately, we could not achieve this goal. Any manipulation of the $mrs6^{S335P}$ and $mrs6^{S335E}$ strains to delete the Rag GTPase genes resulted in disappearance of the original low TORC1 activity phenotype. Furthermore, a similar result was obtained

during transformation of the *mrs6-2* temperature-sensitive strain (which has the G227V and S335P mutations). Second, as indicated in figure 3.14, the S335P and E mutations lie on a region adjacent to the Mrs6 Rab-binding platform.

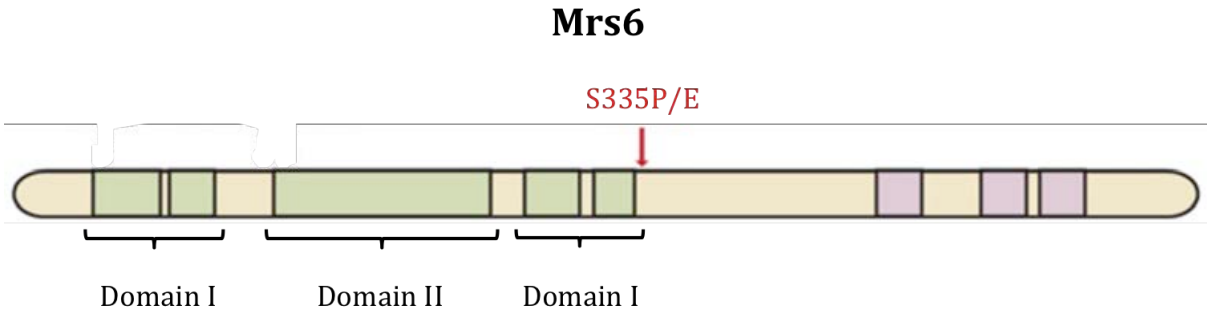

Figure 3.14 Location of the S335P and E amino acid substitutions in Mrs6. Conserved regions of REP proteins are indicated in purple. Conserved structural domains of REP and Rab GDI proteins are indicated in green and they can be further divided in domains I and II. The former functions as Rab-binding platform. The latter promotes the REP-GGTase II interaction (Alory and Balch, 2003). The red arrow allocates the S335P and E mutations in Mrs6. Figure adapted from (Singh and Tyers, 2009).

Mutations in this region cause a decrease in the total amount of prenylated membrane-bound Ypt1 (Alory and Balch, 2003). Ypt1 and its mammalian ortholog Rab1A have been demonstrated to be essential for TORC1/mTORC1 activation. Additionally, GTP-bound Ypt1 interacts with TORC1 (Thomas et al., 2014). As part of the Rab GTPases cycle, GTP loading of Ypt1 requires prenylation and membrane attachment of the GTPase (Alory and Balch, 2001). Therefore, it could be possible that the Mrs6 S335P and E mutations alter TORC1 activation also via reduction of the Ypt1 active fraction. This hypothesis could be test by evaluating the interaction of the Mrs6 mutated proteins with Ypt1 by co-immunoprecipitation. Alternatively, it could be assessed if the amount of membrane-bound Ypt1 is reduced in the *mrs6* mutants (Alory and Balch, 2001). However, mutagenesis of the residue S335 could result in alteration of many other regulatory pathways. Indeed, it has been suggested that the Sfp1 transcription factor competes with Ypt1 for the same interface on Mrs6. (Singh and Tyers, 2009). If the S335 residue is specifically involved in Gtr2 regulation, the interaction of the $Mrs6^{S335P}$ and $Mrs6^{S335E}$ proteins with Gtr2 should be tested. Furthermore, eventual modifications of Gtr2 localization in the $mrs6^{S335P}$ and $mrs6^{S335E}$ strains might be checked. Otherwise, a mutagenesis approach would be required to find hypothetical mutations not impinging on the REP and Sfp1 regulatory functions of Mrs6.

In support of the GDI model, Mrs6 specifically binds Gtr2. Co-immunoprecipitation experiments have shown that Mrs6 binds the GTP-locked Gtr2^{Q66L}. However, the interaction with Gtr2^{Q66L} is not surprising. Sestrin proteins, which have been proposed to negatively regulate TORC1 by functioning as GDIs for RagA/B, can actually bind to a GTP-locked RagB (Peng et al., 2014). A similar behavior could be expected from the Mrs6- Gtr2^{Q66L} interaction. An *in vitro* binding assay using purified Mrs6 and Gtr2 could further confirm the interactions seen *in vivo*. Regarding the absence of interaction between Mrs6 and Gtr2^{S23L}, the result could be explained by either an expression/stability problem for *gtr2^{S23L}* allele (as mentioned in 3.2.6) or the nature of the S23L mutation. The Gtr2^{S23L} protein is predicted to be nucleotide free and not GDP-locked. We need to take in account that Gtr2^{S23L} could have a different conformation from GDP-bound Gtr2, and therefore it could not properly interact with Mrs6. The observation that the Mrs6-Gtr2 interaction is stable during glucose starvation and weakened upon glucose readdition complicates our GDI model for Mrs6. It could be speculated that Mrs6 needs a third factor to regulate Gtr2 that is inactive during glucose starvation. Thus, the observed interaction with Gtr2 might be ineffective. Upon glucose readdition, Mrs6 binds less Gtr2 maybe as a consequence of a homeostatic mechanism to avoid over stimulation of TORC1. Eventually, Mrs6 pull-down in presence and absence of glucose could clarify, by mass-spectrometry analysis, if a specific Mrs6 interactor is missing during glucose deprivation. Additionally, the Mrs6-Gtr2 interaction should be tested also during nitrogen starvation.

Our experiments contributed to the characterization of the biological behavior of Mrs6. We could demonstrate that stresses such as nutrient deprivation prompt a partial relocation of Mrs6 in the nucleus. A similar result was obtained by switching yeast cells from glucose to glycerol as a main carbon source (Singh and Tyers, 2009). The subcellular localization is controlled by a nuclear localization signal (NLS) that has to PKA conserved motifs (RRXS). Alanine mutagenesis of the S residues of the PKA motifs is sufficient to trigger accumulation of a fraction of Mrs6 in the nucleus independently from glucose availability. Our *mrs6* NLS alanine mutant (*mrs6^{AAA}*) was expressed from a plasmid over the endogenous *MRS6* gene, thus we could only evaluate the effect of the mutation on Mrs6 localization. It would be interesting to test a genomically-mutated Mrs6^{AAA} and, if viable, to see if it has an effect on TORC1 signaling, if its interaction with Gtr2 is changed by the mutation and if the localization of Gtr2 is altered in a *mrs6^{AAA}*

mutant strain. We could exclude that TORC1 regulates phosphorylation of the NLS because neither rapamycin nor cycloheximide treatment altered Mrs6 cytosolic localization. Furthermore, TORC1 did not phosphorylate these sites *in vitro* (Serena Raucci, personal communication). Gtr2 and Mrs6 did not co-localize during glucose starvation. However, it is just a fraction of Mrs6 that moves to the nucleus. Therefore, the remaining cytosolic fraction of Mrs6 could still interact with Gtr2, even though no vacuolar recruitment of Mrs6 was observed. To better understand where Mrs6 and Gtr2 are interacting, it could be used a split-GFP system in which a fragment of split-GFP is appended to Mrs6 and the other to Gtr2. Therefore, a GFP signal should be visualized only when Mrs6 and Gtr2 are interacting, thus allowing the two GFP fragments to reassemble in a functional GFP molecule.

Curiously, in the paragraph 2.2.7 we noticed that a fraction of Gtr2 is likely recruited in the nucleus in a *gtr1Δ* strain. Is this effect dependent on Mrs6? Ideally, a conditional *mrs6* mutant, such as the temperature sensitive strain *mrs6-2*, could answer this question by looking at the Gtr2 localization in both permissive and not-permissive conditions.

In conclusion, we could not demonstrate that Mrs6 is a GDI for Gtr2, even though we obtained few "hints" regarding the Mrs6 regulation. Our genetic experiments presented technical limitations that could not be quickly solved. Currently, we are testing by *in vitro* nucleotide exchange assays if Mrs6 could still function as a GDI for Gtr2.

General Discussion

Future perspectives for refined understanding of the function of the Lst4-Lst7 complex

The discovery of the Lst4-Lst7 complex as a GAP for the Rag GTPase Gtr2 gives is an important contribution to the understanding of the TORC1 signaling pathway. However, as for every new finding, new questions arose that are partially or still unsolved. We demonstrated that the Lst4-Lst7 complex is recruited to the vacuolar membrane during amino acid starvation and rapamycin treatment. Additionally, it has been reported that prolonged glucose starvation (one hour) triggers a similar recruitment of the Lst4-Lst7 complex to the membrane (Pacitto et al., 2015). Following amino acid readdition to starved cells, the Lst4-Lst7 complex leaves the vacuolar membrane. How is the Lst4-Lst7 localization regulated? An ongoing study in our laboratory addresses the possibility that several serine and threonine residues within Lst4 may be directly phosphorylated by TORC1 *in vitro*. Most of these residues are located in a large region predicted to be unstructured within the C-terminal DENN domain (intra-DENN loop) (Pacitto et al., 2015). Mutagenesis of these residues to alanines generated an *lst4* mutant that constitutively localized at the vacuolar membrane. Conversely, mutagenesis of these sites in the phospho-mimetic amino acid aspartate generated an *lst4* mutant that could not be recruited to the vacuolar membrane. Thus, it could be speculated that TORC1 phosphorylates Lst4 to trigger Lst4-Lst7 complex removal from the vacuolar membrane and to prevent its recruitment, as part of a feedback inhibitory loop. This mechanism could be required to accurately tune TORC1 activation and avoid its over stimulation (Marie-Pierre Péli-Gulli, personal communication). It is currently not clear if Lst4 directly binds to the vacuolar membrane or whether it has a binding partner, which locates already at the vacuolar surface. Pull-down experiment with Lst4 under two different conditions (exponentially growing cells treated with vehicle or rapamycin for 30 minutes) could possibly identify presumed Lst4-interacting partners on the vacuole surface.

Following amino acid starvation, recruitment of the Lst4-Lst7 complex to the vacuolar membrane is not sufficient to trigger its interaction with Gtr2, which requires readdition of amino acids. It might be reasoned that a third factor is either required for Lst4/Lst7 to interact with Gtr2 upon amino acid readdition, or to inhibit binding of Lst4-Lst7 to Gtr2 upon amino acid starvation. The second hypothesis seems to be more

plausible because Lst4-Lst7 purified from bacteria do not need other factors to activate Gtr2 GTP hydrolysis activity *in vitro*. However, the first hypothesis cannot be discarded because we do not know if our *in vitro* biochemical data are just reflecting the Lst4-Lst7 basal GAP activity. We previously compared the list of binding partners of Lst7 in exponentially growing and rapamycin treated cells (data not shown). Unfortunately, we could not find interesting candidate proteins that specifically interacted with Lst7 under one of these conditions. It would be required to improve the experimental settings. Furthermore, we only looked at Lst7 interacting proteins, but Lst4 pull-down should be tested as well, because of possible specific interactions with one of the two subunits of the Lst4-Lst7 complex. Finally, a more physiological condition (*i.e.* amino acid starvation) should be tested instead of rapamycin treatment when carrying on these pull-down experiments.

Amino acids readdition to starved cells is sufficient to trigger the interaction of Lst4-Lst7 with Gtr2. Strikingly, specific amino acids such as glutamine can trigger this interaction as well and consequently re-activate TORC1. How the Lst4-Lst7 complex senses the amino acid availability signal is still an open question. One possibility would be that Lst4 and/or Lst7 could directly sense changes in concentration for specific amino acids. Recent studies in mammals have shown that Sestrin2 and CASTOR1, two negative regulators of mTORC1, can directly bind leucine and arginine, respectively, thus functioning as direct sensors. The leucine/arginine binding of Sestrin2/CASTOR1 results in conformational changes that abolish their negative effect on mTORC1 signaling. A similar mechanism could instead activate the interaction of the Lst4-Lst7 complex with Gtr2. The crystal structure of the Lst4-Lst7 heterodimer would be required to test this hypothesis. At the moment, only the Lst4 N-terminal longin domain has been crystallized and no obvious amino acid binding region has been found (Pacitto et al., 2015). Furthermore, it could be tested if the Lst4-Lst7 complex binds specific amino acids by using their radioactive form. Alternatively, amino acid availability could be sensed indirectly via a third partner protein, such as a vacuolar amino acid transporter. In mammals, the lysosomal membrane-localized glutamine/arginine transporter SLC38A9 interacts with the Rag GTPases in an amino acid-dependent manner and directly communicates amino acid levels to the Rag GTPases. The transporter has a positive role in mTORC1 signaling since its disruption results in the decrease of mTORC1 activity in response to arginine stimulation (Rebsamen et al.,

2015; Wang et al., 2015). It is not excluded that an analogous mechanism could regulate the Lst4-Lst7 complex. Amino acids could be sensed by a vacuolar amino acid permease, which in turn may stimulate the interaction between Lst4-Lst7 and Gtr2, the GTP-to-GDP transition of Gtr2, and finally the activation of TORC1. Members of the Avt family of amino acid permeases (*i.e.* Avt1-7) might be interesting candidates to fulfill such a role. Furthermore, Avt2 appears to be the most closely related yeast protein to SLC38A9.
At the moment, the main function of the Lst4-Lst7 complex in the TORC1 signaling pathway seems to be elucidated. However, its regulation is only partially understood and more efforts are still required to better characterize this regulatory branch.

Implication of FLCN-FNIP1/2 complex in human diseases

The Birt-Hogg-Dubé (BHD) syndrome is a hereditary cancer syndrome caused by germline mutations in the FLCN gene, the human Lst7 homolog, that predispose to chromophobe RCC, hybrid oncocytic renal tumors, and renal oncocytomas (Nickerson et al., 2002). The FLCN mutations described often cause FLCN loss of function because of premature stop codons (Schmidt and Linehan, 2015). Furthermore, conditional inactivation of FLCN in adult mouse kidney epithelial cells results in mTORC1 activation, abnormal cell proliferation, polycystic kidney disease and renal failure (Baba et al., 2008). Similarly, double knockout FNIP1 and 2 mice developed enlarged polycystic kidneys, while *Fnip1* heterozygous/*Fnip2* homozygous knockout mice produced kidney tumors (Baba et al., 2012; Hasumi et al., 2015). Because of these results, FLCN and FNIP1/2 are considered tumor suppressor genes. However, it has been demonstrated that the FLCN-FNIP1/2 complex (and its yeast counterpart, the Lst4-Lst7 complex) is a positive regulator of mTORC1, and is required to support the RagC/D GDP bound form (Tsun et al., 2013). Strikingly, an activator of the mTORC1 pathway (as the FLCN-FNIP1/2 complex is) is not expected to be a tumor suppressor, but rather a proto-oncogene. Activation of mTORC1 signaling was shown in human and in some mouse kidney cells upon loss of FLCN (Hasumi et al., 2009). However, activation/inactivation of mTORC1 caused by FLCN loss is thought to be dependent on experimental conditions and the cell type used (Baba et al., 2016). Tsun and colleagues proposed that impairment of the mTORC1 signaling caused by FLCN loss could be suppressed by de-regulation of other pathways, therefore explaining the increased

mTORC1 activity in FLCN null cells (Tsun et al., 2013). This hypothesis is supported by the pleiotropic role of FLCN. Indeed, FLCN not only regulates activation of the mTORC1 pathway, but it is also involved in modulation of the AKT pathway, cell-cell adhesion and RhoA signaling (Schmidt and Linehan, 2015). Furthermore, the FLCN-FNIP1/2 complex has been proposed both as a positive and negative regulator of the AMPK pathway (Reyes et al., 2015; Siggs et al., 2016). The important effects of FLCN and FNIP1 in cancer warrant future investigations on the role of the FLCN-FNIP1/2 complex in the AMPK, AKT and mTORC1 pathways.

Identification of novel Gtr1/Gtr2 and TORC1 regulators

The small-scale screening described in chapter II demonstrated its high potential in finding Gtr1/Gtr2 and/or TORC1 regulators. Interestingly, we discovered the *gtr2*^{C231W} mutant that is no longer sensitive to Gtr1^{S20L}-mediated growth inhibition even though this mutation does not alter its positive role in signaling toward TORC1, at least in the conditions we tested. Potentially, this approach could allow us to further increase the knowledge regarding already known TORC1 regulators, via characterization of their mutant versions. Regarding the *gtr2*^{C231W} mutant, more experiments are required to clarify its biological effect. The properties of this mutant support a model in which Gtr1^{S20L} (and likely Gtr1^{GDP}) impacts on TORC1 via Gtr2. It has already been reported that the GTP/GDP loading status of Gtr2 can likely influence the GTP-hydrolysis rate of Gtr1 (Panchaud et al., 2013). Although a Gtr1^{GDP} crystal structure has not been obtained, the G domain of Gtr1 is predicted to undergo a conformational change similar to that of Gtr2 when changing from its GTP- to GDP-bound status (Jeong et al., 2012). This prediction would raise the plausible idea that, within the Gtr1-Gtr2 heterodimer, the nucleotide-binding state of one G domain could influence that of the other. C231 locates in the CTD domain of Gtr2, more precisely on the α8-helix that is involved in dimerization with the Gtr1 CTD. Differently from the G domain, the CTD domain of Gtr2 appears not to change its conformation when the GTPase switches between GTP and GDP. However, it makes several interactions with the G domain of GDP-loaded Gtr1. These interactions are predicted to stabilize the GDP-bound conformation (Jeong et al., 2012). We therefore thought about a model in which Gtr1^{S20L} (and probably GDP-loaded Gtr1) induces a conformational change in Gtr2, resulting in TORC1 inactivation and

growth inhibition. The C231W mutation could make Gtr2 less susceptible to this Gtr1-dependent inactivation, thus the *gtr2*^{C231W} strain does not show growth inhibition during Gtr1^{S20L} overexpression. Computational analysis on the effect of the C231W substitution on the Gtr2 structure could help to verify if our model is correct. Furthermore, it should be tested if a *gtr2*^{S23L} and a double *gtr2*$^{S23L/C231W}$ mutant strains, similarly to the *gtr2*^{C231W} strain, can suppress the Gtr1^{S20L}-mediated growth inhibition.

In addition to the genetic approach, further biochemical strategies may also be adopted to identify new Rag GTPase regulators. For this purpose, the APEX2 system is of particular interest. The method takes advantage of the properties of the monomeric peroxidase reporter 2 (APEX2), an engineered protein that can oxidize numerous phenol derivatives to phenoxyl radicals, which can, in turn, covalently react with electron-rich amino acids such as tyrosine. Briefly, addition of H_2O_2 and biotin-phenol to living cells expressing the APEX2 protein generate a biotin-phenoxyl radical that covalently tag endogenous proteins proximal to APEX2 within a minute. Biotinylated proteins can then next be purified and analyzed by mass spectrometry. Genetic targeting of APEX2 to a cellular organelle or protein complex of interest by protein fusion results in spatial restriction of the biotinylated proteins. Hence, the APEX2 tool allows for proteomic mapping of subcellular compartments as well as identification of dynamic protein complexes (Lam et al., 2015; Rhee et al., 2013). This method has been demonstrated to be successful also in *S. pombe*, where APEX2 was fused to the Golgi protein Dsc5, and the specific Dsc5 binding partner Cdc48 could be recovered (Hwang and Espenshade, 2016). Ideally, an APEX2-Gtr1 or Gtr2 fusion protein would allow the identification of their binding partners. Additionally, under different growth condition (*i.e.* upon amino acid starvation or restimulation) different interacting proteins could be discovered.

Materials and Methods

Strains and plasmids

Strains and plasmids used in this study are listed in tables in the next section.

Growth conditions

Unless stated otherwise, prototrophic strains were pre-grown overnight in synthetic dropout (SD) medium (0.17% yeast nitrogen base, 0.5% ammonium sulfate, 0.2% dropout mix, and 2% glucose) to maintain plasmids. Before each experiment, cells were diluted to an OD_{600} of 0.2 and further grown at 30°C until they reached an OD_{600} of 0.8.

Doxycycline induction

Doxycycline (stock solution: 5 mg/ml in ethanol) was added to the specified medium to a final concentration of 5 µg/ml to express genes under control of the Tet_{ON} promoter.

Galactose induction

For galactose induction, precultures were grown on SD. Exponentially growing cells were further grown in synthetic galactose medium (SGal; 0.17% yeast nitrogen base, 0.5% ammonium sulfate, 2% galactose).

Amino acid deprivation and re-addition

For amino acid deprivation experiments, cells were grown in synthetic complete medium without ammonium sulfate (SC w/o AS; 0.17% yeast nitrogen base, 0.2% of the complete mix of all amino acids, and 2% glucose). At an OD_{600} of 0.8, cells were filtered and transferred to nitrogen starvation medium (SNM; 0.17% yeast nitrogen base, and 2% glucose). For restimulation by amino acids, cells in SNM medium were filtered and transferred back to SC w/o AS.

Nitrogen deprivation and re-addition

For nitrogen deprivation experiments, cells were grown in synthetic complete medium (SC; 0.17% yeast nitrogen base, 0.5% ammonium sulfate, 0.2% of the complete mix of all amino acids, and 2% glucose). At an OD_{600} of 0.8, cells were filtered and transferred to nitrogen starvation medium (SNM; 0.17% yeast nitrogen base, and 2% glucose). For restimulation by nitrogen, cells in SNM medium were filtered and transferred back to SC.

Glucose deprivation and re-addition

For glucose deprivation experiments, cells were grown in SC. At an OD_{600} of 0.8, cells were filtered and transferred to glucose starvation medium (SGM; 0.17% yeast nitrogen base, 0.5% ammonium sulfate, and 0.2% of the complete mix of all amino acids). For restimulation by glucose, cells in SGM medium were filtered and transferred back to SC. Alternatively, yeast cells were grown in YPD (1% yeast extract, 2% peptone, and 2% glucose). Cells were filtered and transferred in YP (1% yeast extract, 2% peptone) for glucose starvation. Glucose refeeding was performed by filtering and transferring cells back to YPD.

Chemical treatments

For rapamycin treatment (stock solution: 1 mg/ml in ethanol:tween20 90:10), rapamycin (200 ng/ml) was added to exponentially growing cells. Incubation time varied among experiments. For cycloheximide treatment (stock solution: 50 mg/ml in ethanol), cycloheximide (25 μg/ml) was added to exponentially growing cells. Incubation time varied among experiments. To test the EGO phenotype (recovery from rapamycin treatment), cells were grown exponentially in specified medium, treated for six hours with rapamycin (200 ng/ml), and washed twice. Finally, serial 10-fold dilutions were spotted on specified solid medium.

TORC1 Activity Assays

TORC1 activity was assessed as the ratio between the phosphorylation on Thr737 of full-length Sch9 compared to the total amount of Sch9 using phosphospecific anti-pThr737-Sch9 and anti-Sch9 antibodies both produced by GenScript.

Co-immunoprecipitation.

Mrs6-myc_{13} expressing cells were centrifuged, washed once with Tris-buffered saline, centrifuged again and subsequently frozen (-80°C). Lysates were prepared by mechanical disruption of frozen cells in lysis buffer (50 mM TRIS (pH 7.5), 1 mM EDTA, 150 mM NaCl, 0.5% NP40 and 1x protease and phosphatase inhibitor cocktails (Roche)) with glass beads (0.5-mm diameter) using a Precellys cell disruptor and subsequent clarification by centrifugation (5 min at maximum speed). Mrs6-myc_{13} was

immunoprecipated with anti-myc magnetic beads (Pierce) and co-immunoprecipitation of Glc7-HA, Gtr1-HA_3, Gtr2-V5, $Gtr2^{Q66L}$-V5, or $Gtr2^{S23L}$-V5 was assessed by immunoblot analysis using anti-HA and anti-V5 antibodies.

Fluorescence microscopy

Mid-log phase cells cultured in specified synthetic dropout medium were imaged with an inverted Spinning Disk Confocal Microscope (VisiScope CSU-W1) equipped with an Evolve 512 (Photometrics) EM-CCD camera and a 100x 1.3 NA oil immersion Nikon CFI series objective. The signal intensity at the vacuolar membrane was quantified using the ImageJ software as follows: For each cell the median intensity value of the total GFP-signal was measured and subtracted from the respective median intensity value of the GFP-signal at the vacuolar membrane. Quantifications were done on three independent experiments (with at least 9 cells analyzed in each experiment). All used construct (genome and plasmid expressed GFP, mCherry and TDimer fusion proteins) were tested for functionality. For staining of the vacuolar membrane by FM4-64, cells were grown until OD_{600} of 0.4. Next, 1.5 ml of the culture was pelleted, resuspended in 100 µl of medium and 1µl of FM4-64 (16 mM in DMSO) was added. Cells, were incubated for 30 minutes with shaking, washed twice, and finally resuspended in 1 ml of medium and left at 30°C with shaking for one additional hour.

Protein purification

Escherichia coli Rosetta strain (Novagen) was used for all protein purifications. Cells were grown at 37°C on LB medium (1% NaCl, 1% Bactotryptone, and 0.5% yeast extract). GST-Gtr2, GST-$Gtr1^{Q65L}$-His_6/Gtr2-His_6, Gtr1-His_6/GST-$Gtr2^{Q66L}$-His6, GST-Cdc42 and His_6-Lst4/His_6-Lst7 were produced in the *E. coli* after induction with 0.5 mM IPTG during 5 hours at 18°C (GST-Gtr2, GST-$Gtr1^{Q65L}$-His_6/Gtr2-His_6, Gtr1-His_6/GST-$Gtr2^{Q66L}$-His_6), or at 37°C (GST-Cdc42) or overnight at 16°C (His_6-Lst4/His_6-Lst7). Cells were collected by centrifugation and lysed with a microfluidizer in the appropriate buffer. Purification of GST-tagged proteins was done using Glutathione-Sepharose beads (GE Healthcare) in Buffer A (50 mM Tris-HCl, pH 7.5, 200 mM NaCl, 1.5 mM $MgCl_2$, 5% glycerol, 1 mM DTT, 0.1% NP40, and 0.1 mM GDP) and proteins were finally eluted with Buffer A + 10 mM reduced glutathione. His_6 purification (His_6-Lst4/His_6-Lst7) was performed using Ni-NTA agarose beads (Qiagen) in Buffer B (50 mM NaH_2PO_4 pH 8.0,

300 mM NaCl, 0.1% NP40, and 50 mM imidazole) and elution was achieved in Buffer B + 250 mM imidazole. Glycerol was added to a final concentration of 20% and proteins were stored at -80°C.

GTP Hydrolysis Assays

Purified GTPases (100 nM) were incubated for 30 min at room temperature in loading buffer (20 mM Tris-HCl [pH 8.0], 2 mM EDTA, and 1 mM DTT) in the presence of 40 nM [α-^{32P}]-GTP (Hartman Analytic; 3,000 Ci/mmol). Unless otherwise stated, 200 nM of His_6-Lst4/His_6-Lst7 or Iml1-His_6 were then added to the mix, together with 10 mM $MgCl_2$ to start the reaction. Reactions were stopped after 20 min of incubation at room temperature by the addition of elution buffer (1% SDS, 25 mM EDTA, 5 mM GDP, and 5 mM GTP). Samples were then heat denatured for 2 min at 65°C. Single turnover GAP assays were performed as described above, except that 1.7 mM unlabeled GTP was added concomitantly with the $MgCl_2$. The concentration of His_6-Lst4/His_6-Lst7 was constant (200 nM), and samples were taken at times 0 and 30 min. [α-^{32P}]-GTP and [α-^{32P}]-GDP were separated by thin-layer chromatography (TLC) on PEI Cellulose F Plates (Merck). The TLC tank was equilibrated with buffer containing 1.0 M acetic acid and 0.8 M LiCl. Results were visualized using a phosphorimager and quantified with ImageQuant software.

Genomic DNA preparation

Samples of 30 ml of yeast cultures were grown in YPD to an OD_{600} of 1.0. Cells were collected by centrifugation and washed twice with H2O. The resulting cell pellets were resuspended in 200 µl of breaking buffer (2% Triton X@100, 1% SDS, 100 mM NaCl, 10 mM Tris-HCl pH 8.0, and 1 mM EDTA [pH 8.0]) and 0.3 g of glass beads and 200 µl of phenol/chloroform/isoamyl alcohol (25:24:1) were added. Cells were vortexed for 3 minutes. Next, 200 µl of TE buffer (10 mM Tris-HCl [pH 7.5] and 1 mM EDTA [pH 8.0]) were added and samples were centrifuged (5 min at maximum speed.). The aqueous layer (upper phase) was transferred to a new eppendorf tube and 1 ml of absolute ethanol was added. After centrifugation (3 min at maximum speed), the supernatant was removed and the pellet resuspended in 0.4 ml of TE buffer. Samples were treated with 30 µl of 1 mg/ml DNAse-free RNaseA and incubated for 5 minutes at 37°C. DNA was precipitated with 10 µl of 5 M ammonium acetate and 1 ml of absolute ethanol.

Following centrifugation (3 min at maximum speed), pellets were dried and resuspended in 100 µl TE buffer. A volume of 2.5 µl was loaded into a 1% agarose gel to verify the DNA integrity. Quantification of DNA concentration was performed with Qubit fluorometer (Qubit® 2.0 Fluorometer) and 2 µg of DNA were sent for library construction and whole genome sequencing.

Analysis of Next Generation Sequencing data (performed by L. Falquet)

Samples were subjected to Next Generation Sequencing (NGS). NGS Paired-End (100 bp) reads were analyzed to remove sources of error/bias with "FastQC" filtering by quality with "Sickle". Reads were aligned to the reference genome remapping the reads with "bwa". Afterwards, the likelihood of variation at each locus was predicted based on the quality scores and allele counts of the aligned reads at that locus. SNPs and small indels were called with "Samtools" and "bcftools", and variants were annotated using "snpEFF". The results were filtered with "SnpSift" to keep only good quality variants that are not common to all strains and that are responsible for critical effects (Stop-Gain, Non-Synonymous, Frameshift, etc.). Finally, manual inspection of the candidate variants was performed with integrative genomic viewer (IGV) to look for genes of interest.

Supplementary Tables

Table 1. Strains Used in Chapter I

Strain	Genotype	Source	Figure
YL515	[BY4741/2] *MATα*; *his3Δ1, leu2Δ0, ura3Δ0*	(Binda et al., 2009)	1A-D; S1
MP347-4A	[YL515] *MATα; lst4Δ::KanMX*	This study	1A-D; S1
MP348-3C	[YL515] *MATα; lst7Δ::KanMX*	This study	1A-D; S1
MP354-9A	[YL515] *MATα; lst4Δ::KanMX, lst7Δ::KanMX*	This study	1A-C; S1
MB36-4B	[YL515] *MATα; gtr1Δ::kanMX*	This study	1A-C; S1
MB33	[YL515] *MATa; gtr2Δ::kanMX*	(Binda et al., 2009)	1A-C; S1
NP04-C4	[YL515] *MATα; iml1Δ::KanMX*	(Panchaud et al., 2013)	1A-C; S1
MP06-8B	[YL515] *MATα; gtr1Δ::kanMX, gtr2Δ::kanMX*	(Binda et al., 2009)	1C
MB27	[YL515] *MATα; gtr1Δ::HIS3*	(Binda et al., 2009)	1D
MP359-5A	[YL515] *MATα; lst4Δ::KanMX gtr1Δ::HIS3*	This study	1D
MP360-2C	[YL515] *MATα; lst7Δ::KanMX gtr1Δ::HIS3*	This study	1D
MB28	[YL515] *MATα; gtr2Δ::HIS3*	(Binda et al., 2009)	1D
MP361-7D	[YL515] *MATα; lst4Δ::KanMX gtr2Δ::HIS3*	This study	1D
MP362-4A	[YL515] *MATα; lst7Δ::KanMX gtr2Δ::HIS3*	This study	1D
KT1961	*MATa*; *his3, leu2, ura3-52, trp1*	(Pedruzzi et al., 2003)	S3B, C
KP09	[KT1961] *MATa; lst4Δ::KanMX*	This study	S3B, C
KP10	[KT1961] *MATa; lst7Δ::KanMX*	This study	2A; S3B, C
MP409-2A	[KT1961] *MATa; LST4-GFP::HIS3MX*	This study	2B, D; 4D, E; S3A
MP410-5B	[KT1961] *MATa; LST7-GFP::HIS3MX*	This study	2B
MP374-1C	[KT1961] *MATa; LST4-GFP::HIS3MX, lst7Δ::KanMX*	This study	2A, C
MP372-2D	[KT1961] *MATa*; *LST7-GFP::HIS3MX, lst4Δ::KanMX*	This study	2C
MP406-8A	[KT1961] *MATa; LST4-GFP::HIS3MX, gtr1Δ::natMX, gtr2Δ::natMX*	This study	2E; 4A-C, F; S2
MP405-3D	[KT1961] *MATa; LST7-GFP::HIS3MX, gtr1Δ::natMX, gtr2Δ::natMX*	This study	2F; 4F
MP268-2B	[KT1961] *MATa; gtr1Δ::natMX, gtr2Δ::natMX*	This study	S3B, C

Table 2. Plasmids Used in Chapter I

Plasmid	Genotype	Source	Figure
pRS413	CEN, ARS, *HIS3*	(Brachmann et al., 1998)	1A-D; 2A, E, F; S3B, C
pRS414	CEN, ARS, *TRP1*	(Brachmann et al., 1998)	2A-D; 4A, C-E; S2; S3A-C
pRS415	CEN, ARS, *LEU2*	(Brachmann et al., 1998)	1A-D; 2A-C, E, F; 4A, D-F; S3A-C
pRS416	CEN, ARS, *URA3*	(Brachmann et al., 1998)	1D; 2A-D; 4A, D, E; S3A-C
pJU1030	[pRS416] *SCH9p-SCH9^{T570A}-HA$_5$*	(Urban et al., 2007)	1A, C, D
pJU793	[pRS416] *SCH9p-GFP-SCH9*	(Urban et al., 2007)	1B
pJU1058	[pRS415] *SCH9p-SCH9^{T570A}-HA$_5$*	(Urban et al., 2007)	1D
YCplac33	CEN, ARS, *URA3*	(Gietz and Sugino, 1988)	
pMB1393	[YCplac33] *TetON-GTR1*	(Binda et al., 2009)	1D
pMB1394	[YCplac33] *TetON-GTR1^{Q65L}*	(Binda et al., 2009)	1D
pMB1395	[YCplac33] *TetON-GTR1^{S20L}*	(Binda et al., 2009)	1D
YCplac111	CEN, ARS, *LEU2*	(Gietz and Sugino, 1988)	
pPM1621	[YCplac111] *TetON-GTR2*	(Binda et al., 2009)	1D
pPM1622	[YCplac111] *TetON-GTR2^{Q66L}*	(Binda et al., 2009)	1D
pPM1623	[YCplac111] *TetON-GTR2^{S23L}*	(Binda et al., 2009)	1D
pMP2562	[pRS414] *LST7p-LST7-V5-HIS$_6$*	This study	2A
pYM2847	[YCplac111] *VAC8p-VAC8-Cherry*	This study	2D
pMPG2177	[pRS414] *GTR2p-GTR2-V5-HIS$_6$*	This study	2E, F; 4F
pNP2055	[YCplac111] *ADH1p-IML1- HIS6-TEV-ProtA*	(Panchaud et al., 2013)	3B
pNP2035	[pET-24d] *GST-TEV-GTR1*	(Panchaud et al., 2013)	3B
pNP2038	[pET-24d] *GST-TEV-GTR2*	(Panchaud et al., 2013)	3A-E
pJU1046	[pGEX-6P] *GST-TEV-GTR1^{Q65L}-HIS$_6$*	R. Loewith	3A-E
pJU1048	[pGEX-6P] *GST-TEV-GTR2^{Q66L}-HIS$_6$*	(Panchaud et al., 2013)	3B
pMP2101	[pGEX-4T] *GST-CDC42*	(Panchaud et al., 2013)	3B
pAS2570	[pET28b$^+$] *HIS$_6$-LST4*	This study	3A-E
pAS2571	[pET15b$^+$] *HIS$_6$-LST7*	This study	3A-E
pJU650	[pRS416] *GTR1p-GTR1*	R. Loewith	4A
pJU652	[pRS416] *GTR1p-GTR1^{S20L}*	R. Loewith	4A, B
pJU653	[pRS416] *GTR1p-GTR1^{Q65L}*	R. Loewith	4A
pMP2337	[pRS416] *GTR1p-GTR1-HA$_3$*	This study	2E, F; 4A, C, F; S2
pMP2338	[pRS416] *GTR1p-GTR1^{S20L}-HA$_3$*	This study	4C
pMP2339	[pRS416] *GTR1p-GTR1^{Q65L}-HA$_3$*	This study	4C
pJU661	[pRS415] *GTR2p-GTR2*	R. Loewith	4A
pJU658	[pRS415] *GTR2p-GTR2^{S23L}*	R. Loewith	4A
pJU659	[pRS415] *GTR2p-GTR2^{Q66L}*	R. Loewith	4A
pMP2136	[pRS415] *GTR2p-GTR2-V5-HIS$_6$*	This study	4C, S2
pMP2777	[pRS415] *GTR2p-GTR2^{S23L}-V5-HIS$_6$*	This study	4C
pMP2778	[pRS415] *GTR2p-GTR2^{Q66L}-V5-HIS$_6$*	This study	4C

pMP2782	[pRS414] *GTR2p-GTR2^{Q66L}-V5-HIS$_6$*	This study	4B
pPL132	CEN, ARS*, LEU2*, *HA$_3$-TOR1*	(Reinke et al., 2006)	4B
pPL155	CEN, ARS*, LEU2*, *HA$_3$-TOR1^{A1957V}*	(Reinke et al., 2006)	4B
pPL156	CEN, ARS*, LEU2*, *HA$_3$-TOR1^{I1954V}*	(Reinke et al., 2006)	4B

Table 3. Strains Used in Chapter II

Strain	Genotype	Source	Figure
MB36-4B	[YL515] *MATα; gtr1Δ::kanMX*	This study	2.1; 2.3-2.9; 2.11
MP02-7B	[YL515] *MAT*α; *gtr1Δ::kanMX, tco89Δ::HIS3*	(Binda et al., 2009)	2.1
MP07-1D	[YL516] *MAT***a**; *vam6Δ::kanMX*	(Binda et al., 2009)	2.5-2.8
MP06-8B	[YL515] *MATα; gtr1Δ::kanMX, gtr2Δ::kanMX*	(Binda et al., 2009)	2.10
MP11-4C	[YL515] *MATα; gtr1Δ::kanMX, vam6Δ::kanMX*	This study	2.9
YAS063	[YL515] *MATα; gtr1Δ::kanMX, vps33^{L18P}*	This study	2.3-2.8
YAS064	[YL515] *MATα; gtr1Δ::kanMX, ego1^{R9*}, vid27^{K513T}*	This study	2.3-2.8
YAS065	[YL515] *MATα; gtr1Δ::kanMX, rsc1^{P387L}*	This study	2.3-2.8
YAS066	[YL515] *MATα; gtr1Δ::kanMX, dpb11^{N92H}, pep5^{Q76*}*	This study	2.3-2.8
YAS067	[YL515] *MATα; gtr1Δ::kanMX, vam6^{Q391*}*	This study	2.3-2.8; 2.9
YAS068	[YL515] *MATα; gtr1Δ::kanMX, apl6^{M613R}*	This study	2.3-2.8; 2.12
YAS069	[YL515] *MATα; gtr1Δ::kanMX, apl6^{M1V}*	This study	2.3-2.8; 2.12
YAS070	[YL515] *MATα; gtr1Δ::kanMX, gtr2^{C231W}*	This study	2.3-2.8; 2.11
YAS071	[YL515] *MATα; gtr1Δ::kanMX, tco89?*	This study	2.3; 2.4

Table 4. Plasmids Used in Chapter II

Plasmid	Genotype	Source	Figure
pRS413	CEN, ARS, *HIS3*	(Brachmann et al., 1998)	2.1; 2.3; 2.4; 2.9; 2.11
pRS415	CEN, ARS, *LEU2*	(Brachmann et al., 1998)	
pRS416	CEN, ARS, *URA3*	(Brachmann et al., 1998)	2.1; 2.9; 2.11
YCplac33	CEN, ARS, *URA3*	(Gietz and Sugino, 1988)	
YCplac111	CEN, ARS, *LEU2*	(Gietz and Sugino, 1988)	
pPM1396	[YCplac111] *TetON-GTR1*	This study	2.1
pPM1397	[YCplac111] *TetON-GTR1^{Q65L}*	(Panchaud et al., 2013)	2.1
pPM1398	[YCplac111] *TetON-GTR1^{S20L}*	(Panchaud et al., 2013)	2.1; 2.11
pMB1395	[YCplac33] *TetON-GTR1^{S20L}*	(Binda et al., 2009)	2.3
YCpIF2	CEN, *LEU2, GAL1-GST*	(Foreman and Davis, 1994)	
pMB1580	[YCpIF2] *GAL1-GST-GTR1^{S20L}*	(Binda et al., 2009)	2.3; 2.4; 2.9
pFD1123	[YCplac33] *TCO89p-TCO89*	This study	2.4
pRH2911	[pRS416] *GTR1p-GFP-GTR1*	This study	2.5-2.8
pRH2836	[pRS415] *GTR2p-GFP-GTR2*	This study	2.10
pAS3192	[pRS415] *GTR2p-GFP-GTR2^{C231W}*	This study	2.10
pRS316	CEN, ARS, *URA3*	(Sikorski and Hieter, 1989)	
pSK384	[pRS316] *EGO1p- EGO1-GFP*	T. Noda	2.12
pJU660	[pRS415] *GTR1p-GTR1*	R. Loewith	2.11
pJU650	[pRS416] *GTR1p-GTR1*	R. Loewith	2.10

Table 5. Strains Used in Chapter III

Strain	Genotype	Source	Figure
YL515	[BY4741/2] *MATα*; *his3Δ1, leu2Δ0, ura3Δ0*	(Binda et al., 2009)	3.2-3.6
KT1961	*MATa*; *his3, leu2, ura3-52, trp1*	(Pedruzzi et al., 2003)	3.10
mrs6-2	[BY4741] *MAT*a; *his3Δ1, leu2Δ0, met15Δ0, ura3Δ0, mrs6-2::kanMX*	(Li et al., 2011)	3.2
MB33	[YL515] *MATα; gtr2Δ::kanMX*	(Binda, 2009)	3.3-3.5; 3.13
MP06-8B	[YL515] *MATα; gtr1Δ::kanMX, gtr2Δ::kanMX*	(Binda et al., 2009)	3.11
YAS043	[YL515] *MATα; mrs6^{S335P}::natMX*	This study	3.3-3.6
YAS045	[YL515] *MATα; mrs6^{S335E}::natMX*	This study	3.3-3.6
YAS044	[YL515] *MATα; mrs6^{S335A}::natMX*	This study	3.3-3.5
YAS073	[KT1961] *MATa; MRS6-GFP::HIS3MX, HHF2-TDimer::TRP1*	This study	3.7
YAS072	[KT1961] *MATa; MRS6-GFP::HIS3MX*	This study	3.8; 3.13
YAS074	[YL515] *MATα; MRS6-myc$_{13}$::HIS3MX, gtr1Δ::kanMX, gtr2Δ::kanMX*	This study	3.11; 3.12

Table 6. Plasmids Used in Chapter III

Plasmid	Genotype	Source	Figure
pRS413	CEN, ARS, *HIS3*	(Brachmann et al., 1998)	3.5; 3.6; 3.10
pRS415	CEN, ARS, *LEU2*	(Brachmann et al., 1998)	3.5; 3.7; 3.8; 3.10
pRS414	CEN, ARS, *TRP1*	(Brachmann et al., 1998)	3.8; 3.13
pRS416	CEN, ARS, *URA3*	(Brachmann et al., 1998)	3.5; 3.7; 3.8; 3.13
YCplac33	CEN, ARS, *URA3*	(Gietz and Sugino, 1988)	
YCplac111	CEN, ARS, *LEU2*	(Gietz and Sugino, 1988)	
pMB1393	[YCplac33] *TetON-GTR1*	(Binda et al., 2009)	3.6
pMB1394	[YCplac33] *TetON-GTR1^{Q65L}*	(Binda et al., 2009)	3.6
pPM1621	[YCplac111] *TetON-GTR2*	(Binda et al., 2009)	3.6
pPM1623	[YCplac111] *TetON-GTR2^{S23L}*	(Binda et al., 2009)	3.6
pFD652	CEN, ARS, *URA3*, *GLC7-GLC7-HA*	This study	3.11
pMP2337	[pRS416] *GTR1p-GTR1-HA$_3$*	This study	3.11; 3.12
pMP2136	[pRS415] *GTR2p-GTR2-V5-HIS$_6$*	This study	3.11; 3.12
pRH2836	[pRS415] *GTR2p-GFP-GTR2*	This study	3.13B
pMP2778	[pRS415] *GTR2p-GTR2^{Q66L}-V5-HIS$_6$*	This study	3.11B
pMP2777	[pRS415] *GTR2p-GTR2^{S23L}-V5-HIS$_6$*	This study	3.11B
pFLJ2135	[pRS416] *CYC1p-HHF2-TDimer*	This study	3.10
pFLJ2149	[pRS416] *CYC1p-HHF2-TDimer*	This study	3.13B
pRH2866	[pRS415] *GTR2p-yEmRFP-GTR2*	This study	3.13A
pAS3193	[YCplac33] *MRS6p-MRS6-GFP*	This study	3.10A
pAS3195	[YCplac33] *MRS6p-MRS6$^{S3E-S9E-S16E}$-GFP*	This study	3.10B
pAS3194	[YCplac33] *MRS6p-MRS6$^{S3A-S9A-S16A}$-GFP*	This study	3.10C

References

Albuquerque, C.P., Smolka, M.B., Payne, S.H., Bafna, V., Eng, J., and Zhou, H. (2008). A multidimensional chromatography technology for in-depth phosphoproteome analysis. Mol. Cell Proteomics *7*, 1389–1396.

Alexandrov, K., Horiuchi, H., Steele-Mortimer, O., Seabra, M.C., and Zerial, M. (1994). Rab escort protein-1 is a multifunctional protein that accompanies newly prenylated rab proteins to their target membranes. Embo J. *13*, 5262–5273.

Alory, C., and Balch, W.E. (2001). Organization of the Rab-GDI/CHM superfamily: the functional basis for choroideremia disease. Traffic *2*, 532–543.

Alory, C., and Balch, W.E. (2003). Molecular evolution of the Rab-escort-protein/guanine-nucleotide-dissociation-inhibitor superfamily. Mol. Biol. Cell *14*, 3857–3867.

Andres, D.A., Seabra, M.C., Brown, M.S., Armstrong, S.A., Smeland, T.E., Cremers, F.P., and Goldstein, J.L. (1993). cDNA cloning of component A of Rab geranylgeranyl transferase and demonstration of its role as a Rab escort protein. Cell *73*, 1091–1099.

Ashrafi, K., Farazi, T.A., and Gordon, J.I. (1998). A role for *Saccharomyces cerevisiae* fatty acid activation protein 4 in regulating protein N-myristoylation during entry into stationary phase. Journal of Biological Chemistry *273*, 25864–25874.

Baba, M., Furihata, M., Hong, S.-B., Tessarollo, L., Haines, D.C., Southon, E., Patel, V., Igarashi, P., Alvord, W.G., Leighty, R., et al. (2008). Kidney-targeted Birt-Hogg-Dube gene inactivation in a mouse model: Erk1/2 and Akt-mTOR activation, cell hyperproliferation, and polycystic kidneys. J. Natl. Cancer Inst. *100*, 140–154.

Baba, M., Keller, J.R., Sun, H.-W., Resch, W., Kuchen, S., Suh, H.-C., Hasumi, H., Hasumi, Y., Kieffer-Kwon, K.-R., Gonzalez, C.G., et al. (2012). The folliculin-FNIP1 pathway deleted in human Birt-Hogg-Dubé syndrome is required for murine B-cell development. Blood *120*, 1254–1261.

Baba, M., Toyama, H., Sun, L., Takubo, K., Suh, H.-C., Hasumi, H., Nakamura-Ishizu, A., Hasumi, Y., Klarmann, K.D., Nakagata, N., et al. (2016). Loss of Folliculin Disrupts Hematopoietic Stem Cell Quiescence and Homeostasis Resulting in Bone Marrow Failure. Stem Cells *34*, 1068–1082.

Bajaj, K., Madhusudhan, M.S., Adkar, B.V., Chakrabarti, P., Ramakrishnan, C., Sali, A., and Varadarajan, R. (2007). Stereochemical criteria for prediction of the effects of proline mutations on protein stability. PLoS Comput. Biol. *3*, e241.

Baker, R.W., Jeffrey, P.D., and Hughson, F.M. (2013). Crystal Structures of the Sec1/Munc18 (SM) Protein Vps33, Alone and Bound to the Homotypic Fusion and Vacuolar Protein Sorting (HOPS) Subunit Vps16*. PLoS ONE *8*, e67409.

Balderhaar, H.J.K., and Ungermann, C. (2013). CORVET and HOPS tethering complexes - coordinators of endosome and lysosome fusion. J. Cell. Sci. *126*, 1307–1316.

Bar-Peled, L., Chantranupong, L., Cherniack, A.D., Chen, W.W., Ottina, K.A., Grabiner, B.C., Spear, E.D., Carter, S.L., Meyerson, M., and Sabatini, D.M. (2013). A Tumor suppressor

complex with GAP activity for the Rag GTPases that signal amino acid sufficiency to mTORC1. Science *340*, 1100–1106.

Bar-Peled, L., Schweitzer, L.D., Zoncu, R., and Sabatini, D.M. (2012). Ragulator is a GEF for the rag GTPases that signal amino acid levels to mTORC1. Cell *150*, 1196–1208.

Barbacid, M. (1987). ras genes. Annu. Rev. Biochem. *56*, 779–827.

Barral, Y., and Kinoshita, M. (2008). Structural insights shed light onto septin assemblies and function. Curr. Opin. Cell Biol. *20*, 12–18.

Bialek-Wyrzykowska, U., Bauer, B.E., Wagner, W., Kohlwein, S.D., Schweyen, R.J., and Ragnini, A. (2000). Low levels of Ypt protein prenylation cause vesicle polarization defects and thermosensitive growth that can be suppressed by genes involved in cell wall maintenance. Molecular Microbiology *35*, 1295–1311.

Binda, M. (2009). The Target of Rapamycin Complex 1, regulator of growth of yeast cells in response to amino acids.

Binda, M., PEli-Gulli, M.-P., Bonfils, G., Panchaud, N., Urban, J., Sturgill, T.W., Loewith, R., and De Virgilio, C. (2009). The Vam6 GEF Controls TORC1 by Activating the EGO Complex. Molecular Cell *35*, 563–573.

Blumberg, H., and Silver, P. (1991). A split zinc-finger protein is required for normal yeast growth. Gene *107*, 101–110.

Bonfils, G., Jaquenoud, M., Bontron, S., Ostrowicz, C., Ungermann, C., and De Virgilio, C. (2012). Leucyl-tRNA synthetase controls TORC1 via the EGO complex. Molecular Cell *46*, 105–110.

Bos, J.L., Rehmann, H., and Wittinghofer, A. (2007). GEFs and GAPs: critical elements in the control of small G proteins. Cell *129*, 865–877.

Bourne, H.R., Sanders, D.A., and McCormick, F. (1990). The GTPase superfamily: a conserved switch for diverse cell functions. Nature *348*, 125–132.

Bourne, H.R., Sanders, D.A., and McCormick, F. (1991). The GTPase superfamily: conserved structure and molecular mechanism. Nature *349*, 117–127.

Brachmann, C.B., Davies, A., Cost, G.J., Caputo, E., Li, J., Hieter, P., and Boeke, J.D. (1998). Designer deletion strains derived from *Saccharomyces cerevisiae* S288C: a useful set of strains and plasmids for PCR-mediated gene disruption and other applications. Yeast *14*, 115–132.

Brondyk, W.H., McKiernan, C.J., Burstein, E.S., and Macara, I.G. (1993). Mutants of Rab3A analogous to oncogenic Ras mutants. Sensitivity to Rab3A-GTPase activating protein and Rab3A-guanine nucleotide releasing factor. Journal of Biological Chemistry *268*, 9410–9415.

Buhrman, G., Holzapfel, G., Fetics, S., and Mattos, C. (2010). Allosteric modulation of Ras positions Q61 for a direct role in catalysis. Proc. Natl. Acad. Sci. U.S.a. *107*, 4931–4936.

Bun-Ya, M., Harashima, S., and Oshima, Y. (1992). Putative GTP-binding protein, Gtr1, associated with the function of the Pho84 inorganic phosphate transporter in *Saccharomyces cerevisiae*. Mol. Cell. Biol. *12*, 2958–2966.

Bungard, D., Reed, M., and Winter, E. (2004). RSC1 and RSC2 are required for expression of mid-late sporulation-specific genes in *Saccharomyces cerevisiae*. Eukaryotic Cell *3*, 910–918.

Cabrera-Vera, T.M., Vanhauwe, J., Thomas, T.O., Medkova, M., Preininger, A., Mazzoni, M.R., and Hamm, H.E. (2003). Insights into G protein structure, function, and regulation. Endocr. Rev. *24*, 765–781.

Caplan, S., Hartnell, L.M., Aguilar, R.C., Naslavsky, N., and Bonifacino, J.S. (2001). Human Vam6p promotes lysosome clustering and fusion in vivo. J. Cell Biol. *154*, 109–122.

Carvalho, A.T.P., Szeler, K., Vavitsas, K., Åqvist, J., and Kamerlin, S.C.L. (2015). Modeling the mechanisms of biological GTP hydrolysis. Arch. Biochem. Biophys. *582*, 80–90.

Castro, A.F., Rebhun, J.F., Clark, G.J., and Quilliam, L.A. (2003). Rheb binds tuberous sclerosis complex 2 (TSC2) and promotes S6 kinase activation in a rapamycin- and farnesylation-dependent manner. Journal of Biological Chemistry *278*, 32493–32496.

Chantranupong, L., Scaria, S.M., Saxton, R.A., Gygi, M.P., Shen, K., Wyant, G.A., Wang, T., Harper, J.W., Gygi, S.P., and Sabatini, D.M. (2016). The CASTOR Proteins Are Arginine Sensors for the mTORC1 Pathway. Cell *165*, 153–164.

Chantranupong, L., Wolfson, R.L., Orozco, J.M., Saxton, R.A., Scaria, S.M., Bar-Peled, L., Spooner, E., Isasa, M., Gygi, S.P., and Sabatini, D.M. (2014). The Sestrins Interact with GATOR2 to Negatively Regulate the Amino-Acid-Sensing Pathway Upstream of mTORC1. Cell Rep.

Chappie, J.S., Acharya, S., Leonard, M., Schmid, S.L., and Dyda, F. (2010). G domain dimerization controls dynamin's assembly-stimulated GTPase activity. Nature *465*, 435–440.

Chattopadhyay, S., and Pearce, D.A. (2002). Interaction with Btn2p is required for localization of Rsglp: Btn2p-mediated changes in arginine uptake in *Saccharomyces cerevisiae*. Eukaryotic Cell *1*, 606–612.

Cherfils, J., and Zeghouf, M. (2013). Regulation of small GTPases by GEFs, GAPs, and GDIs. Physiol. Rev. *93*, 269–309.

Coleman, D.E., Berghuis, A.M., Lee, E., Linder, M.E., Gilman, A.G., and Sprang, S.R. (1994). Structures of active conformations of Gi alpha 1 and the mechanism of GTP hydrolysis. Science *265*, 1405–1412.

Connolly, T., and Gilmore, R. (1989). The signal recognition particle receptor mediates the GTP-dependent displacement of SRP from the signal sequence of the nascent polypeptide. Cell *57*, 599–610.

Cowles, C.R., Odorizzi, G., Payne, G.S., and Emr, S.D. (1997). The AP-3 adaptor complex is

essential for cargo-selective transport to the yeast vacuole. Cell *91*, 109–118.

Cox, A.D., and Der, C.J. (2002). Ras family signaling: therapeutic targeting. Cancer Biol. Ther. *1*, 599–606.

Cybulski, N., and Hall, M.N. (2009). TOR complex 2: a signaling pathway of its own. Trends Biochem. Sci. *34*, 620–627.

Daumke, O., Weyand, M., Chakrabarti, P.P., Vetter, I.R., and Wittinghofer, A. (2004). The GTPase-activating protein Rap1GAP uses a catalytic asparagine. Nature *429*, 197–201.

De Virgilio, C., and Loewith, R. (2006). The TOR signalling network from yeast to man. Int. J. Biochem. Cell Biol. *38*, 1476–1481.

Demetriades, C., Doumpas, N., and Teleman, A.A. (2014). Regulation of TORC1 in response to amino acid starvation via lysosomal recruitment of TSC2. Cell *156*, 786–799.

Demetriades, C., Plescher, M., and Teleman, A.A. (2016). Lysosomal recruitment of TSC2 is a universal response to cellular stress. Nat Commun *7*, 10662.

Dubouloz, F., Deloche, O., Wanke, V., Cameroni, E., and De Virgilio, C. (2005). The TOR and EGO protein complexes orchestrate microautophagy in yeast. Molecular Cell *19*, 15–26.

Durán, R.V., and Hall, M.N. (2012). Regulation of TOR by small GTPases. Nature Publishing Group *13*, 121–128.

Efeyan, A., Comb, W.C., and Sabatini, D.M. (2015). Nutrient-sensing mechanisms and pathways. Nature *517*, 302–310.

Eltschinger, S., and Loewith, R. (2015). TOR Complexes and the Maintenance of Cellular Homeostasis. Trends Cell Biol.

Farnsworth, C.L., and Feig, L.A. (1991). Dominant inhibitory mutations in the Mg(2+)-binding site of RasH prevent its activation by GTP. Mol. Cell. Biol. *11*, 4822–4829.

Fawal, M.-A., Brandt, M., and Djouder, N. (2015). MCRS1 Binds and Couples Rheb to Amino Acid-Dependent mTORC1 Activation. Dev. Cell *33*, 67–81.

Felici, A., Wurthner, J.U., Parks, W.T., Giam, L.R.-Y., Reiss, M., Karpova, T.S., McNally, J.G., and Roberts, A.B. (2003). TLP, a novel modulator of TGF-beta signaling, has opposite effects on Smad2- and Smad3-dependent signaling. Embo J. *22*, 4465–4477.

Feuerstein, J., Goody, R.S., and Wittinghofer, A. (1987). Preparation and characterization of nucleotide-free and metal ion-free p21 "apoprotein". Journal of Biological Chemistry *262*, 8455–8458.

Fingerman, I., Nagaraj, V., Norris, D., and Vershon, A.K. (2003). Sfp1 plays a key role in yeast ribosome biogenesis. Eukaryotic Cell *2*, 1061–1068.

Focia, P.J., Shepotinovskaya, I.V., Seidler, J.A., and Freymann, D.M. (2004). Heterodimeric

GTPase core of the SRP targeting complex. Science *303*, 373–377.

Foreman, P.K., and Davis, R.W. (1994). Cloning vectors for the synthesis of epitope-tagged, truncated and chimeric proteins in *Saccharomyces cerevisiae*. Gene *144*, 63–68.

Fujimura, K., Tanaka, K., Nakano, A., and Toh-e, A. (1994). The *Saccharomyces cerevisiae* MSI4 gene encodes the yeast counterpart of component A of Rab geranylgeranyltransferase. Journal of Biological Chemistry *269*, 9205–9212.

Gao, M., and Kaiser, C.A. (2006). A conserved GTPase-containing complex is required for intracellular sorting of the general amino-acid permease in yeast. Nat. Cell Biol. *8*, 657–667.

Gao, S., Malsburg, von der, A., Paeschke, S., Behlke, J., Haller, O., Kochs, G., and Daumke, O. (2010). Structural basis of oligomerization in the stalk region of dynamin-like MxA. Nature *465*, 502–506.

Garami, A., Zwartkruis, F.J.T., Nobukuni, T., Joaquin, M., Roccio, M., Stocker, H., Kozma, S.C., Hafen, E., Bos, J.L., and Thomas, G. (2003). Insulin activation of Rheb, a mediator of mTOR/S6K/4E-BP signaling, is inhibited by TSC1 and 2. Molecular Cell *11*, 1457–1466.

Gasper, R., Meyer, S., Gotthardt, K., Sirajuddin, M., and Wittinghofer, A. (2009). It takes two to tango: regulation of G proteins by dimerization. Nature Reviews Molecular Cell Biology *10*, 423–429.

Gaubitz, C., Prouteau, M., Kusmider, B., and Loewith, R. (2016). TORC2 Structure and Function. Trends Biochem. Sci. *41*, 532–545.

Gietz, R.D., and Sugino, A. (1988). New yeast-Escherichia coli shuttle vectors constructed with in vitro mutagenized yeast genes lacking six-base pair restriction sites. Gene *74*, 527–534.

Gilman, A.G. (1987). G proteins: transducers of receptor-generated signals. Annu. Rev. Biochem. *56*, 615–649.

Gong, R., Li, L., Liu, Y., Wang, P., Yang, H., Wang, L., Cheng, J., Guan, K.-L., and Xu, Y. (2011). Crystal structure of the Gtr1p-Gtr2p complex reveals new insights into the amino acid-induced TORC1 activation. Genes Dev. *25*, 1668–1673.

González, A., Shimobayashi, M., Eisenberg, T., Merle, D.A., Pendl, T., Hall, M.N., and Moustafa, T. (2015). TORC1 promotes phosphorylation of ribosomal protein S6 via the AGC kinase Ypk3 in *Saccharomyces cerevisiae*. PLoS ONE *10*, e0120250.

Han, J.M., Jeong, S.J., Park, M.C., Kim, G., Kwon, N.H., Kim, H.K., Ha, S.H., Ryu, S.H., and Kim, S. (2012). Leucyl-tRNA synthetase is an intracellular leucine sensor for the mTORC1-signaling pathway. Cell *149*, 410–424.

Hara, K., Maruki, Y., Long, X., Yoshino, K.-I., Oshiro, N., Hidayat, S., Tokunaga, C., Avruch, J., and Yonezawa, K. (2002). Raptor, a binding partner of target of rapamycin (TOR), mediates TOR action. Cell *110*, 177–189.

Hasumi, H., Baba, M., Hasumi, Y., Lang, M., Huang, Y., Oh, H.F., Matsuo, M., Merino, M.J., Yao, M., Ito, Y., et al. (2015). Folliculin-interacting proteins Fnip1 and Fnip2 play critical roles in kidney tumor suppression in cooperation with Flcn. Proc. Natl. Acad. Sci. U.S.a. *112*, E1624–E1631.

Hasumi, Y., Baba, M., Ajima, R., Hasumi, H., Valera, V.A., Klein, M.E., Haines, D.C., Merino, M.J., Hong, S.-B., Yamaguchi, T.P., et al. (2009). Homozygous loss of BHD causes early embryonic lethality and kidney tumor development with activation of mTORC1 and mTORC2. Proc. Natl. Acad. Sci. U.S.a. *106*, 18722–18727.

Heitman, J., Movva, N.R., and Hall, M.N. (1991). Targets for cell cycle arrest by the immunosuppressant rapamycin in yeast. Science *253*, 905–909.

Hsu, Y.-C., Chern, J.J., Cai, Y., Liu, M., and Choi, K.-W. (2007). Drosophila TCTP is essential for growth and proliferation through regulation of dRheb GTPase. Nature *445*, 785–788.

Huh, W.-K., Falvo, J.V., Gerke, L.C., Carroll, A.S., Howson, R.W., Weissman, J.S., and O'Shea, E.K. (2003). Global analysis of protein localization in budding yeast. Nature *425*, 686–691.

Hwang, J., and Espenshade, P.J. (2016). Proximity-dependent biotin labelling in yeast using the engineered ascorbate peroxidase APEX2. Biochem. J. *473*, 2463–2469.

Im, E., Lintig, von, F.C., Chen, J., Zhuang, S., Qui, W., Chowdhury, S., Worley, P.F., Boss, G.R., and Pilz, R.B. (2002). Rheb is in a high activation state and inhibits B-Raf kinase in mammalian cells. Oncogene *21*, 6356–6365.

Inoki, K., Li, Y., Xu, T., and Guan, K.-L. (2003a). Rheb GTPase is a direct target of TSC2 GAP activity and regulates mTOR signaling. Genes Dev. *17*, 1829–1834.

Inoki, K., Li, Y., Zhu, T., Wu, J., and Guan, K.-L. (2002). TSC2 is phosphorylated and inhibited by Akt and suppresses mTOR signalling. Nat. Cell Biol. *4*, 648–657.

Inoki, K., Zhu, T., and Guan, K.-L. (2003b). TSC2 mediates cellular energy response to control cell growth and survival. Cell *115*, 577–590.

Jacinto, E., Loewith, R., Schmidt, A., Lin, S., Rüegg, M.A., Hall, A., and Hall, M.N. (2004). Mammalian TOR complex 2 controls the actin cytoskeleton and is rapamycin insensitive. Nat. Cell Biol. *6*, 1122–1128.

Jeong, J.-H., Lee, K.-H., Kim, Y.-M., Kim, D.-H., Oh, B.-H., and Kim, Y.-G. (2012). Crystal structure of the Gtr1p(GTP)-Gtr2p(GDP) protein complex reveals large structural rearrangements triggered by GTP-to-GDP conversion. J. Biol. Chem. *287*, 29648–29653.

Jiang, Y., and Broach, J.R. (1999). Tor proteins and protein phosphatase 2A reciprocally regulate Tap42 in controlling cell growth in yeast. Embo J. *18*, 2782–2792.

Jiang, Y., and Ferro-Novick, S. (1994). Identification of yeast component A: reconstitution of the geranylgeranyltransferase that modifies Ypt1p and Sec4p. Proc. Natl. Acad. Sci. U.S.a. *91*, 4377–4381.

John, J., Rensland, H., Schlichting, I., Vetter, I., Borasio, G.D., Goody, R.S., and Wittinghofer, A. (1993). Kinetic and structural analysis of the Mg(2+)-binding site of the guanine nucleotide-binding protein p21H-ras. Journal of Biological Chemistry *268*, 923–929.

Jorgensen, P., Rupes, I., Sharom, J.R., Schneper, L., Broach, J.R., and Tyers, M. (2004). A dynamic transcriptional network communicates growth potential to ribosome synthesis and critical cell size. Genes Dev. *18*, 2491–2505.

Kamada, Y., Yoshino, K.-I., Kondo, C., Kawamata, T., Oshiro, N., Yonezawa, K., and Ohsumi, Y. (2010). Tor directly controls the Atg1 kinase complex to regulate autophagy. Mol. Cell. Biol. *30*, 1049–1058.

Kim, D.-H., Sarbassov, D.D., Ali, S.M., King, J.E., Latek, R.R., Erdjument-Bromage, H., Tempst, P., and Sabatini, D.M. (2002). mTOR interacts with raptor to form a nutrient-sensitive complex that signals to the cell growth machinery. Cell *110*, 163–175.

Kim, E., Goraksha-Hicks, P., Li, L., Neufeld, T.P., and Guan, K.-L. (2008). Regulation of TORC1 by Rag GTPases in nutrient response. Nat. Cell Biol. *10*, 935–945.

Kim, H., An, S., Ro, S.-H., Teixeira, F., Jin Park, G., Kim, C., Cho, C.-S., Kim, J.S., Jakob, U., Hee Lee, J., et al. (2015a). Janus-faced Sestrin2 controls ROS and mTOR signalling through two separate functional domains. Nat Commun *6*, 10025.

Kim, J.S., Ro, S.-H., Kim, M., Park, H.-W., Semple, I.A., Park, H., Cho, U.-S., Wang, W., Guan, K.-L., Karin, M., et al. (2015b). Sestrin2 inhibits mTORC1 through modulation of GATOR complexes. Sci Rep *5*, 9502.

Kingsbury, J.M., Sen, N.D., Maeda, T., Heitman, J., and Cardenas, M.E. (2014). Endolysosomal membrane trafficking complexes drive nutrient-dependent TORC1 signaling to control cell growth in *Saccharomyces cerevisiae*. Genetics *196*, 1077–1089.

Kira, S., Tabata, K., Shirahama-Noda, K., Nozoe, A., Yoshimori, T., and Noda, T. (2014). Reciprocal conversion of Gtr1 and Gtr2 nucleotide-binding states by Npr2-Npr3 inactivates TORC1 and induces autophagy. Autophagy *10*, 1565–1578.

Kozlov, M.M., and Chernomordik, L.V. (2015). Membrane tension and membrane fusion. Curr. Opin. Struct. Biol. *33*, 61–67.

Lachmann, J., Glaubke, E., Moore, P.S., and Ungermann, C. (2014). The Vps39-like TRAP1 is an effector of Rab5 and likely the missing Vps3 subunit of human CORVET. Cell Logist *4*, e970840.

Lam, S.S., Martell, J.D., Kamer, K.J., Deerinck, T.J., Ellisman, M.H., Mootha, V.K., and Ting, A.Y. (2015). Directed evolution of APEX2 for electron microscopy and proximity labeling. Nat. Methods *12*, 51–54.

Lee, J.H., Cho, U.-S., and Karin, M. (2016). Sestrin regulation of TORC1: Is Sestrin a leucine sensor? Science Signaling *9*, re5–re5.

Lempiäinen, H., Uotila, A., Urban, J., Dohnal, I., Ammerer, G., Loewith, R., and Shore, D.

(2009). Sfp1 interaction with TORC1 and Mrs6 reveals feedback regulation on TOR signaling. Molecular Cell *33*, 704–716.

Li, Z., Vizeacoumar, F.J., Bahr, S., Li, J., Warringer, J., Vizeacoumar, F.S., Min, R., VanderSluis, B., Bellay, J., DeVit, M., et al. (2011). Systematic exploration of essential yeast gene function with temperature-sensitive mutants. Nat. Biotechnol. *29*, 361–367.

Lin, J.-R., Mondal, A.M., Liu, R., and Hu, J. (2012). Minimalist ensemble algorithms for genome-wide protein localization prediction. BMC Bioinformatics *13*, 157.

Loewith, R., Jacinto, E., Wullschleger, S., Lorberg, A., Crespo, J.L., Bonenfant, D., Oppliger, W., Jenoe, P., and Hall, M.N. (2002). Two TOR complexes, only one of which is rapamycin sensitive, have distinct roles in cell growth control. Molecular Cell *10*, 457–468.

Low, H.H., Sachse, C., Amos, L.A., and Löwe, J. (2009). Structure of a bacterial dynamin-like protein lipid tube provides a mechanism for assembly and membrane curving. Cell *139*, 1342–1352.

Lürick, A., Kuhlee, A., Bröcker, C., Kümmel, D., Raunser, S., and Ungermann, C. (2015). The Habc domain of the SNARE Vam3 interacts with the HOPS tethering complex to facilitate vacuole fusion. J. Biol. Chem. *290*, 5405–5413.

Ma, L., Chen, Z., Erdjument-Bromage, H., Tempst, P., and Pandolfi, P.P. (2005). Phosphorylation and functional inactivation of TSC2 by Erk implications for tuberous sclerosis and cancer pathogenesis. Cell *121*, 179–193.

Manning, B.D., Tee, A.R., Logsdon, M.N., Blenis, J., and Cantley, L.C. (2002). Identification of the tuberous sclerosis complex-2 tumor suppressor gene product tuberin as a target of the phosphoinositide 3-kinase/akt pathway. Molecular Cell *10*, 151–162.

Marcet-Houben, M., and Gabaldón, T. (2015). Beyond the Whole-Genome Duplication: Phylogenetic Evidence for an Ancient Interspecies Hybridization in the Baker's Yeast Lineage. PLoS Biol. *13*, e1002220.

Marshall, C.B., Ho, J., Buerger, C., Plevin, M.J., Li, G.Y., Li, Z., Ikura, M., and Stambolic, V. (2009). Characterization of the Intrinsic and TSC2-GAP-Regulated GTPase Activity of Rheb by Real-Time NMR. Science Signaling *2*, ra3–ra3.

Masumoto, H., Sugino, A., and Araki, H. (2000). Dpb11 controls the association between DNA polymerases alpha and epsilon and the autonomously replicating sequence region of budding yeast. Mol. Cell. Biol. *20*, 2809–2817.

Mazhab-Jafari, M.T., Marshall, C.B., Ishiyama, N., Ho, J., Di Palma, V., Stambolic, V., and Ikura, M. (2012). An autoinhibited noncanonical mechanism of GTP hydrolysis by Rheb maintains mTORC1 homeostasis. Structure *20*, 1528–1539.

Messler, S., Kropp, S., Episkopou, V., Felici, A., Würthner, J., Lemke, R., Jerabek-Willemsen, M., Willecke, R., Scheu, S., Pfeffer, K., et al. (2011). The TGF-β signaling modulators TRAP1/TGFBRAP1 and VPS39/Vam6/TLP are essential for early embryonic development. Immunobiology *216*, 343–350.

Mishra, A.K., and Lambright, D.G. (2016). Invited review: Small GTPases and their GAPs. Biopolymers *105*, 431–448.

Moser, C., Mol, O., Goody, R.S., and Sinning, I. (1997). The signal recognition particle receptor of Escherichia coli (FtsY) has a nucleotide exchange factor built into the GTPase domain. Proc. Natl. Acad. Sci. U.S.a. *94*, 11339–11344.

Nada, S., Hondo, A., Kasai, A., Koike, M., Saito, K., Uchiyama, Y., and Okada, M. (2009). The novel lipid raft adaptor p18 controls endosome dynamics by anchoring the MEK-ERK pathway to late endosomes. Embo J. *28*, 477–489.

Nakamura, N., Hirata, A., Ohsumi, Y., and Wada, Y. (1997). Vam2/Vps41p and Vam6/Vps39p are components of a protein complex on the vacuolar membranes and involved in the vacuolar assembly in the yeast *Saccharomyces cerevisiae*. Journal of Biological Chemistry *272*, 11344–11349.

Nakashima, A., Otsubo, Y., Yamashita, A., Sato, T., Yamamoto, M., and Tamanoi, F. (2012). Psk1, an AGC kinase family member in fission yeast, is directly phosphorylated and controlled by TORC1 and functions as S6 kinase. J. Cell. Sci. *125*, 5840–5849.

Nakashima, A., Yoshino, K.-I., Miyamoto, T., Eguchi, S., Oshiro, N., Kikkawa, U., and Yonezawa, K. (2007). Identification of TBC7 having TBC domain as a novel binding protein to TSC1-TSC2 complex. Biochem. Biophys. Res. Commun. *361*, 218–223.

Nakashima, N., Noguchi, E., and Nishimoto, T. (1999). *Saccharomyces cerevisiae* putative G protein, Gtr1p, which forms complexes with itself and a novel protein designated as Gtr2p, negatively regulates the Ran/Gsp1p G protein cycle through Gtr2p. Genetics *152*, 853–867.

Nickerson, M.L., Warren, M.B., Toro, J.R., Matrosova, V., Glenn, G., Turner, M.L., Duray, P., Merino, M., Choyke, P., Pavlovich, C.P., et al. (2002). Mutations in a novel gene lead to kidney tumors, lung wall defects, and benign tumors of the hair follicle in patients with the Birt-Hogg-Dubé syndrome. Cancer Cell *2*, 157–164.

Odorizzi, G., Cowles, C.R., and Emr, S.D. (1998). The AP-3 complex: a coat of many colours. Trends Cell Biol. *8*, 282–288.

Ostrowicz, C.W., Meiringer, C.T.A., and Ungermann, C. (2008). Yeast vacuole fusion: a model system for eukaryotic endomembrane dynamics. Autophagy *4*, 5–19.

Ögmundsdóttir, M.H., Heublein, S., Kazi, S., Reynolds, B., Visvalingam, S.M., Shaw, M.K., and Goberdhan, D.C.I. (2012). Proton-assisted amino acid transporter PAT1 complexes with Rag GTPases and activates TORC1 on late endosomal and lysosomal membranes. PLoS ONE *7*, e36616.

Pacitto, A., Ascher, D.B., Wong, L.H., Blaszczyk, B.K., Nookala, R.K., Zhang, N., Dokudovskaya, S., Levine, T.P., and Blundell, T.L. (2015). Lst4, the yeast Fnip1/2 orthologue, is a DENN-family protein. Open Biol. *5*, 150174–11.

Pan, X., Eathiraj, S., Munson, M., and Lambright, D.G. (2006). TBC-domain GAPs for Rab GTPases accelerate GTP hydrolysis by a dual-finger mechanism. Nature *442*, 303–306.

Panchaud, N., PEli-Gulli, M.-P., and De Virgilio, C. (2013). Amino acid deprivation inhibits TORC1 through a GTPase-activating protein complex for the Rag family GTPase Gtr1. Science Signaling *6*, ra42.

Parmigiani, A., Nourbakhsh, A., Ding, B., Wang, W., Kim, Y.C., Akopiants, K., Guan, K.-L., Karin, M., and Budanov, A.V. (2014). Sestrins Inhibit mTORC1 Kinase Activation through the GATOR Complex. Cell Rep.

Pedruzzi, I., Dubouloz, F., Cameroni, E., Wanke, V., Roosen, J., Winderickx, J., and De Virgilio, C. (2003). TOR and PKA signaling pathways converge on the protein kinase Rim15 to control entry into G0. Molecular Cell *12*, 1607–1613.

Peng, M., Yin, N., and Li, M.O. (2014). Sestrins Function as Guanine Nucleotide Dissociation Inhibitors for Rag GTPases to Control mTORC1 Signaling. Cell *159*, 122–133.

Peterson, T.R., Laplante, M., Thoreen, C.C., Sancak, Y., Kang, S.A., Kuehl, W.M., Gray, N.S., and Sabatini, D.M. (2009). DEPTOR is an mTOR inhibitor frequently overexpressed in multiple myeloma cells and required for their survival. Cell *137*, 873–886.

Pfeffer, S.R., Dirac-Svejstrup, A.B., and Soldati, T. (1995). Rab GDP dissociation inhibitor: putting rab GTPases in the right place. Journal of Biological Chemistry *270*, 17057–17059.

Pfeffer, S.R. (2012). Rab GTPase localization and Rab cascades in Golgi transport. Biochem. Soc. Trans *40*, 1373–1377.

Powis, K., and De Virgilio, C. (2016). Conserved regulators of Rag GTPases orchestrate amino acid-dependent TORC1 signaling. Nature Publishing Group *2*, 15049.

Powis, K., Zhang, T., Panchaud, N., Wang, R., De Virgilio, C., and Ding, J. (2015). Crystal structure of the Ego1-Ego2-Ego3 complex and its role in promoting Rag GTPase-dependent TORC1 signaling. Cell Res. *25*, 1043–1059.

Rebsamen, M., Pochini, L., Stasyk, T., de Araújo, M.E.G., Galluccio, M., Kandasamy, R.K., Snijder, B., Fauster, A., Rudashevskaya, E.L., Bruckner, M., et al. (2015). SLC38A9 is a component of the lysosomal amino acid sensing machinery that controls mTORC1. Nature.

Regelmann, J., Schüle, T., Josupeit, F.S., Horak, J., Rose, M., Entian, K.-D., Thumm, M., and Wolf, D.H. (2003). Catabolite degradation of fructose-1,6-bisphosphatase in the yeast *Saccharomyces cerevisiae*: a genome-wide screen identifies eight novel GID genes and indicates the existence of two degradation pathways. Mol. Biol. Cell *14*, 1652–1663.

Rehmann, H., Brüning, M., Berghaus, C., Schwarten, M., Köhler, K., Stocker, H., Stoll, R., Zwartkruis, F.J., and Wittinghofer, A. (2008). Biochemical characterisation of TCTP questions its function as a guanine nucleotide exchange factor for Rheb. FEBS Lett. *582*, 3005–3010.

Reiner, D.J., and Lundquist, E.A. (2016). Small GTPases. WormBook 1–99.

Reinke, A., Anderson, S., McCaffery, J.M., Yates, J., Aronova, S., Chu, S., Fairclough, S., Iverson, C., Wedaman, K.P., and Powers, T. (2004). TOR complex 1 includes a novel component, Tco89p (YPL180w), and cooperates with Ssd1p to maintain cellular integrity in *Saccharomyces cerevisiae*. Journal of Biological Chemistry *279*, 14752–14762.

Reinke, A., Chen, J.C.-Y., Aronova, S., and Powers, T. (2006). Caffeine targets TOR complex I and provides evidence for a regulatory link between the FRB and kinase domains of Tor1p. Journal of Biological Chemistry *281*, 31616–31626.

Rensland, H., John, J., Linke, R., Simon, I., Schlichting, I., Wittinghofer, A., and Goody, R.S. (1995). Substrate and product structural requirements for binding of nucleotides to H-ras p21: the mechanism of discrimination between guanosine and adenosine nucleotides. Biochemistry *34*, 593–599.

Reyes, N.L., Banks, G.B., Tsang, M., Margineantu, D., Gu, H., Djukovic, D., Chan, J., Torres, M., Liggitt, H.D., Hirenallur-S, D.K., et al. (2015). Fnip1 regulates skeletal muscle fiber type specification, fatigue resistance, and susceptibility to muscular dystrophy. Proc. Natl. Acad. Sci. U.S.a. *112*, 424–429.

Rhee, H.-W., Zou, P., Udeshi, N.D., Martell, J.D., Mootha, V.K., Carr, S.A., and Ting, A.Y. (2013). Proteomic mapping of mitochondria in living cells via spatially restricted enzymatic tagging. Science *339*, 1328–1331.

Roth, A.F., Wan, J., Bailey, A.O., Sun, B., Kuchar, J.A., Green, W.N., Phinney, B.S., Yates, J.R., and Davis, N.G. (2006). Global analysis of protein palmitoylation in yeast. Cell *125*, 1003–1013.

Rubio-Texeira, M., Van Zeebroeck, G., Voordeckers, K., and Thevelein, J.M. (2010). *Saccharomyces cerevisiae* plasma membrane nutrient sensors and their role in PKA signaling. FEMS Yeast Res. *10*, 134–149.

Rush, M.G., Drivas, G., and D'Eustachio, P. (1996). The small nuclear GTPase Ran: how much does it run? Bioessays *18*, 103–112.

Rybin, V., Ullrich, O., Rubino, M., Alexandrov, K., Simon, I., Seabra, M.C., Goody, R., and Zerial, M. (1996). GTPase activity of Rab5 acts as a timer for endocytic membrane fusion. Nature *383*, 266–269.

Sancak, Y., Bar-Peled, L., Zoncu, R., Markhard, A.L., Nada, S., and Sabatini, D.M. (2010). Ragulator-Rag complex targets mTORC1 to the lysosomal surface and is necessary for its activation by amino acids. Cell *141*, 290–303.

Sancak, Y., Peterson, T.R., Shaul, Y.D., Lindquist, R.A., Thoreen, C.C., Bar-Peled, L., and Sabatini, D.M. (2008). The Rag GTPases bind raptor and mediate amino acid signaling to mTORC1. Science *320*, 1496–1501.

Sancak, Y., Thoreen, C.C., Peterson, T.R., Lindquist, R.A., Kang, S.A., Spooner, E., Carr, S.A., and Sabatini, D.M. (2007). PRAS40 is an insulin-regulated inhibitor of the mTORC1 protein kinase. Molecular Cell *25*, 903–915.

Saraste, M., Sibbald, P.R., and Wittinghofer, A. (1990). The P-loop--a common motif in ATP- and GTP-binding proteins. Trends Biochem. Sci. *15*, 430–434.

Sarbassov, D.D., Ali, S.M., Kim, D.-H., Guertin, D.A., Latek, R.R., Erdjument-Bromage, H., Tempst, P., and Sabatini, D.M. (2004). Rictor, a novel binding partner of mTOR, defines a rapamycin-insensitive and raptor-independent pathway that regulates the cytoskeleton. Current Biology *14*, 1296–1302.

Sarbassov, D.D., Ali, S.M., and Sabatini, D.M. (2005). Growing roles for the mTOR pathway. Curr. Opin. Cell Biol. *17*, 596–603.

Sato, T., Nakashima, A., Guo, L., and Tamanoi, F. (2009). Specific activation of mTORC1 by Rheb G-protein in vitro involves enhanced recruitment of its substrate protein. Journal of Biological Chemistry *284*, 12783–12791.

Saucedo, L.J., Gao, X., Chiarelli, D.A., Li, L., Pan, D., and Edgar, B.A. (2003). Rheb promotes cell growth as a component of the insulin/TOR signalling network. Nat. Cell Biol. *5*, 566–571.

Saxton, R.A., Chantranupong, L., Knockenhauer, K.E., Schwartz, T.U., and Sabatini, D.M. (2016a). Mechanism of arginine sensing by CASTOR1 upstream of mTORC1. Nature *536*, 229–233.

Saxton, R.A., Knockenhauer, K.E., Schwartz, T.U., and Sabatini, D.M. (2016b). The apo-structure of the leucine sensor Sestrin2 is still elusive. Science Signaling *9*, ra92–ra92.

Saxton, R.A., Knockenhauer, K.E., Wolfson, R.L., Chantranupong, L., Pacold, M.E., Wang, T., Schwartz, T.U., and Sabatini, D.M. (2015). Structural basis for leucine sensing by the Sestrin2-mTORC1 pathway. Science.

Scheffzek, K., and Ahmadian, M.R. (2005). GTPase activating proteins: structural and functional insights 18 years after discovery. Cell. Mol. Life Sci. *62*, 3014–3038.

Scheffzek, K., Ahmadian, M.R., Kabsch, W., Wiesmüller, L., Lautwein, A., Schmitz, F., and Wittinghofer, A. (1997). The Ras-RasGAP complex: structural basis for GTPase activation and its loss in oncogenic Ras mutants. Science *277*, 333–338.

Schleiff, E., Jelic, M., and Soll, J. (2003). A GTP-driven motor moves proteins across the outer envelope of chloroplasts. Proc. Natl. Acad. Sci. U.S.a. *100*, 4604–4609.

Schmelzle, T., and Hall, M.N. (2000). TOR, a central controller of cell growth. Cell *103*, 253–262.

Schmidt, L.S., and Linehan, W.M. (2015). Molecular genetics and clinical features of Birt-Hogg-Dubé syndrome. Nat Rev Urol *12*, 558–569.

Schürmann, A., Brauers, A., Massmann, S., Becker, W., and Joost, H.G. (1995). Cloning of a novel family of mammalian GTP-binding proteins (RagA, RagBs, RagB1) with remote similarity to the Ras-related GTPases. Journal of Biological Chemistry *270*, 28982–28988.

Scrima, A., Thomas, C., Deaconescu, D., and Wittinghofer, A. (2008). The Rap-RapGAP complex: GTP hydrolysis without catalytic glutamine and arginine residues. Embo J. *27*, 1145–1153.

Segev, N. (2011). GTPases in intracellular trafficking: an overview. Semin. Cell Dev. Biol. *22*, 1–2.

Sehgal, S.N., Baker, H., and Vézina, C. (1975). Rapamycin (AY-22,989), a new antifungal antibiotic. II. Fermentation, isolation and characterization. J. Antibiot. *28*, 727–732.

Sekiguchi, T., Hirose, E., Nakashima, N., Ii, M., and Nishimoto, T. (2001). Novel G proteins, Rag C and Rag D, interact with GTP-binding proteins, Rag A and Rag B. Journal of Biological Chemistry *276*, 7246–7257.

Sekiguchi, T., Kamada, Y., Furuno, N., Funakoshi, M., and Kobayashi, H. (2014). Amino acid residues required for Gtr1p-Gtr2p complex formation and its interactions with the Ego1p-Ego3p complex and TORC1 components in yeast. Genes Cells *19*, 449–463.

Sengottaiyan, P., Spetea, C., Lagerstedt, J.O., Samyn, D., Andersson, M., Ruiz-Pavón, L., and Persson, B.L. (2012). The intrinsic GTPase activity of the Gtr1 protein from *Saccharomyces cerevisiae*. BMC Biochem. *13*, 11.

Shertz, C.A., Bastidas, R.J., Li, W., Heitman, J., and Cardenas, M.E. (2010). Conservation, duplication, and loss of the Tor signaling pathway in the fungal kingdom. BMC Genomics *11*, 510.

Shimobayashi, M., and Hall, M.N. (2015). Multiple amino acid sensing inputs to mTORC1. Cell Res. *26*, 1–14.

Siderovski, D.P., and Willard, F.S. (2005). The GAPs, GEFs, and GDIs of heterotrimeric G-protein alpha subunits. Int. J. Biol. Sci. *1*, 51–66.

Siggs, O.M., Stockenhuber, A., Deobagkar-Lele, M., Bull, K.R., Crockford, T.L., Kingston, B.L., Crawford, G., Anzilotti, C., Steeples, V., Ghaffari, S., et al. (2016). Mutation of Fnip1 is associated with B-cell deficiency, cardiomyopathy, and elevated AMPK activity. Proc. Natl. Acad. Sci. U.S.a. *113*, E3706–E3715.

Sikorski, R.S., and Hieter, P. (1989). A system of shuttle vectors and yeast host strains designed for efficient manipulation of DNA in *Saccharomyces cerevisiae*. Genetics *122*, 19–27.

Simon, I., Zerial, M., and Goody, R.S. (1996). Kinetics of interaction of Rab5 and Rab7 with nucleotides and magnesium ions. Journal of Biological Chemistry *271*, 20470–20478.

Singh, J., and Tyers, M. (2009). A Rab escort protein integrates the secretion system with TOR signaling and ribosome biogenesis. Genes Dev. *23*, 1944–1958.

Sturgill, T.W., Cohen, A., Diefenbacher, M., Trautwein, M., Martin, D.E., and Hall, M.N. (2008). TOR1 and TOR2 have distinct locations in live cells. Eukaryotic Cell *7*, 1819–1830.

Swaney, D.L., Beltrao, P., Starita, L., Guo, A., Rush, J., Fields, S., Krogan, N.J., and Villén, J. (2013). Global analysis of phosphorylation and ubiquitylation cross-talk in protein degradation. Nat. Methods *10*, 676–682.

Syrovatkina, V., Alegre, K.O., Dey, R., and Huang, X.-Y. (2016). Regulation, Signaling, and Physiological Functions of G-Proteins. J. Mol. Biol. *428*, 3850–3868.

Tee, A.R., Manning, B.D., Roux, P.P., Cantley, L.C., and Blenis, J. (2003). Tuberous sclerosis complex gene products, Tuberin and Hamartin, control mTOR signaling by acting as a GTPase-activating protein complex toward Rheb. Current Biology *13*, 1259–1268.

Thomas, J.D., Zhang, Y.-J., Wei, Y.-H., Cho, J.-H., Morris, L.E., Wang, H.-Y., and Zheng, X.F.S. (2014). Rab1A Is an mTORC1 Activator and a Colorectal Oncogene. Cancer Cell *26*, 754–769.

Trahey, M., and McCormick, F. (1987). A cytoplasmic protein stimulates normal N-ras p21 GTPase, but does not affect oncogenic mutants. Science *238*, 542–545.

Tsun, Z.-Y., Bar-Peled, L., Chantranupong, L., Zoncu, R., Wang, T., Kim, C., Spooner, E., and Sabatini, D.M. (2013). The folliculin tumor suppressor is a GAP for the RagC/D GTPases that signal amino acid levels to mTORC1. Molecular Cell *52*, 495–505.

Urano, J., Tabancay, A.P., Yang, W., and Tamanoi, F. (2000). The *Saccharomyces cerevisiae* Rheb G-protein is involved in regulating canavanine resistance and arginine uptake. Journal of Biological Chemistry *275*, 11198–11206.

Urban, J., Soulard, A., Huber, A., Lippman, S., Mukhopadhyay, D., Deloche, O., Wanke, V., Anrather, D., Ammerer, G., Riezman, H., et al. (2007). Sch9 is a major target of TORC1 in *Saccharomyces cerevisiae*. Molecular Cell *26*, 663–674.

Valbuena, N., Guan, K.-L., and Moreno, S. (2012). The Vam6 and Gtr1-Gtr2 pathway activates TORC1 in response to amino acids in fission yeast. J. Cell. Sci. *125*, 1920–1928.

Valencia, A., Chardin, P., Wittinghofer, A., and Sander, C. (1991). The ras protein family: evolutionary tree and role of conserved amino acids. Biochemistry *30*, 4637–4648.

Vézina, C., Kudelski, A., and Sehgal, S.N. (1975). Rapamycin (AY-22,989), a new antifungal antibiotic. I. Taxonomy of the producing streptomycete and isolation of the active principle. J. Antibiot. *28*, 721–726.

Wang, S., Tsun, Z.-Y., Wolfson, R.L., Shen, K., Wyant, G.A., Plovanich, M.E., Yuan, E.D., Jones, T.D., Chantranupong, L., Comb, W., et al. (2015). Lysosomal amino acid transporter SLC38A9 signals arginine sufficiency to mTORC1. Science *347*, 188–194.

Wang, X., Fonseca, B.D., Tang, H., Liu, R., Elia, A., Clemens, M.J., Bommer, U.-A., and Proud, C.G. (2008). Re-evaluating the roles of proposed modulators of mammalian target of rapamycin complex 1 (mTORC1) signaling. Journal of Biological Chemistry *283*, 30482–30492.

Wedegaertner, P.B., Wilson, P.T., and Bourne, H.R. (1995). Lipid modifications of trimeric G proteins. Journal of Biological Chemistry *270*, 503–506.

Wennerberg, K., Rossman, K.L., and Der, C.J. (2005). The Ras superfamily at a glance. J. Cell. Sci. *118*, 843–846.

Willard, F.S., Kimple, R.J., and Siderovski, D.P. (2004). Return of the GDI: the GoLoco motif in cell division. Annu. Rev. Biochem. *73*, 925–951.

Wittinghofer, A., and Pai, E.F. (1991). The structure of Ras protein: a model for a universal molecular switch. Trends Biochem. Sci. *16*, 382–387.

Wittinghofer, A., and Vetter, I.R. (2011). Structure-function relationships of the G domain, a canonical switch motif. Annu. Rev. Biochem. *80*, 943–971.

Wolfson, R.L., Chantranupong, L., Saxton, R.A., Shen, K., Scaria, S.M., Cantor, J.R., and Sabatini, D.M. (2015). Sestrin2 is a leucine sensor for the mTORC1 pathway. Science 1–9.

Wullschleger, S., Loewith, R., and Hall, M.N. (2006). TOR signaling in growth and metabolism. Cell *124*, 471–484.

Yamagata, K., Sanders, L.K., Kaufmann, W.E., Yee, W., Barnes, C.A., Nathans, D., and Worley, P.F. (1994). rheb, a growth factor- and synaptic activity-regulated gene, encodes a novel Ras-related protein. Journal of Biological Chemistry *269*, 16333–16339.

Yang, J., Zhang, Z., Roe, S.M., Marshall, C.J., and Barford, D. (2009). Activation of Rho GTPases by DOCK exchange factors is mediated by a nucleotide sensor. Science *325*, 1398–1402.

Yerlikaya, S., Meusburger, M., Kumari, R., Huber, A., Anrather, D., Costanzo, M., Boone, C., Ammerer, G., Baranov, P.V., and Loewith, R. (2016). TORC1 and TORC2 work together to regulate ribosomal protein S6 phosphorylation in *Saccharomyces cerevisiae*. Mol. Biol. Cell *27*, 397–409.

Yu, F., Imamura, Y., Ueno, M., Suzuki, S.W., Ohsumi, Y., Yukawa, M., and Tsuchiya, E. (2015). The yeast chromatin remodeler Rsc1-RSC complex is required for transcriptional activation of autophagy-related genes and inhibition of the TORC1 pathway in response to nitrogen starvation. Biochem. Biophys. Res. Commun. *464*, 1248–1253.

Yu, Y., Li, S., Xu, X., Li, Y., Guan, K., Arnold, E., and Ding, J. (2005). Structural basis for the unique biological function of small GTPase RHEB. Journal of Biological Chemistry *280*, 17093–17100.

Zaman, S., Lippman, S.I., Zhao, X., and Broach, J.R. (2008). How Saccharomyces responds to nutrients. Annu. Rev. Genet. *42*, 27–81.

Zheng, M., Wang, Y.-H., Wu, X.-N., Wu, S.-Q., Lu, B.-J., Dong, M.-Q., Zhang, H., Sun, P., Lin, S.-C., Guan, K.-L., et al. (2011). Inactivation of Rheb by PRAK-mediated phosphorylation is essential for energy-depletion-induced suppression of mTORC1. Nat. Cell Biol. *13*, 263–272.

Zurita-Martinez, S.A., Puria, R., Pan, X., Boeke, J.D., and Cardenas, M.E. (2007). Efficient

Tor signaling requires a functional class C Vps protein complex in *Saccharomyces cerevisiae*. Genetics *176*, 2139–2150.

Appendix

Acknowledgements

So... it looks like the end of this thesis. Thus, it is time to say thanks to...

Prof. Claudio De Virgilio, because of so many reasons I could write a new chapter with figures, discussions and general remarks... and probably Marie would have to correct it! Well, I will "just" say that you gave me the awesome opportunity to move to Switzerland, to work in your laboratory, to learn so much about science and to meet other amazing people. I will never forget what you did for me.

Prof. Robbie Loewith and Prof. Jörn Dengjel, for accepting to review this thesis and being members of my thesis jury board.

Marie, because you have been a mentor during my PhD. You gave me valuable advices, strongly contributing to my scientific education. You also carefully corrected this thesis, often sacrificing your free time. You heroically tried to fight my stubbornness, having success where others failed. Thanks again.

Serena, per la tua amicizia, complicità e pazienza. Per avermi sempre detto qualsiasi cosa tu pensassi in modo diretto e sincero. Per aver condiviso insieme momenti felici una miriade di volte. Per avermi sopportato cinque giorni a settimana, per quattro lunghi anni di fila (ci vuole coraggio). Custodirò nel cuore tutti questi ricordi, com'è ovvio che sia.

Nicolas P, because you have been a great friend/colleague. You taught me how anyone can work hard in the lab and still have a great social life. Marta and Fernando, again, a unique example of the right attitude in life/work. I was really lucky to meet you in my life. Séverine, because you taught me how to be independent. Riko, one of my "senseis", for our many scientific discussions and protocols you shared with me. Emma, for your kindness when I was still new in the lab. Malika and Floriane, always ready to help me. Nico T, Judith, Yvan, Jonas, Katie, and Ladislav for the time we shared in the lab... and outside as well.

Ai miei amici italiani e ticinesi. Siete parte della mia forza (e spesso causa delle mie vicissitudini sociali).

Alla mia famiglia, in particolare mio padre e mia madre. Nonostante la distanza geografica, vi ho sempre sentito al mio fianco. Mi avete sempre dato il giusto consiglio per andare avanti con questa esperienza. Non sarei arrivato fin qui senza di voi.

A Irene... perché mi sei sempre stata vicina in quest'avventura in Svizzera, e hai sempre cercato di tirarmi fuori un sorriso quando la voglia di sorridere non c'era e molti altri ci avrebbero rinunciato. Grazie per amarmi incondizionatamente, nonostante che in questi anni abbia avuto la mente in laboratorio un giorno sì e l'altro pure. Grazie di cuore per essere quello che sei.

Alessandro Sardu

Curriculum Vitae

Personal Information

Address	32, Avenue Beauregard - 1700 Fribourg, Switzerland.		
Nationality	Italian	Date of birth	29 July 1988
E-mail	alessandro.sardu@gmail.com	Mobile	+41 (0) 78 879 32 88

Education and Training

Dates	**03/2013 – ongoing**
Title of Qualification	PhD in Life Science.
Principal Subjects	Research on nutrient signal transduction and control of quiescence in budding yeast, especially focusing on the regulation of the TOR complex 1 by Rag GTPases.
Type of Organisation providing Education and Training	University of Fribourg, Department of Biology. 10, Chemin du Musée - 1700 Fribourg, Switzerland.
Dates	**10/2010 – 10/2012**
Title of Qualification Awarded	Master Diploma in Molecular Biology, final mark 110/110 cum laude.
Master Thesis Title	"Analysis of the yeast transcriptome structure using a new bioinformatic tool"
Type of Organisation providing Education and Training	University of Padua, Faculty of Science MM. FF. NN, Department of Biology. 2, Via 8 Febbraio - 35122 Padua, Italy.
Dates	**10/2007 – 09/2010**
Title of Qualification Awarded	First Level Diploma in Molecular Biology.
Degree Thesis Title	"Drosophila as model organism to study functions and regulation of VDAC protein"
Type of Organisation providing Education and Training	University of Padua, Faculty of Science MM. FF. NN, Department of Biology. 2, Via 8 Febbraio - 35122 Padua, Italy
Dates	**09/2002 – 07/2007**
Title of Qualification Awarded	Secondary School Diploma focusing on Sciences Studies.
Type of Organisation providing Education and Training	Liceo Scientifico Statale "Lorenzo Mossa". Via Campidano – 07026 Olbia, Italy.

Personal Skills

Mother tongue: **Italian**

Self-Assessment

European level (*)

English

Understanding				**Speaking**				**Writing**	
Listening		Reading		Spoken interaction		Spoken production			
C1	Independent user	C1	Independent user	C1	Independent user	C1	Independent user	C1	Independent user

(*) Common European Framework of Reference for Languages

Social Competences

Good communication skills and sense of team spirit gained through lot of experiences such as group work during research projects.

Technical Competences

Molecular Biology: PCR, qRT-PCR, RNA extraction, DNA gel electrophoresis, cloning, gene deletion and genomic tagging in yeast, site-directed mutagenesis, co-immunoprecipitation.

Cell Biology: protein extraction, Western Blot, fluorescence microscopy, split-ubiquitin-based yeast two hybrid system, SGA screening.

Biochemistry: recombinant protein purification from bacteria, tandem-affinity purification from yeast, *in vitro* protein interaction, *in vitro* GTP hydrolysis assays.

Computer Competences

Operating system: Full command of Microsoft Windows and OS X operating system. Competences in administration and configuration of Linux Debian and Ubuntu system.

General software: Full command of Microsoft Office, LibreOffice and Google document tools. Good knowledge of statistic analysis software like R or Prism and of graphic design applications like Photoshop.

Programming languages: Good knowledge of bioinformatics language Perl and dedicated BioPerl packages.

Bioinformatic software and competences: Proficient in the management of Next-Generation Sequencing coming from GS FLX+ System, Solexa and SOLiD sequencing technologies. Experience in finishing work for genome sequence assembly and oligonucleotide selection for gap filling.

Interests

Live music, sport, cooking, photography, traveling.

Driving Licence

Swiss A and B category.

References

Available upon request

Prof. Claudio De Virgilio, Full Professor, University of Fribourg, Department of Biology; e-mail: claudio.devirgilio@unifr.ch; tel. 026/300.86.56

Dr. Stefano Campanaro, Researcher, University of Padua, Department of Biology – CRIBI Biotecnology Centre; e-mail: stefano.campanaro@unipd.it; tel. 00390498276306;

Scientific Publications

Péli-Gulli, M.-P., Sardu, A., et al., 2015. Amino Acids Stimulate TORC1 through Lst4-Lst7, a GTPase-Activating Protein Complex for the Rag Family GTPase Gtr2. Cell reports, 13(1), pp.1–15.

Numrich, J. et al., 2015. The I-BAR protein Ivy1 is an effector of the Rab7 GTPase Ypt7 involved in vacuole membrane homeostasis. Journal of cell science, p.jcs.164905.

Sardu, A., Treu, L. & Campanaro, S., 2014. Transcriptome structure variability in Saccharomyces cerevisiae strains determined with a newly developed assembly software. BMC genomics, 15(1), p.1045.

Treu, L. et al., 2014. The impact of genomic variability on gene expression in environmental Saccharomyces cerevisiae strains. Environmental microbiology, 16(5), pp.1378–1397.